Offical journal of the Association of Clinical Biochemistry Specialists

ISSN 2587-2362

INTERNATIONAL JOURNAL OF MEDICAL BIOCHEMISTRY

YEAR 2026 VOLUME 9 ISSUE 1

www.internationalbiochemistry.com

INTERNATIONAL JOURNAL OF MEDICAL BIOCHEMISTRY

ISSN 2587-2362

VOLUME IX ISSUE I YEAR 2026

The Owner and Publishing Manager on behalf of the Association of Clinical Biochemistry Specialists (Klinik Biyokimya Uzmanları Derneği): PROF. DILDAR KONUKOGLU

Address: Maslak Mah. AOS 55. Sok. No: 2, 42 Maslak A Blok Daire: 231 Sarıyer, İstanbul-Türkiye
Phone: +90 212 241 26 53
Fax: +90 212 241 26 54
e-mail: www.kbud.org.tr
web: info@kbud.org.tr

Publisher: KARE MEDIA
Address: Göztepe Mah. Fahrettin Kerim Gökay Cad. No: 200 D: 2, Göztepe, Kadıköy, İstanbul
Phone: +90 216 550 61 11
Fax: +90 216 550 61 12
e-mail: info@karepb.com
web: www.kareyayincilik.com

Yayın Turu: Uluslararası Sureli
Basım Tarihi: Ocak 2026
Basım: Filmevi Grafik Renk Ayırımı Sistemleri San. Tic. LTD. ŞTİ. İstanbul-Türkiye

International Journal of Medical Biochemistry is a peer-reviewed journal published triannually.

This publication is printed on paper that meets the international standard ISO 9706:1994.
National Library of Medicine (USA) recommends the use of permanent, acid-free paper in the production of biomedical literature.

INTERNATIONAL JOURNAL OF
MEDICAL BIOCHEMISTRY

AIM AND SCOPE

International Journal of Medical Biochemistry (IJMB) publishes articles relating to clinical and experimental chemistry, molecular biology, genetics, therapeutic drug monitoring, toxicology, immunology, hematology and laboratory medicine with the focus on analytical and clinical investigation of laboratory tests used for diagnosis, prognosis, and monitoring of diseases.

BASIC PUBLICATION RULES

Authors are responsible for the accuracy of data. The journal is in compliance with the uniform requirements for manuscripts submitted to biomedical journals published by the ICMJ. The editorial and publication processes of the journal are conducted in accordance with the guidelines of the World Association of Medical Editors (WAME), International Committee of Medical Journal Editors (ICMJE), the Council of Science Editors (CSE), the European Association of Science Editors (EASE), and the Committee on Publication Ethics (COPE) as well.

DISCLAIMER

Statements or opinions expressed in the manuscripts published in International Journal of Medical Biochemistry reflect the views of the author(s) and not the opinions of the editors, the editorial board and the publisher; the editors, the editorial board and the publisher disclaim any responsibility or liability for such materials.

ABSTRACTING AND INDEXING

International Journal of Medical Biochemistry is indexed in TUBITAK TR Index (2019), CNKI (2019), TurkMedline (2019), Open Ukrainian Citation Index (2019), ProQuest (2019), CABI (2021), CEEAS (2021), EBSCO (2022), CAS (American Chemical Society) (2022), Directory of Open Access Journals - DOAJ (2022), Scopus (2023), Gale Cengage (2023), Sherpa Romeo (2024), ASCI (2024) and Web of Science - ESCI (2025).

ABBREVIATION

Int J Med Biochem

PUBLICATION FEE

International Journal of Medical Biochemistry is an open access journal. Manuscripts are available on the journal web page at no cost.

As of March 1, 2025, in order to further improve the quality and accessibility of the journal, a fee will be charged as a contribution to the cost of production. This fee will be charged during the process of application of submitted articles and will be charged regardless of eventual acceptance/rejection of the manuscript.

Foreign authors can complete the article submission process after depositing to the USD account below. No publication fee is charged for articles submitted by authors from Türkiye.

ACCESS TO JOURNAL CONTENT

The abstracts and full texts of published articles can be accessed free of charge at www.internationalbiochemistry.com.

JOURNAL FREQUENCY

The International Journal of Medical Biochemistry published three issues per year from its establishment until 2024. The journal has started publishing four issues per year since 2025. The publication months are January, April, July, and October.

INTERNATIONAL JOURNAL OF
MEDICAL BIOCHEMISTRY

ISSN 2587-2362

CONTENTS

VOLUME IX ISSUE 1 YEAR 2026

EDITORIAL

ORIGINAL ARTICLES

REVIEW

LETTER TO THE EDITOR

INTERNATIONAL JOURNAL OF
MEDICAL BIOCHEMISTRY

EDITORIAL

Dear Colleagues,

We are pleased to present the first issue of 2026, following a landmark achievement for our journal in 2025: acceptance into Web of Science. This milestone reflects the scientific rigor of our authors, the diligence of our reviewers, and our shared commitment to high-quality research in clinical biochemistry and laboratory medicine.

The articles in this issue represent the breadth of our field—from prognostic biomarkers in non-ST elevation myocardial infarction and emerging endocrine mediators in Type 2 diabetes, to oxidative stress markers in brucellosis and amino acid profiling in chronic renal failure. Genetic considerations in polycythemia, advances in total laboratory automation, and the evolving role of digital platforms in clinical biochemistry education further highlight the dynamic transformation of laboratory medicine.

In addition, our review on Alzheimer's disease emphasizes the critical integration of biological biomarkers into diagnostic practice, reinforcing the translational mission of our discipline.

As we move forward with increased international visibility, we remain committed to methodological excellence, clinical relevance, and interdisciplinary collaboration.

We thank our contributors and readers for their continued support.

Sincerely,

Prof. Dildar Konukoglu, MD.

Editor-in-Chief

INTERNATIONAL JOURNAL OF
MEDICAL BIOCHEMISTRY

DOI: 10.14744/ijmb.2025.83723
Int J Med Biochem 2026;9(1):1–8

Research Article

Comparative analysis of turnaround times before and after the implementation of a new total laboratory automation system

Berrak Guven, Murat Can

Department of Biochemistry, Zonguldak Bülent Ecevit University School of Medicine, Zonguldak, Türkiye

Abstract

Objectives: This study aimed to evaluate the impact of Total Laboratory Automation (TLA) with the implementation of the Beckman Coulter DxA Fit 5000 on laboratory workload and performance.

Methods: A comparative analysis was conducted at the Biochemistry Laboratory of Zonguldak Bülent Ecevit Hospital, covering the pre-automation period (May 1–June 30, 2024) and the post-automation period (May 1–June 30, 2025). Key performance indicators included mean turnaround time (TAT), median TAT, 90th percentile TAT, the proportion of outliers at 60 and 120 minutes, and achievement of emergency department (ED) benchmarks (≤45 minutes). Test volumes were monitored to ensure stability as a covariate.

Results: Following the introduction of TLA, mean TAT decreased by up to 20%, median TAT by 18%, and 90th percentile TAT by 25% across inpatient and outpatient tests. Outlier rates at 60 minutes declined from 12% to 10% in inpatients and from 83% to 55% in outpatients. For STAT testing, the proportion of samples meeting the 45-minute ED benchmark increased from 65% to 88%.Total test volumes remained largely stable between periods, indicating that observed TAT improvements were attributable to automation rather than changes in sample volume. Glucose exhibited the shortest mean TAT, whereas gamma-glutamyl transferase had the longest. In outpatient testing, C-reactive protein demonstrated the highest compliance with the 60-minute TAT benchmark, while human chorionic gonadotropin showed the lowest; however, all outpatient tests were completed within 120 minutes.

Conclusion: The implementation of TLA significantly improved numerical TAT metrics, reduced outlier frequencies, and increased achievement of ED benchmarks, while maintaining stable test volumes, highlighting enhanced efficiency, predictability, and workflow stability in a high-volume university hospital laboratory setting.

Keywords: DxA Fit 5000, total laboratory automation, tunaround time

How to cite this article: Guven B, Can M. Comparative analysis of turnaround times before and after the implementation of a new total laboratory automation system. Int J Med Biochem 2026;9(1):1–8.

Clinical laboratories are integral components of hospital services, providing critical diagnostic information that guides patient management and treatment. In recent years, the demand for laboratory testing has increased steadily, driven by an aging population, the rising prevalence of chronic diseases, the discovery of novel clinically relevant biomarkers, and the overall growth in healthcare utilization. To meet these demands, laboratories have increasingly adopted advanced automation technologies to accelerate processes, enhance standardization, and improve reliability [1].

One of the most comprehensive applications of such technologies is Total Laboratory Automation (TLA) [2]. TLA integrates all phases of the laboratory workflow—preanalytical (sample acceptance, sorting, centrifugation, aliquoting), analytical,

Address for correspondence: Murat Can, MD. Department of Biochemistry, Zonguldak Bülent Ecevit University School of Medicine, Zonguldak, Türkiye
Phone: +90 532 556 85 02 **E-mail:** drcanmurat@yahoo.com **ORCID:** 0000-0002-1539-3973

Submitted: October 22, 2025 **Revised:** December 03, 2025 **Accepted:** December 06, 2026 **Available Online:** February 18, 2026

and postanalytical (storage and archiving)—within a single continuous platform. By minimizing manual intervention, TLA improves process standardization and reduces overall error rates. Given that the majority of laboratory errors occur in the preanalytical phase, automating these steps plays a crucial role in improving the quality of the total testing process [3]. Furthermore, integration of TLA with a Laboratory Information System (LIS) enables synchronization of analytical results with patient records, thereby enhancing both efficiency and the clinical utility of laboratory data [4].

In an era of increasingly constrained healthcare budgets, investments in TLA must demonstrate clear clinical and operational benefits [5]. Among the most widely recognized indicators of such benefit is the reduction of turnaround time (TAT), defined as the interval between test initiation and result reporting. TAT is a well-established quality metric in laboratory medicine, with shorter TAT consistently associated with faster clinical decision-making and improved patient care [6]. Although multiple definitions of TAT exist, laboratories and accreditation bodies most commonly monitor in-laboratory TAT, which refers to the period between the receipt of a barcoded sample and the release of results [7, 8].

Building on this context, the present study was designed to systematically evaluate the impact of implementing the Beckman Coulter DxA Fit 5000 TLA system in the Medical Biochemistry Laboratory, with particular focus on its effect on in-laboratory TAT.

Materials and Methods

The study was approved by the Zonguldak Bülent Ecevit University Ethics Committee (No: 2025/06, Date: 19/03/2025) following the principles of the Declaration of Helsinki. This study was performed at the Biochemistry Laboratory of the University Hospital of Zonguldak Bülent Ecevit, that is a tertiary care 619-bed hospital equipped with an integrated informatics platform that manages both patient records and laboratory test orders. Laboratory data are treated through a software package, allowing clinicians real-time consultation of laboratory reports after laboratory staff clinical validation.

In this study, TATs were systematically observed and analyzed over a two-month period. Laboratory automation was implemented in April 2025 to improve operational efficiency. To evaluate the impact of automation, we compared data from two distinct periods: The pre-automation phase (May 1 to June 30, 2024) and the post-automation phase (May 1 to June 30, 2025). For the calculation of TAT, the time interval was defined from the moment the sample was received in the LIS to the moment the result was verified and reported. These timestamps were identical in both pre-TLA and post-TLA periods, ensuring consistent measurement of turnaround times. Preanalytical steps, such as sample collection and transportation, were not included, as they were performed uniformly across both periods. Repeat or reflex tests, add-on requests, and failed samples were excluded from the TAT analysis. All tests were processed individually; therefore, the observed TAT outliers are not attributable to differences in processing and measurements were consistent across all test types. This comparative design enabled us to assess the effect of TLA on TATs and overall laboratory performance.

Pre-TLA

Before the implementation of automation, the preanalytical area was equipped with a Cobas p612 system. The analytical section consisted of two Cobas 6000 systems (Roche Diagnostics, Mannheim, Germany), including two Cobas c501 modules and one Cobas e601 module, as well as an additional standalone Cobas e601 module used exclusively for STAT samples (Table 1). Samples were manually registered into the Hospital Information Management System and delivered to the centrifugation stage (NF 1200; Nüve, Turkey) by laboratory personnel. After centrifugation, several manual steps were required, including tube decapping, liquid-level detection, barcode verification, sample quality assessment, and aliquoting of both primary and secondary tubes, all facilitated through the Cobas p612 system.

Automation software (Cobas Infinity, Roche Diagnostics, Mannheim, Germany) allowed staff to manage workload orders from the LIS and monitor the operational status of analytical instruments. At the end of each working day, samples were placed in refrigerated storage and discarded after two business days.

Table 1. Instrument configurations and features in pre- and post-TLA periods

Pre-TLA				Post-TLA			
Instrument	**Number of modules**	**Capacity**	**Throughput**	**Instrument**	**Number of modules**	**Capacity**	**Throughput**
Input Module	1	600 tubes	1400 tubes/hr	Input Module	1	336 tubes	375 tubes/hr
Centrifuge	3 (offline)	144 tubes	288 tubes/hr	Centrifuge	1	56 tubes	325 tubes/hr
Decapper	1	N/A	300 tubes/hr	Decapper	1	N/A	375 tubes/hr
Aliquoter	1	N/A	300 tubes/hr	Aliquoter	---------	----------	----------
e601	3	25 position	170 test/hr	DXI 800	2	50 position	400 test/hr
c501	4	63 position	600 test/hr	AU 5800	2	54 positions	2000 test/hr

N/A: Not applicable.

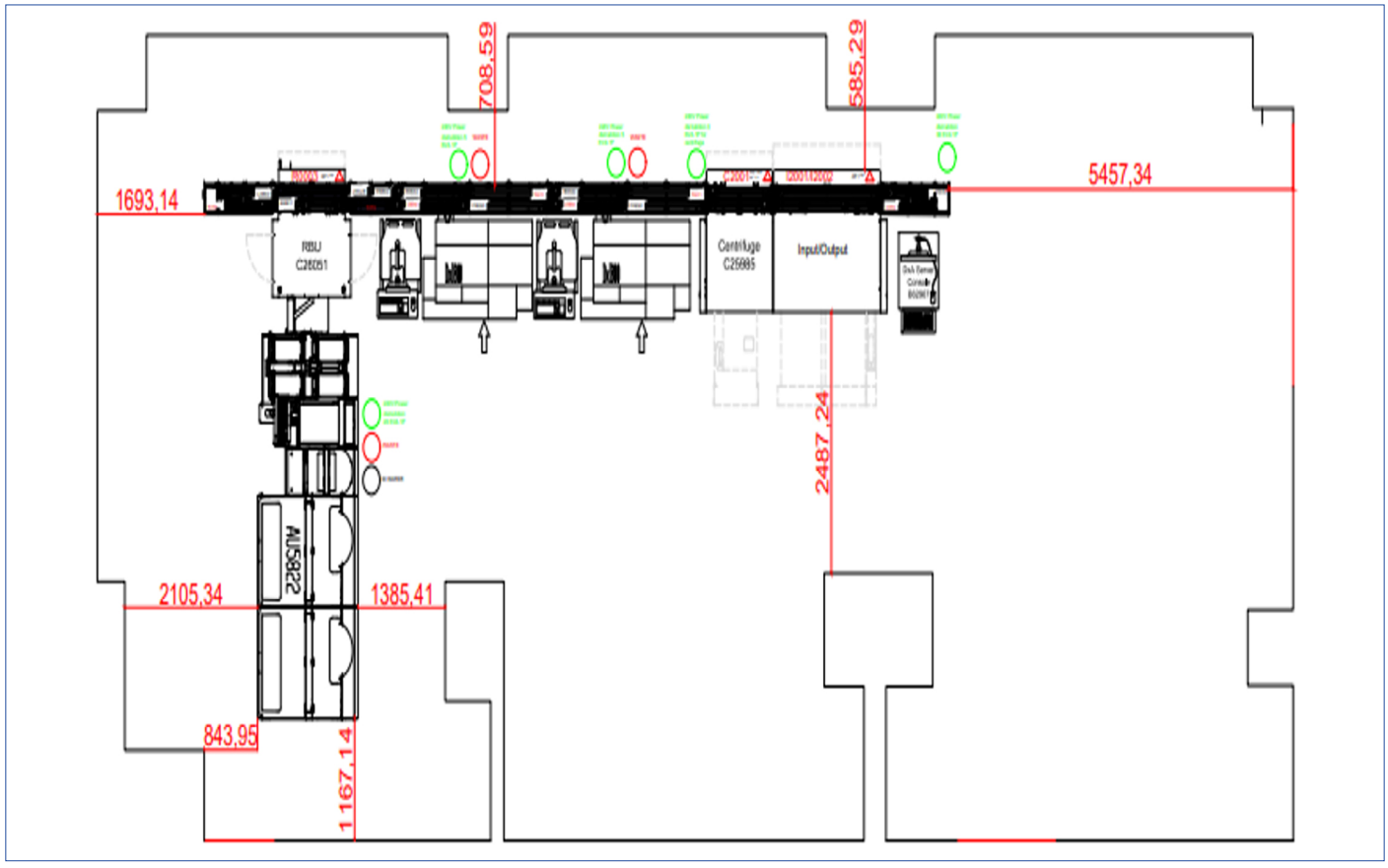

Figure 1. Design of the instruments included along the automation line at the laboratory.

Post-TLA

Following the installation of the TLA system, laboratory workflows were redesigned and centralized. During the preanalytical phase, personnel inspected samples for preanalytical errors (e.g. barcode inconsistencies, or inappropriate tube types) after sample acceptance. Verified samples were then transferred to the sample input area of the DxA Fit 5000 system. The automated laboratory layout included the DxA Fit 5000 Workflow Automation System (Beckman Coulter, CA, USA), two DxI 800 immunoassay analyzers and two AU 5800 clinical chemistry analyzer with an ISE module (Beckman Coulter, CA, USA) (Table 1). This integrated platform allowed standardized handling and management of samples within a unified workstation.

Once the barcode is scanned and work orders are received from the LIS, the automated workflow initiates seamlessly within the system. Robotic arms facilitate the efficient execution of tasks throughout the process. Initially, samples undergo centrifugation, followed by a leveling determination. Upon reaching the lid-opening module, the sample lids are automatically removed and directed towards the analyzers, where hormone and biochemical tests are conducted. The automation software, REMISOL Advance (Beckman Coulter, Brea, CA), empowers staff to effectively manage workload orders from the LIS and monitor the operational status of the associated analytical instruments.

Samples are pipetted into analyzers in precise volumes according to test requirements and subsequently transferred to the DxA Fit 5000 outlet module, which has a storage capacity of 600 tubes. Tubes in this outlet module could be retrieved at any time by staff. Repeat testing is processed automatically without manual intervention, further enhancing efficiency and accuracy. At the end of each day, remaining samples were stored in a refrigerator and discarded after two business days. The schematic layout of the automated system is illustrated in Figure 1.

In this study, predefined outcome measures were established to evaluate the impact of TLA on laboratory performance. The primary outcome was the TAT for outpatient, inpatient, and STAT samples, assessed using mean TAT, median TAT, and 90th percentile TAT for each analyte. These metrics allowed a detailed assessment of the direct effect of TLA implementation on processing times. Secondary outcomes were defined to evaluate workflow quality, stability, and clinical relevance. These included the proportion of samples exceeding accepted TAT limits (outlier rates), the percentage of STAT samples meeting the critical ≤45-minute TAT benchmark, the proportion of samples completed at the 60- and 120-minute marks, and improvements in distribution variability reflected by upper percentile reductions (especially the 90th percentile). This comprehensive approach enabled assessment not only of reductions in average TAT but also of improvements in delay rates, predictability, and performance for emergency testing.

Table 2. Test numbers of inpatient, outpatient and stat samples

	Outpatient		Inpatient		STAT	
	PreTLA (2024)	PostTLA (2025)	PreTLA (2024)	PostTLA (2025)	PreTLA (2024)	PostTLA (2025)
Glucose	9651	9263	16772	11142	2707	1973
Urea	17679	18403	15815	15518	2843	2741
Creatinine	14850	15356	17683	15384	3179	2718
ALT	17839	18079	13588	13467	3172	2709
AST	17306	17261	13532	13467	3168	2706
Total Bilirubin	4680	5162	6752	7374	2052	2129
Potasium	14200	14590	15922	15765	3194	2742
Lipaz	695	764	3633	4364	1139	1049
ALP	7692	7315	6203	7101	772	1043
GGT	9431	8598	7193	8145	623	984
CRP	7371	7539	11408	12918	2239	2131
HCG	1069	1245	345	266	285	236
Troponin I/T	471	529	3359	2777	1817	1972
CK-MB	147	148	3245	2608	1777	1931
TSH	9178	10113	--------	--------	--------	--------
Vit D	3378	3776	--------	--------	--------	--------
B12	5636	7300	--------	--------	--------	--------
Folat	2892	4524	--------	--------	--------	--------
Ferritin	4977	6971	--------	--------	--------	--------
Total	149.142	156.936	135.450	130.296	28.967	27.064

Statistical Analysis

Data analysis was performed using IBM SPSS Statistics version 19.0 (IBM Corp., Armonk, NY, USA). The normality of data distributions was assessed using the Kolmogorov-Smirnov test. Depending on the outcome, comparisons between pre- and post-automation periods were conducted using either a independent-samples t-test for normally distributed variables or the Mann–Whitney U test for non-normally distributed variables. When the t-test was applied, comparisons were based on the mean TAT values, whereas for the Mann–Whitney U test, comparisons were based on the median TAT values. Continuous variables are presented as mean (95% CI), median, and 90th percentile TAT values. All tests were two-tailed, and $p \leq 0.05$ was considered statistically significant.

Results

Upon detailed analysis of the laboratory workload, a noticeable change in the volume of received tubes was observed across all categories, including inpatient, outpatient, and STAT samples. Laboratory performance was evaluated based on 19 outpatient tests and 14 inpatient and STAT tests. Overall, the data indicated a 5% increase in outpatient test volume, a 3.8% decrease in inpatient tests, and a 6.5% reduction in STAT tests between the pre- and post-TLA periods (Table 2). This relative stability in total test numbers supports the interpretation that observed improvements in turnaround time (TAT) primarily reflect workflow efficiency rather than fluctuations in sample volume.

The primary outcomes, defined as mean, median, and 90th percentile TAT, were calculated for each analyte separately for outpatient, inpatient, and STAT samples. For outpatient tests (Table 3), all analytes including Glucose, Urea, Creatinine, ALT, AST, Total Bilirubin, Potassium, Lipase, ALP, GGT, CRP, HCG, Troponin I/T, CK-MB, TSH, B12, Folate, and Ferritin exhibited a significant reduction in TAT across all three metrics ($p<0.001$), except for Vitamin D, which showed only modest changes. Among outpatient tests, Potassium demonstrated the lowest mean TAT at 67 minutes, whereas Vitamin D had the highest mean TAT at 141 minutes. Notably, Vitamin D also showed the highest TAT values at both the 60- and 120-minute time points, while ALT had the lowest values. These results indicate that the impact of automation was observed across both routine and complex assays, with certain analytes demonstrating larger absolute reductions in TAT.

For inpatient and STAT tests (Table 4, 5), the mean TAT ranged from 39 minutes for Glucose to 43 minutes for GGT among inpatient samples. For STAT samples, the mean TAT ranged from 31 minutes for GGT to 39 minutes for HCG. The median and 90th percentile TAT values consistently reflected reductions post-TLA, suggesting both improvements in central tendency and decreased variability. Across outpatient tests, the 60-minute TAT completion rate varied from 5% for HCG to 13% for CRP, whereas by the 120-minute mark, all tests were completed, demonstrating efficient throughput.

Secondary outcomes were systematically assessed to evaluate workflow quality and predictability. Outlier analysis indicated

Table 3. Total Laboratory Automation (TLA), mean, median and 9^{0th} percentile laboratory Turnaround Time (TAT), and Percentage of Outlier (OP) at 60 min and 120 min during the study period for outpatient tests

Test	Mean TAT (%95 CI)		Median TAT		90th percentile		OP 60 min		OP 120 min		p
	Pre-TLA	Post-TLA	Pre-TLA	Post-TLA	Pre-TLA	Post-TLA	Pre-TLA	Post-TLA	Pre-TLA	Post-TLA	
Glucose	119.71 (18.8–120.8)	80.3 (79.4–81.3)	115	67	182	146	90.6	56.8	45.1	17.7	<0.001[a]
Urea	107.4 (106.7–108.0)	75.1 (74.5–75.8)	102	63	169	133	83.7	52.3	34.9	13.3	<0.001[a]
Creatinine	104.6 (103.8–105.3)	75.0 (74.3–75.7)	99	62	167	131	81.7	51.9	32.6	12.9	<0.001[a]
ALT	110.1 (109.5–110.8)	67.9 (67.4–68.4)	104	57	172	114	85.3	45.9	37.1	8.6	<0.001[a]
AST	109.3 (108.7–110.1)	68.4 (67.9–69.0)	104	58	171	114	84.9	46.8	36.4	8.5	<0.001[a]
Total Bilirubin	112.1 (110.8–113.4)	77.5 (76.3–78.7)	107	63	173	143	87.1	53.3	39.6	15.6	<0.001[a]
Potasium	106.4 (105.7–107.2)	67.6 (67.0–68.2)	101	57	168	114	83.8	55.1	34.1	8.4	<0.001[b]
Lipaz	109.0 (105.4–112.8)	69.8 (67.2–72.3)	102	58	179	117	85.3	47.5	34.8	9.2	<0.001[a]
ALP	114.3 (113.3–115.4)	70.9 (70.0–71.8)	109	60	178	119	87.1	49.5	40.9	9.7	<0.001[a]
GGT	112.2 (111.3–113.2)	74.7 (71.4–73.2)	107	63	175	127	86.0	53.3	38.8	11.9	<0.001[a]
CRP	112.4 (111.2–113.5)	89.6 (88.5–90.7)	107	77	175	156	86.4	65.2	39.4	23.2	<0.001[a]
HCG	153.2 (149.6–156.8)	114.1 (109.8–118.5)	153	96	224	179	95.2	82.3	68.5	31.4	<0.001[a]
Troponin I/T	151.1 (146.2–155.9)	107.9 (103.4–112.4)	154	98	208	167	94.5	85.1	74.5	33.6	<0.001[a]
CK-MB	136.0 (127.7–144.4)	119.8 (108.2–131.4)	135	100	201	206	90.5	81.1	61.9	39.9	<0.001[a]
TSH	146.9 (145.9–147.9)	118.0 (116.7–119.3)	147	102	20 3	186	97.3	87.8	68.6	38.8	<0.001[a]
Vit D	141.4 (139.4–143.4)	140.9 (138.3–143.6)	144	124	191	222	97.2	94.6	61.8	52.2	>0.05[b]
B12	140.3 (138.8–141.9)	125.4 (123.8–127.0)	141	110	193	197	97.6	92.6	60.6	43.0	<0.001[a]
Folat	138.4 (136.3–140.6)	126.6 (124.6–128.6)	138	113	191	199	97.5	94.4	58.1	45.3	<0.001[a]
Ferritin	134.8 (133.2–136.3)	130.0 (128.3–131.7)	134	114	190	209	96.3	92.4	56.6	66.1	<0.001[a]

95% Confidence Interval (CI); [a]: Mann–Whitney U test, Pre-TLA compared with Post-TLA for non-normally distributed data; [b]: Independent t-test, Pre-TLA compared with Post-TLA for normally distributed data.

a substantial reduction in the proportion of samples exceeding acceptable TAT limits, particularly among STAT samples where the proportion meeting the ≤45-minute ED benchmark increased notably. Troponin I and CK-MB tests, critical for emergency diagnostics, had the highest outpatient TAT values at both 60- and 120-minute intervals; however, automation resulted in a meaningful decrease in outliers and improved adherence to the ED standard. Conversely, creatinine and Potassium tests consistently demonstrated the lowest TAT values, reflecting optimized processing for high-frequency assays.

Discussion

The implementation of a TLA system in our biochemistry laboratory in 2025, comprising the Beckman Coulter DxA Fit

Table 4. Total Laboratory Automation (TLA), Mean, Median and 90th Percentile Laboratory Turnaround Time (TAT), and Percentage of Outlier (OP) at 60 min and 120 min during the study period for inpatient tests

Test	Mean TAT (%95 CI)		Median TAT		90th percentile		OP 60 min		OP 120 min		p
	Pre-TLA	Post-TLA	Pre-TLA	Post-TLA	Pre-TLA	Post-TLA	Pre-TLA	Post-TLA	Pre-TLA	Post-TLA	
Glucose	40.1 (39.7–40.5)	39.2 (38.9–39.4)	37	36	61	58	10.1	8.8	0	0	<0.001[a]
Urea	43.5 (43.3–43.7)	40.1 (39.7–40.4)	41	36	63	60	12.2	10.0	0	0	<0.001[a]
Creatinine	42.9 (42.7–43.2)	41.9 (41.0–41.8)	41	37	62	63	11.5	11.5	0	0	<0.001[a]
ALT	43.3 (43.1–43.6)	41.6 (41.3–42.0)	41	37	63	62	12.5	11.1	0	0	<0.001[a]
AST	44.8 (44.5–45.1)	41.8 (41.4–42.1)	42	37	64	62	13.8	11.0	0	0	<0.001[a]
Total Bilirubin	46.2 (45.8–46.6)	43.2 (42.8–43.8)	44	38	67	63	17.5	11.9	0	0	<0.001[a]
Potasium	42.5 (42.3–42.8)	40.6 (40.2–40.9)	40	36	62	60	11.8	9.8	0	0	<0.001[b]
Lipaz	46.3 (45.4–47.2)	39.9 (39.4–40.5)	42	36	68	58	16.8	8.7	0	0	<0.001[b]
ALP	47.7 (47.2–48.2)	42.9 (42.4–43.4)	45	37	69	63	18.8	11.8	0	0	<0.001[a]
GGT	48.3 (47.8–48.8)	43.3 (42.8 –43.8)	45	38	70	63	19.5	12.2	0	0	<0.001[b]
CRP	46.2 (45.9–46.4)	44.1 (43.7–44.5)	42	39	66	64	16.2	13.3	0	0	<0.001[a]
HCG	42.3 (41.2–43.5)	39.6 (37.4–41.8)	41	34	58	56	8.6	5.5	0	0	<0.001[a]
Troponin I/T	46.1 (45.7–46.6)	40.4 (39.7–41.0)	44	36	60	56	10.1	8.2	0.1	0	<0.001[a]
CK-MB	46.0 (45.5–46.4)	39.9 (39.2–40.6)	44	36	60	55	9.6	7.7	0	0	<0.001[a]

95% Confidence Interval (CI); [a]: Mann–Whitney U test, Pre-TLA compared with Post-TLA for non-normally distributed data; [b]: Independent t-test, Pre-TLA compared with Post-TLA for normally distributed data.

5000, two Dxl 800 immunoassay analyzers, and two AU 5800 chemistry analyzers, represents a significant advancement in laboratory modernization. This transition required not only technological upgrades but also a fundamental shift in the philosophy of sample processing. Software customization posed the greatest challenge, highlighting the importance of accurate operational data collection and close collaboration among LIS personnel, IT specialists, and laboratory staff, whereas hardware transition proceeded smoothly.

The primary focus of this study was the impact of TLA on TAT. Our results indicate that automation can substantially reduce TAT and stabilize workflow variability. Tornel et al. [9] reported that online centrifugation within TLA added 9–10 minutes compared with offline methods. In our setting, offline centrifugation alone required at least 10 minutes, resulting in total processing times comparable to online workflows, with a mean of 23 minutes. These observations suggest that while manual processing may be faster for very small STAT sample volumes, TLA provides superior performance for high-volume and accessible STAT testing.

In emergency department (ED) testing, achieving a TAT ≤45 minutes is clinically meaningful [10]. Following TLA implementation, median troponin I TAT decreased from 42 to 34 minutes, reaching this benchmark. Similar improvements have been reported by Angeletti et al. [4], Lam et al. [11], and Chung et al. [12], demonstrating the feasibility and clinical benefit of intra-laboratory TAT <45 minutes.

Potassium TAT, evaluated as a benchmark analyte, showed a substantial reduction in outlier rates, decreasing from 12% to 10% in inpatients and from 83% to 55% in outpatients. This aligns with Holland et al. [13], who reported minimal changes in mean potassium TAT but significant reductions in extreme delays (>40 minutes). These improvements emphasize the value of automation in stabilizing workflow variability, which is highly regarded by clinicians.

Table 5. Total Laboratory Automation (TLA), Mean, Median and 90th Percentile Laboratory Turnaround Time (TAT), and Percentage of Outlier (OP) at 60 min and 120 min during the Study Period for STAT Tests

Test	Mean TAT (%95 CI)		Median TAT		90th percentile		OP 60 min		OP 120 min		p
	Pre-TLA	Post-TLA	Pre-TLA	Post-TLA	Pre-TLA	Post-TLA	Pre-TLA	Post-TLA	Pre-TLA	Post-TLA	
Glucose	37.6 (37.0–38.3)	34.3 (32.7–34.0)	34	30	50	49	5.4	5.2	0.5	0.7	<0.001[a]
Urea	34.9 (34.4–35.3)	32.5 (31.9–33.1)	34	28	47	46	4.7	2.1	0.6	0.6	<0.001[a]
Creatinine	34.5 (34.1–34.8)	32.5 (31.9–33.2)	33	28	46	46	4.7	1.7	0.4	0.1	<0.001[a]
ALT	35.3 (34.8–35.8)	31.6 (31.0–32.2)	34	27	47	45	4.4	2.3	0.6	0.1	<0.001[a]
AST	35.9 (35.4–36.2)	32.1 (31.5–32.7)	35	28	48	46	4.4	2.5	0.6	0.1	<0.001[a]
Total Bilirubin	35.5 (34.8–36.0)	32.3 (31.3–33.3)	35	28	48	46	4.8	2.2	0.7	0	<0.001[a]
Potasium	34.6 (34.0–34.8)	32.1 (31.5–32.7)	34	28	46	45	4.4	1.9	0.6	0	<0.001[b]
Lipaz	35.3 (34.6–36.0)	31.7 (30.7–32.7)	34	28	48	45	4.3	2.6	0.6	0	<0.001[a]
ALP	35.0 (34.2–35.7)	31.6 (29.6–31.7)	34	27	48	45	4.0	2.1	0.4	0	<0.001[a]
GGT	35.7 (34.9–36.7)	31.4 (30.1–32.6)	35	28	49	45	4.5	2.4	0.3	0	<0.001[a]
CRP	36.5 (35.8–37.0)	34.0 (33.3–34.7)	35	30	50	48	5.3	3.0	0.6	0.1	<0.001[a]
HCG	42.4 (40.7–43.5)	39.3 (36.9–41.8)	41	34	55	54	8.1	5.6	0	0	<0.001[a]
Troponin I/T	43.9 (43.3–44.5)	37.6 (36.6–37.9)	42	34	56	49	6.5	5.7	0.3	0.1	<0.001[a]
CK-MB	43.8 (43.2–44.4)	37.8 (36.7–38.1)	43	34	56	50	6.4	5.8	0.2	0	<0.001[a]

95% Confidence Interval (CI); [a]: Mann–Whitney U test, Pre-TLA compared with Post-TLA for non-normally distributed data; [b]: Independent t-test, Pre-TLA compared with Post-TLA for normally distributed data.

Secondary metrics including outlier rates, the proportion of tests meeting ED benchmarks, and percentile-based measures of TAT demonstrated consistent improvements post-TLA. Lam et al. [11], Chung et al. [12], Ellison et al. [14], Kim et al. [15], Osuna et al. [16], and Yıldız et al. [17] similarly report reductions in mean, 90th, 95th, and 99th percentile TAT, improvements in delayed-result frequency, and enhanced workflow predictability. These findings collectively indicate that TLA not only reduces median TAT but also stabilizes extreme delays and improves overall laboratory efficiency.

Although preanalytical TAT could theoretically influence total TAT, accessioning and barcode scanning were identical in both pre- and post-TLA periods; therefore, improvements are predominantly attributable to intralaboratory automation.

The present study has several limitations that should be considered. It is a single-center study with a pre/post design without randomization, which may limit generalizability. Unmeasured seasonal differences could influence TAT. The reliance on LIS time stamps introduces potential measurement bias, and no direct measurement of preanalytical error rates was performed. Economic evaluation was not conducted despite discussion of labor savings.

Conclusion

Overall, the implementation of TLA significantly enhanced efficiency, predictability, and workflow stability. Instrument configuration upgrades increased analytical capacity, which likely contributed indirectly to TAT improvements by enabling the laboratory to manage high sample volumes more effectively. Future studies should investigate the quantitative relationship between throughput and TAT reduction to fully elucidate the operational benefits of automation.

Disclosures

Ethics Committee Approval: The study was approved by the Zonguldak Bülent Ecevit University Ethics Committee (no: 2025/06, date: 19/03/2025).

Informed Consent: Informed consent was obtained from all participants.

Conflict of Interest Statement: The authors have no conflicts of interest to declare.

Funding: The authors declared that this study received no financial support.

Use of AI for Writing Assistance: No AI technologies utilized.

Authorship Contributions: Concept – M.C., B.G.; Design – M.C.; Supervision – M.C.; Funding – M.C., B.G.; Materials – M.C., B.G.; Data collection and/or processing – M.C.; Data analysis and/or interpretation – M.C., B.G.; Literature search – M.C.; Writing – M.C.; Critical review – M.C., B.G.

Peer-review: Externally peer-reviewed.

References

1. Nam Y, Park HD. Revolutionizing laboratory practices: Pioneering trends in total laboratory automation. Ann Lab Med 2025;45(5):472–83. [CrossRef]
2. Ialongo C, Porzio O, Giambini I, Bernardini S. Total automation for the core laboratory: Improving the turnaround time helps to reduce the volume of ordered STAT tests. J Lab Autom 2016;21(3):451–8. [CrossRef]
3. Armbruster DA, Overcrash DR, Reyes J. Clinical chemistry laboratory automation in the 21st century – amat victoria curam (victory loves careful preparation). Clin Biochem Rev 2014;35:143–53.
4. Angeletti S, De Cesaris M, Hart JG, Urbano M, Vitali MA, Fragliasso F, Dicuonzo G. Laboratory automation and intra-laboratory turnaround time: Experience at the university hospital campus Bio-Medico of Rome. J Lab Autom 2015;20(6):652–8. [CrossRef]
5. Lou AH, Elnenaei M, Sadek I, Thompson S, Crocker BD, Nassar B. Evaluation of the impact of a total automation system in a large core laboratory on turnaround time. Clin Biochem 2016;49:1254–8. [CrossRef]
6. Holland LL, Smith LL, Blick KE. Reducing laboratory turnaround time outliers can reduce emergency department patient length of stay: An 11-hospital study. Am J Clin Pathol 2005;124:672–4. [CrossRef]
7. Dolci A, Giavarina D, Pasqualetti S, Szőke D, Panteghini M. Total laboratory automation: Do stat tests still matter? Clin Biochem 2017;50(10–11):605–11. [CrossRef]
8. Breil B, Fritz F, Thiemann V, Dugas M. Mapping turnaround times (TAT) to a generic timeline: A systematic review of TAT definitions in clinical domains. BMC Med Inform Decis Mak 2011;11:34. [CrossRef]
9. Tornel PL, Ayuso E, Martinez P. Evaluation of the turnaround time of an integrated preanalytical and analytical automated modular system in a medium-sized laboratory. Clin Biochem 2005;38(6):548–51. [CrossRef]
10. O'Gara PT, Kushner FG, Ascheim DD, Casey DE Jr, Chung MK, de Lemos JA, et al. 2013 ACCF/AHA guideline for the management of ST-elevation myocardial infarction: A report of the American College of Cardiology Foundation/American Heart Association Task Force on Practice Guidelines. J Am Coll Cardiol 2013;61:e78–e140.
11. Lam C, Jacob E. Implementing a laboratory automation system: Experience of a large clinical laboratory. J Lab Autom 2012;17(1):16–23. [CrossRef]
12. Chung HJ, Song YK, Hwang SH, Lee DH, Sugiura T. Experimental fusion of different versions of the total laboratory automation system and improvement of laboratory turnaround time. J Clin Lab Anal 2018;32:e22400. [CrossRef]
13. Holland LL, Smith LL, Blick KE. Total laboratory automation can help eliminate the laboratory as a factor in emergency department length of stay. Am J Clin Pathol 2006;125(5):765–70. [CrossRef]
14. Ellison TL, Alharbi M, Alkaf M, Elimam S, Alfaries M, Nounou RA, et al. Implementation of total laboratory automation at a tertiary care hospital in Saudi Arabia: Effect on turnaround time and cost efficiency. Ann Saudi Med 2018;38(5):352–7. [CrossRef]
15. Kim K, Lee SG, Kim TH, Lee SG. Economic evaluation of total laboratory automation in the clinical laboratory of a tertiary care hospital. Ann Lab Med 2022;42:89–95. [CrossRef]
16. García-Osuna Á, Guiñón Muñoz L, Costa Pallaruelo M, Mansilla Usero A, Cuevas Eduardo B, Llanos Ramos J, et al. Characterization of add-on testing before and after automation at a core laboratory. Heliyon 2023;9(11):e22096. [CrossRef]
17. Yıldız R, Ulman C. Corrective steps in a total laboratory automation: Experience of a university laboratory. Turk Klin Biyokim Derg 2023;21(3):134–44. [CrossRef]

INTERNATIONAL JOURNAL OF
MEDICAL BIOCHEMISTRY

DOI: 10.14744/ijmb.2025.53325
Int J Med Biochem 2026;9(1):9–15

Research Article

Examination of NRF2, Heme Oxygenase, and neopterin levels in brucellosis

Nihayet Bayraktar[1], Busra Ozturk[1], Mehmet Celik[2], Mehmet Resat Ceylan[2], Mehmet Bayraktar[3]

[1]Department of Medical Biochemistry, Harran University Faculty of Medicine, Sanliurfa, Türkiye
[2]Department of İnfection Diseases, Harran University Faculty of Medicine, Sanliurfa, Türkiye
[3]Department of Medical Microbiology, Harran University Faculty of Medicine, Sanliurfa, Türkiye

Abstract

Objectives: *Brucella* species are highly infectious organisms that can gain access to the human body through various routes, including the gastrointestinal and respiratory tracts, conjunctiva, and eroded skin. In some cases, they may also enter the bloodstream directly, as in transfusion-related cases or via transplacental transmission. The aim of this study was to evaluate the potential role of serum anti-inflammatory and antioxidant factors such as nuclear factor erythropoietin-2 (NRF2), heme oxygenase (HO-1), and neopterin in brucellosis and to investigate their relationship with serologic anti-*Brucella* antibody findings.

Methods: A total of 90 patients with brucellosis and 30 healthy control individuals were included in the study. The patient group was divided into three subgroups according to antibody titers: 30 patients with a 1/160 titer, 30 patients with a 1/320 titer, and 30 patients with a 1/640 titer. Blood samples were collected and transferred into biochemistry tubes containing gel. The tubes were then centrifuged at 4000 rpm for 10 minutes to separate the serum. The separated serum samples were stored at -80°C. Serum levels of NRF2, HO-1, and neopterin were measured using the ELISA method.

Results: No significant differences in biomarker levels were observed between gender or age groups. However, biomarker levels varied significantly according to antibody titer. Healthy controls exhibited the lowest levels of NRF2, HO-1, and neopterin, whereas the 1/640 titer group exhibited the highest levels. NRF2, HO-1, and neopterin levels increased progressively with rising anti-*Brucella* antibody titers ($p<0.01$).

Conclusion: NRF2, HO-1, and neopterin levels were positively correlated with antibody titers, suggesting that these biomarkers may play a role in the immune response to brucellosis. Further studies with larger patient groups are needed to better understand and confirm these findings.

Keywords: Brucellosis, heme oxygenase, neopterin, NRF2

How to cite this article: Bayraktar N, Ozturk B, Celik M, Ceylan MR, Bayraktar M. Examination of NRF2, Heme Oxygenase, and neopterin levels in brucellosis. Int J Med Biochem 2026;9(1):9–15.

Brucellosis is a globally widespread infectious disease in both animals and humans and is considered a debilitating zoonotic disease. It can occur in men and women of all ages, most commonly in the 15–35 age group. The disease also has synonyms such as "Mediterranean fever" or "Malta fever" [1, 2]. Routes of infection include the gastrointestinal tract, respiratory tract, conjunctiva, and abraded skin [3]. When risk groups are examined, priority is given to those who earn their living from livestock farming, slaughterhouse workers, veterinarians, and veterinary research laboratory workers [4, 5]. Nrf2 is a cellular sensor of oxidative and electrophilic stress. Nrf2 is a nuclear factor that controls the expression and coordinated induction of a group of genes encoding detoxifying enzymes, drug transporters, anti-apoptotic proteins, and proteasomes. Modulation of NRF2 protein and enzymes occurs in response to oxidative stress and infection. In the presence of inflammation or oxidative stress, NRF2 undergoes phosphorylation and nuclear translocation, which leads to the transcription of proteins and antioxidant enzymes [6].

Address for correspondence: Mehmet Bayraktar, MD. Department of Medical Microbiology, Harran University Faculty of Medicine, Sanliurfa, Türkiye
Phone: +90 507 634 35 99 **E-mail:** mrtmehmet@yahoo.com **ORCID:** 0000-0003-2306-6531

Submitted: September 29, 2025 **Revised:** December 13, 2025 **Accepted:** December 14, 2025 **Available Online:** February 18, 2026

When Nrf2 is activated in the nucleus, it stimulates and initiates the production of antioxidant enzymes such as catalase, glutathione, and superoxide dismutase. Antioxidant enzymes neutralize up to one million free radicals per second [7]. Nrf2 is activated to correct the body's oxidative stress state, ensure cell survival, and maintain the redox homeostasis of cells by regulating the induced expression of phase II detoxifying enzymes and antioxidant enzymes [8]. The Nrf2 protein is expressed in different tissues of the body (such as the liver, kidney, spleen, and heart). Phosphorylated Nrf2 forms a heterodimer with the Maf protein and is then associated with antioxidant response elements that activate HO-1 expression [9]. HO-1 catabolizes free heme into Fe^{2+}, carbon monoxide (CO), and biliverdin. Heme catabolism by HO-1 produces biliverdin, which can be converted to bilirubin by biliverdin reductase. Heme catabolism by HO-1 also produces CO, a gas transmitter that regulates cellular signaling [10]. The stress-sensitive HO-1 isoenzyme provides protection against programmed cell death. This cytoprotective effect inhibits the pathogenesis of various immune-mediated inflammatory diseases. HO-1 expression is often induced in response to oxidative stress [11]. Heme oxygenase is the rate-limiting enzyme in heme metabolism, and its function is essential to limit oxidative tissue damage in both acute and chronic hemolytic injuries [12]. It has implications in many diseases, particularly cancer, Alzheimer's disease, and infections [13].

Neopterin and its unoxidized form, 7,8-dihydroneopterin, are relatively sensitive inflammatory markers because they are produced at sites of inflammation. It is an antioxidant synthesized by monocytes/macrophages that is produced upon interferon-gamma stimulation. 7,8-dihydroneopterin rapidly scavenges superoxide and hypochlorite, products of the inflammatory response, to form highly fluorescent neopterin [14]. These factors maintain the dual balance of 7,8-dihydroneopterin and neopterin to measure inflammation and oxidative stress [15]. Neopterin is a frequently used clinical marker to indicate immune activation during inflammation in various conditions and stresses [16]. We conducted this study to find out biochemical abnormalities of certain parameters (HO-1, NRF2, and neopterin) in patients with brucellosis and their correlation with *Brucella* Wright agglutination results.

Materials and Methods

This study consisted of brucellosis patients who applied to the Harran University Faculty of Medicine Infectious Diseases Polyclinic. This study was approved by the Harran University Faculty of Medicine Clinical Research Ethics Committee on 18.10.2021, in the 1st session, with decision number HRU/21.18.16. Our study was designed in accordance with the criteria specified in the Declaration of Helsinki. Accordingly, written informed consent was obtained from each subject. The patients were composed of a total of 120 individuals from four groups: 1/160 titer group, 1/320 titer group, 1/640 titer group, and healthy control group without brucellosis.

Preparation of samples: This study consisted of brucellosis patients who did not receive any antimicrobial therapy and presented to the Infectious Diseases Outpatient Clinic of Harran University Faculty of Medicine. A total of 90 patient groups were formed; 1/160 titer groups, 1/320 titer groups, and 1/640 titer groups were composed; 20 were female and 10 were male in each group. The mean age of the 1/160 titer group was (45.20±18.24) years; the mean age of the 1/320 titer group was (40.17±14.95) years; and the mean age of the 1/640 titer group was (42.80±17.16) years; and the mean age of each group was similar. In this study, a healthy control group was recruited from Harran University staff. Thirty healthy individuals, 18 females and 12 males, with a mean age of 40.70±13.91 years were included in the study. The study included 30 volunteers aged 40.70±13.91 years without any disease history or pathology. They were collected from the staff of Harran University, and those with a BMI below 28 were selected (Fig. 1).

Blood samples were collected as patient and control samples. The collected blood was transferred to gel-containing

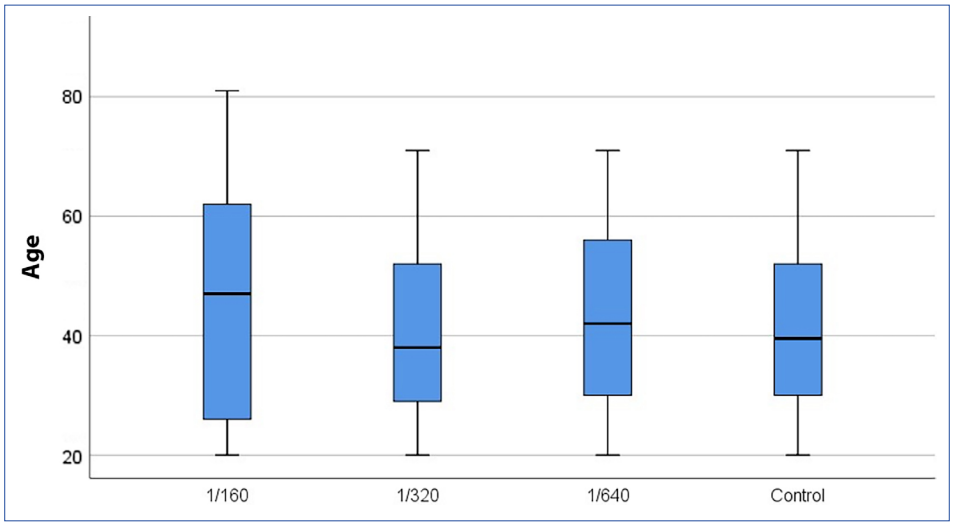

Figure 1. Age levels of the study groups (years; means +/- standart deviation).

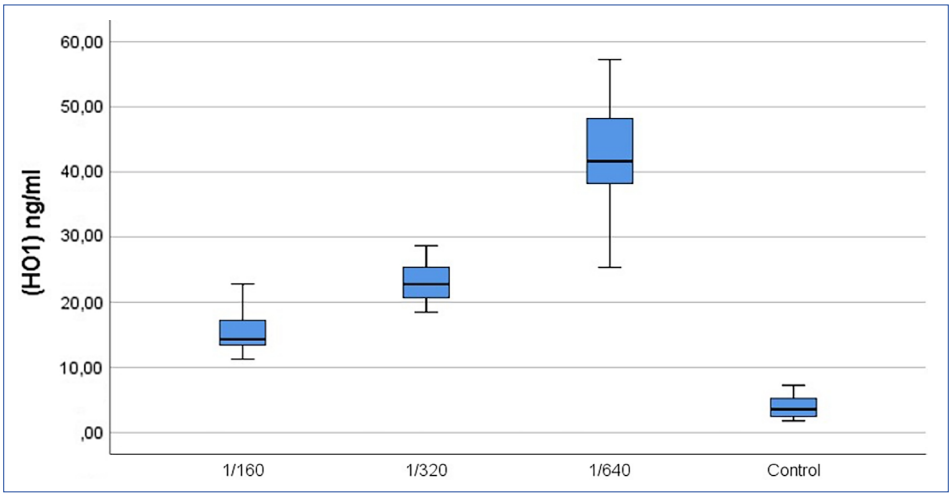

Figure 2. Heme Oxygenase-1 Levels in the study groups (means +/- standart deviation).

(biochemistry) tubes. Then, the blood was centrifuged at 4000 rpm for 15 minutes to separate the serum. The sera were stored in a deep freezer at –80°C for use. The separated sera were studied with the kit branded NRF2 ELISA Kit, Bioassay Technology Laboratory (BT Lab) (Catalog No: E3244Hu), Sensitivity: 0.11 ng/mL, CV (%) = SD/mean × 100; Intra-assay: CV<8%; Inter-assay: CV<10%; Human Heme Oxygenase-1 ELISA Kit (HO-1), Bioassay Technology Laboratory (BT Lab) (Catalog No: E0932Hu), Sensitivity: 0.05 ng/mL; CV (%) = SD/mean × 100; Intra-assay: CV<8%; Inter-assay: CV<10%; and Human Neopterin ELISA Kit, Bioassay Technology Laboratory (BT Lab) (Catalog No: E3155Hu), Sensitivity: 0.061 mmol/L; CV (%) = SD/mean × 100; Intra-assay: CV<8%; Inter-assay: CV<10% (Fig. 2).

Statistical analysis

Statistical analyses were performed using the SPSS version 23.0 program. The conformity of variables to normal distribution was examined using histogram graphics and the Kolmogorov–Smirnov/Shapiro–Wilk test. Mean, standard deviation, and median values were used when presenting descriptive analyses. The Kruskal–Wallis test was used to evaluate variables that did not show a normal distribution (nonparametric) among more than two groups. The Bonferroni multiple comparison test was used to investigate the source of significant differences among the studied groups. Frequency and percentage values were used when presenting categorical variables, and the analysis of categorical variables was performed using the chi-square (exact) test. The Spearman correlation test was used to evaluate the relationships between quantitative variables. Cases in which the p-value was below 0.05 were considered statistically significant.

Results

The study included a total of 120 patients, with a mean age of 42.22±16.08 years. Of the participants, 65% were female. The mean measurements were 21.10±14.70 ng/mL for HMOX1, 64.32±31.13 ng/mL for NRF2, and 10.73±6.43 nmol/L for neopterin. The individuals were classified into four groups (1/160, 1/320, 1/640, and healthy control), each comprising 25% of the total participants (Table 1).

A total of 120 participants were included in the study. Participants were divided into four groups (1/160, 1/320, 1/640, and Healthy Control). Mean measurements for HMOX1, NRF2, and neopterin were shown for the participants (Table 1).

NRF2 levels were significantly lower in the control group compared to the other groups. Furthermore, levels in the 1/320 group were statistically significantly lower than those in the 1/160 and 1/640 groups, and neopterin levels in the 1/160 group showed a statistically significant difference compared to the 1/320 and 1/640 groups (p<0.05; Table 1; Fig. 3).

Table 1. Comparison of clinical measurement values among study groups

	1/160		1/320		1/640		Control		p
	Mean±SD	Median	Mean±SD	Median	Mean±SD	Median	Mean±SD	Median	
Age	45.20±18.24	47.00	40.17±14.95	38.00	42.80±17.16	42.00	40.70±13.91	39.50	0.706
HO-1 (ng/mL)	15.27±2.52	14.31[a]	23.14±2.81	22.77[b]	42.01±8.65	41.65[c]	3.96±1.55	3.55[d]	<0.001
NRF2 (ng/mL)	72.74±35.99	90.74[a]	73.85±5.66	71.86[b]	87.48±11.27	90.79[a]	23.20±7.22	23.23[c]	<0.001
Neopterin (nmol/L)	9.03±1.65	8.76[a]	14.66±2.00	14.88[b]	17.60±2.94	17.95[b]	1.61±0.70	1.66[c]	<0.001

[b,c,d]: Kruskal Wallis Test, Chi-Square Test, Bonferroni Method. The study did not identify a significant correlation between group and gender. Furthermore, there were no significant age differences among the groups. (Fig.1). SD: Standard deviation.

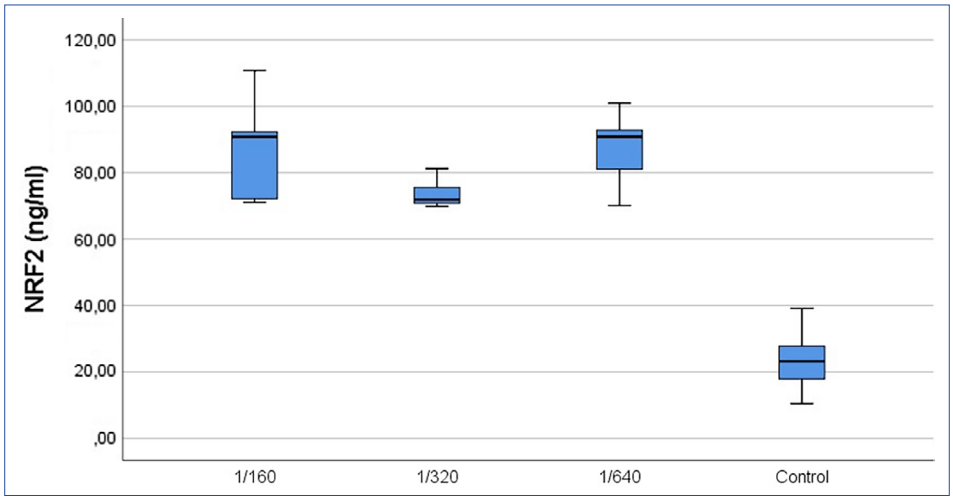

Figure 3. NRF2 levels in the study groups (means +/- standart deviation).

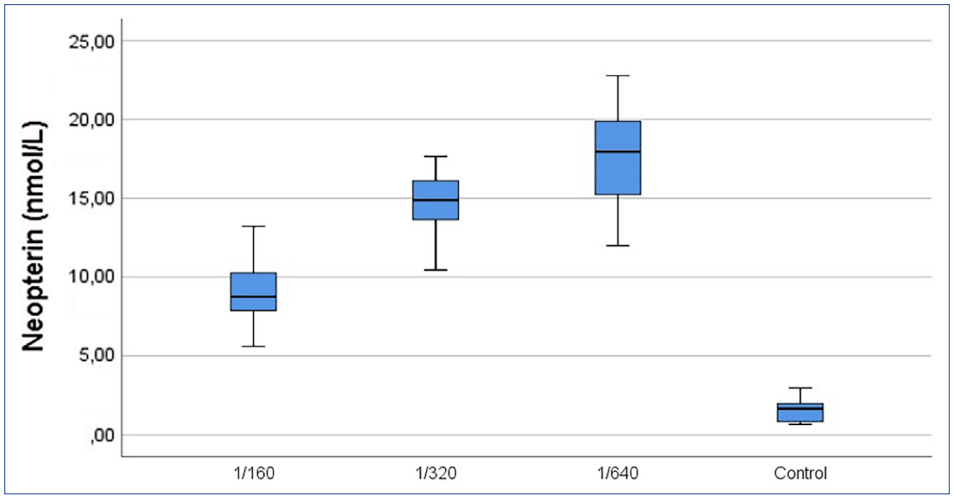

Figure 4. Neopterin Levels in the study groups (means +/- standart deviation).

Neopterin measurement levels were ranked from lowest to highest as follows: Control, 1/160, 1/320, and 1/640 (Fig 4; Table 2). Relationships between variables were examined within each group. As a result of the study, a moderate, negative, and significant correlation was found between HO-1 (ng/mL) and NRF2 (ng/mL) in the 1/160 titer group ($r=-0.407$; $p<0.05$). In addition, a low, positive, and significant correlation was found between HO-1 (ng/mL) and neopterin (nmol/L) measurements in the control group ($r=0.368$; $p<0.05$) (Table 2).

Discussion

The most important feature of *Brucella* is its ability to survive and multiply in both phagocytic and non-phagocytic cells [17]. While the findings of this study provide important information, some diagnostic limitations exist. The inability to confirm the diagnosis of brucellosis with PCR or culture, and the inadequacy of serological tests alone, reduced diagnostic certainty and limited the interpretability of the results. Activation of antioxidant response elements is primarily achieved through the modulation of proteins and enzymes that combat inflammation and oxidative stress. NRF2 is typically degraded via the ubiquitin–proteasome pathway [18]. When the body is exposed to inflammation or oxidative stress, NRF2 is phosphorylated and transported to the nucleus, contributing to the body's antioxidant mechanisms and leading to the transcription of proteins and antioxidant enzymes. These compounds can be regulated to provide protection against oxidative stress [19].

The autonomic nervous system helps restore homeostasis through inflammation and oxidative stress, triggering synapses as a secondary effect. Ngo et al. [20] suggested that NRF2 is a well-known regulator of oxidative stress and that lovastatin (UEI) provides protection against acute viral myocarditis through NRF2 activation; NRF2 can be activated by immune and inflammatory processes. Although there is a lack of correlation between *Brucella* antibody titers and the clinical picture of brucellosis [21], to our knowledge, there is no clinical study in the literature that directly measures the relationship between NRF2/HO-1 and neopterin levels with serological titers (e.g., 1/160 and above) in brucellosis [21]. Significant

Table 2. Correlation of clinical measurements within the groups

(HMOX1) ng/mL	NRF2 (ng/mL)		Neopterin (nmol/L)
(HO-1) ng/mL	1.000	-0.407*	0.092
	.	0.026	0.640
NRF2 (ng/mL)	-0.311	1.000	-0.031
	0.108	.	0.875
Neopterin (nmol/L)	0.092	-0.031	1.000
	0.640	0.875	.
(HO-1) ng/mL	1.000	0.092	-0.027
	.	0.628	0.888
NRF2 (ng/mL)	0.092	1.000	0.192
	0.628	.	0.310
Neopterin (nmol/L)	-0.027	0.192	1.000
	0.888	0.310	.
(HO-1) ng/mL	1.000	-0.058	-0.126
	.	0.765	0.514
NRF2 (ng/mL)	-0.058	1.000	0.160
	0.765	.	0.408
Neopterin (nmol/L)	-0.126	0.160	1.000
	0.514	0.408	.
(HO-1) ng/mL	1.000	0.028	0.368*
	.	0.884	0.046
NRF2 (ng/mL)	0.028	1.000	0.003
	0.884	.	0.986
Neopterin (nmol/L)	0.368*	0.003	1.000
	0.046	0.986	.

changes were observed in NRF2, NO, and neopterin levels in brucellosis patients at different antibody titers (1/160, 1/320, and 1/640) ($p<0.05$; Table 1; Fig. 3). NRF2/HO-1, on the other hand, is involved in the cellular oxidative stress response and the anti-inflammatory response of tissues. There is a clear relationship between increased NRF2 levels and an increased immune response [22]. Our study showed a positive correlation between increased immune response and increased NRF2 levels (Table 1). Activation of the NRF2 signaling pathway can prevent oxidation by reducing the production of free radicals and decreasing oxidative damage in the myocardium [23]. According to some research findings, NRF2 has been shown to reduce cell damage and oxidative stress and to exhibit an anti-inflammatory function that suppresses tumor formation [24].

Neopterin is a biochemical marker associated with cell-mediated immunity. Serum neopterin levels indicate the activation phase of the cellular immune system, which is important in the pathogenesis and progression of various diseases, and elevated neopterin levels have been detected before the onset of clinical symptoms [25]. Skogmar et al. [26] conducted a study on serum neopterin concentrations before, during, and after antituberculosis treatment in patients with tuberculosis. Michalak et al. [27] showed that urinary neopterin levels were significantly higher in patients with active tuberculosis compared to latently infected individuals. Chauvin et al. [28] demonstrated that high neopterin levels were a strong independent predictor of cardiovascular events. Thomas et al. [29] measured neopterin levels in a small cohort of 20 influenza patients and found that 80% of the patients had levels above the upper limit of normal at symptom onset (within 48 hours). Furthermore, a rapid decrease in neopterin levels was observed during recovery between days 5 and 14, with levels returning to normal after day 14. In our study, neopterin levels showed a statistically significant difference between brucellosis patients (1/160, 1/320, and 1/640) and healthy controls ($p<0.05$; Table 1; Fig. 4). These results suggest that neopterin, a biomarker of immune activation, has an anti-inflammatory effect and can provide insight into disease severity and the healing process as an indicator of immune response [30]. The studies mentioned above show that neopterin reduces oxidative stress in various diseases. Neopterin levels can therefore be used to assess disease activity and response to treatment.

HO-1 is considered a primary protein and cytoprotective mechanism involved in diseases caused by oxidative and inflammatory damage. It acts as a catalyst for reactions involving heme, pro-oxidants, and free radicals with an iron atom at the center and has been shown to have antitumor effects [31]. Due to its antioxidant and genome-protective activities, HO-1 may have protective effects against carcinogens and reduce the likelihood of tumor formation [32]. One study investigated the beneficial effects of reducing microglial HO-1 in aged mice exposed to an inflammatory challenge and identified reduced iron accumulation in the brain as a key mechanism. This finding suggests that HO-1 induction is beneficial due to its antioxidant and anti-inflammatory properties [33]. Another study evaluated the role of HMOX1 in *Brucella* infection and demonstrated that it induces HO-1 expression in macrophages. When HO-1 is deactivated or its activity is inhibited, the intracellular growth of *Brucella* is significantly reduced [34, 35]. In our study, statistically significant differences were observed in HO-1 levels in the serum of brucellosis patients at titers of 1/160, 1/320, and 1/640 compared with healthy controls ($p<0.05$; Table 1). Based on the relationship between titers and antigen–antibody levels, higher heme oxygenase levels were found in the 1/640 titer group compared to the other groups. These results were thought to be related to oxidative and inflammatory factors. Ojeda et al. [11] showed that HO-1 activation is reduced in brucellosis patients and that enzyme levels are related to disease severity.

Limitations

The limitation of our study is that the diagnosis of brucellosis was made according to clinical and serological findings, and confirmatory culture positivity and PCR tests were not performed. However, further studies may be conducted in the future that could contribute to the diagnosis and treatment of the disease. Another limitation is the small number of patients. Increasing the number of patients and control groups to improve the reliability of the study could eliminate this limitation and yield more reliable data.

Conclusion

Antibody titers are one of the measures of the systemic humoral immune response to brucellosis. NRF2/HO-1 and neopterin levels increase with increasing antibody titers. These biomarkers are related to cellular oxidative stress and the anti-inflammatory responses of tissues. They indicate an immune response system that reduces oxidative stress and exhibits anti-inflammatory effects against brucellosis and may serve as potential biomarkers for clinical brucellosis outcomes instead of antibody titers.

Disclosures

Ethics Committee Approval: The study was approved by the Harran University Faculty of Medicine Clinical Ethics Committee (no: HRU/21.18.16, date: 18/10/2021).

Informed Consent: Informed consent was obtained from all participants.

Conflict of Interest Statement: The authors have no conflicts of interest to declare.

Funding: This research received Harran University BAP Project Funding. Project number was 21286 supported by Harran University BAP.

Use of AI for Writing Assistance: No AI technologies utilized.

Authorship Contributions: Concept – N.B., M.C., M.R.C., M.B.; Design – N.B., B.O.; Supervision – N.B.; Materials – N.B., M.C., M.R.C., M.B.; Data collection and/or processing – N.B., B.O.; Data analysis and/or interpretation –N.B., B.O., M.B.; Literature search – N.B., M.C., M.R.C., M.B.; Writing – N.B., B.O.; Critical review – M.B.

Peer-review: Externally peer-reviewed.

References

1. Zhang N, Zhou H, Huang DS, Guan P. Brucellosis awareness and knowledge in communities worldwide: A systematic review and meta-analysis of 79 observational studies. PLoS Negl Trop Dis 2019;13:e0007366. [Crossref]
2. Ghssein G, Ezzeddine Z, Tokajian S, Khoury CA, Kobeissy H, Ibrahim JN, et al. Brucellosis: Bacteriology, pathogenesis, epidemiology and role of the metallophores in virulence: a review. Front Cell Infect Microbiol 2025;15:1621230. [Crossref]
3. Yagupsky P, Morata P, Colmenero JD. Laboratory Diagnosis of human brucellosis. Clin Microbiol Rev 2019;33:e00073–19. [Crossref]
4. An CH, Liu ZG, Nie SM, Sun YX, Fan SP, Luo BY, et al. Changes in the epidemiological characteristics of human brucellosis in Shaanxi Province from 2008 to 2020. Sci Rep 2021;11:17367. [Crossref]
5. Rezaei Shahrabi A, Moradkasani S, Goodarzi F, Beig M, Sholeh M. Prevalence of Brucella melitensis and Brucella abortus tetracyclines resistance: A systematic review and meta-analysis. Microb Pathog 2023;183:106321. [Crossref]
6. Banerjee N, Wang H, Wang G, Khan MF. Enhancing the Nrf2 antioxidant signaling provides protection against trichloroethene-mediated inflammation and autoimmune response. Toxicol Sci. 2020;175:64–74. [Crossref]
7. Saha S, Buttari B, Panieri E, Profumo E, Saso L. An overview of Nrf2 signaling pathway and its role in inflammation. Molecules 2020;25:5474. [Crossref]
8. Wang L, Zhang X, Xiong X, Zhu H, Chen R, Zhang S, et al. Nrf2 regulates oxidative stress and its role in cerebral ischemic stroke. Antioxidants (Basel) 2022;11:2377. [Crossref]
9. Jiang Y, Duan LJ, Pi J, Le YZ, Fong GH. Dependence of retinal pigment epithelium integrity on the nrf2-heme oxygenase-1 axis. Invest Ophthalmol Vis Sci 2022;63:30. [Crossref]
10. Luu Hoang KN, Anstee JE, Arnold JN. The Diverse Roles of Heme Oxygenase-1 in Tumor Progression. Front Immunol 2021;12:658315. [Crossref]
11. Ojeda JF, Martinson DA, Menscher EA, Roop RM. The bhuQ gene encodes a heme oxygenase that contributes to the ability of Brucella abortus 2308 to use heme as an iron source and is regulated by Irr. J Bacteriol 2012;194:4052–8. [Crossref]
12. Kochert BA, Fleischhacker AS, Wales TE, Becker DF, Engen JR, Ragsdale SW. Dynamic and structural differences between heme oxygenase-1 and -2 are due to differences in their C-terminal regions. J Biol Chem 2019 17;294:8259–72. [Crossref]
13. Fernández-Fierro A, Funes SC, Rios M, Covián C, González J, Kalergis AM. Immune modulation by inhibitors of the HO system. Int J Mol Sci 2020;22:294. [Crossref]
14. Gieseg SP, Baxter-Parker G, Lindsay A. Neopterin, inflammation, and oxidative stress: what could we be missing? Antioxidants (Basel) 2018;7:80. [Crossref]
15. Heneberk O, Wurfelova E, Radochova V. Neopterin, the cell-mediated immune response biomarker, in inflammatory periodontal diseases: a narrative review of a more than fifty years old biomarker. Biomedicines 2023;11:1294. [Crossref]
16. Tezcan D, Onmaz DE, Sivrikaya A, Hakbilen S, Körez MK, Gülcemal S, et al. Assessment of serum neopterin and calprotectin as biomarkers for subclinical inflammation in patients with familial Mediterranean fever. Ir J Med Sci 2023;192:2015–22. [Crossref]
17. Qureshi KA, Parvez A, Fahmy NA, Abdel Hady BH, Kumar S, Ganguly A, et al. Brucellosis: epidemiology, pathogenesis, diagnosis and treatment-a comprehensive review. Ann Med 2023;55:2295398. [Crossref]
18. Shao Y, Sun L, Yang G, Wang W, Liu X, Du T, et al. Icariin protects vertebral endplate chondrocytes against apoptosis and degeneration via activating Nrf-2/HO-1 pathway. Front Pharmacol 2022;13:937502. [Crossref]
19. Zhang X, Li H, Chen L, Wu Y, Li Y. NRF2 in age-related musculoskeletal diseases: Role and treatment prospects. Genes Dis 2023;11:101180. [Crossref]
20. Ngo V, Duennwald ML. Nrf2 and Oxidative Stress: A General Overview of Mechanisms and Implications in Human Disease. Antioxidants (Basel) 2022;11:2345. [Crossref]
21. Alsubaie SA, Turkistani SA, Zeaiter AA, Thabit AK. Lack of correlation of Brucella antibody titers with clinical outcomes and culture positivity of brucellosis. Trop Dis Travel Med Vaccines. 2021;7:5. [Crossref]
22. Hammad M, Raftari M, Cesário R, Salma R, Godoy P, Emami SN, et al. Roles of oxidative stress and Nrf2 signaling in pathogenic and non-pathogenic cells: A possible general mechanism of resistance to therapy. Antioxidants (Basel) 2023;12:1371. [Crossref]

23. Kim MJ, Jeon JH. Recent advances in understanding Nrf2 agonism and its potential clinical application to metabolic and inflammatory diseases. Int J Mol Sci 2022;23:2846. [Crossref]
24. Zhou J, Zheng Q, Chen Z. The Nrf2 pathway in liver diseases. Front Cell Dev Biol 2022;10:826204. [Crossref]
25. Eisenhut M. Neopterin in diagnosis and monitoring of infectious diseases. J Biomark 2013;2013:196432. [Crossref]
26. Skogmar S, Schön T, Balcha TT, Sturegård E, Jansson M, Björkman P. Plasma levels of neopterin and c-reactive protein (crp) in tuberculosis (tb) with and without hiv coinfection in relation to cd4 cell count. PLoS One. 2015;10:e0144292. [Crossref]
27. Michalak Ł, Bulska M, Strząbała K, Szcześniak P. Neopterin as a marker of cellular immunological response. Postepy Hig Med Dosw (Online). 2017;71:727–36. [Crossref]
28. Chauvin M, Larsen M, Quirant B, Quentric P, Dorgham K, Royer L, et al. Elevated neopterin levels predict fatal outcome in SARS-CoV-2-infected patients. Front Cell Infect Microbiol 2021;11:709893. [Crossref]
29. Thomas B, Bipath P, Viljoen M. Comparison between plasma neopterin and the urine neopterin:creatinine ratio as inflammatory biomarkers. Afr Health Sci 2019;19:2407–13. [Crossref]
30. Uysal HK, Sohrabi P, Habip Z, Saribas S, Kocazeybek E, Seyhan F, et al. Neopterin and soluble CD14 levels as indicators of immune activation in cases with indeterminate pattern and true positive hiv-1 infection. PLoS One. 2016;11:e0152258. [Crossref]
31. Chen S, Liu S, Zhao L, Lin H, Ma K, Shao Z. Heme oxygenase-1-mediated autophagy protects against oxidative damage in rat nucleus pulposus-derived mesenchymal stem cells. Oxid Med Cell Longev 2020;2020:9349762. [Crossref]
32. Tachibana M, Hashino M, Nishida T, Shimizu T, Watarai M. Protective role of heme oxygenase-1 in Listeria monocytogenes-induced abortion. PLoS One 2011;6:e25046. [Crossref]
33. Funes SC, Rios M, Fernández-Fierro A, Covián C, Bueno SM, Riedel CA, et al. Naturally derived heme-oxygenase 1 inducers and their therapeutic application to immune-mediated diseases. Front Immunol 2020;11:1467. [Crossref]
34. Chiang SK, Chen SE, Chang LC. The role of HO-1 and Its crosstalk with oxidative stress in cancer cell survival. Cells 2021;10:2401. [Crossref]
35. Hu H, Tian M, Yin Y, Zuo D, Guan X, Ding C, et al. Brucella induces heme oxygenase-1 expression to promote its infection. Transbound Emerg Dis 2022;69:2697–711. [Crossref]

INTERNATIONAL JOURNAL OF
MEDICAL BIOCHEMISTRY

DOI: 10.14744/ijmb.2025.61482
Int J Med Biochem 2026;9(1):16–21

Research Article

Examination of amino acid profile in patients with chronic renal failure

Nihayet Bayraktar[1], Amer Alkadrou[1], Leyla Cimen[2], Idris Kirhan[3], Mehmet Bayraktar[4]

[1]Department of Medical Biochemistry, Harran University Faculty of Medicine, Sanliurfa, Türkiye
[2]Department of Medical Biochemistry, Gaziantep Islam Science and Technology University Faculty of Medicine, Gaziantep, Türkiye
[3]Department of Department of Internal Medicine, Harran University Faculty of Medicine, Sanliurfa, Türkiye
[4]Department of Medical Microbiology, Harran University Faculty of Medicine, Sanliurfa, Türkiye

Abstract

Objectives: This study aims to analyze the plasma free amino acid profiles pre and post dialysis in patients with chronic kidney failure (CRF), and to evaluate their potential utility in diagnosis and treatment by comparing them with profiles from a healthy control group.

Methods: Plasma samples were collected from 46 healthy control and 46 patients diagnosed with CRF who applied to Şanlıurfa Harran University Medical Faculty Dialysis Department. Plasma free amino acid profiles were analyzed with LC-MS/MS.

Results: Mean values of alanine, arginine, aspartic acid, citrulline, histidine, methionine, tyrosine, hydroxyproline, glycine, leucine, isoleucine, lysine, ornithine, phenylalanine, proline, serine glutamic acid, glutamine, valine, taurine, alloisoleucine, alphaaminoadipic acid, anserine, gammaaminobutyric acid, 1- methylhistidine, 3-methylhistidine, 5-hydroxytryptophan levels in CRF patients exhibited higher levels compared to the control group. Phosphoethanolamine, cystine, alphaaminobutyric acid, betaaminoisobutyric acid and tryptophan were found to be lower in CRF patients than control group. When post-dialysis compared to pre-dialysis; there was an increase in citrulline, histidine, alanine, arginine, aspartic acid, glutamic acid, glycine, cystine, isoleucine, proline, phosphoethanolamine, taurine, alloisoleucin, alphaaminoadipic acid, ancerine, alphaaminobutyric acid, betaaminoisobutyric acid, beta alanin, 1-methylhistidine , 5-hydroxytryptophan levels; there was a decrease was observed in glutamine, leucine, lysine, ornithine, phenylalanine, serine, valine, asparagine, methionine, tryptophan, tyrosine, hydroxyproline, gammaaminobutyric acid, 3-methylhistidine levels. Citrulline, glycine, anserine, alphaaminobutyric acid, gammaaminobutyric acid, phosphoethanolamine and taurine levels were found to be significant in the Paired samples test, which was used to test the significance of the difference between the arithmetic means of the groups ($p<0.05$).

Conclusion: More studies were needed to understand the role of amino acids in CRF.

Keywords: Amino acid, chronic kidney disease, LC/MS, metabolic

How to cite this article: Bayraktar N, Alkadrou A, Cimen L, Kirhan I, Bayraktar M. Examination of amino acid profile in patients with chronic renal failure. Int J Med Biochem 2026;9(1):16–21.

Chronic kidney disease (CKD) refers to a group of diverse conditions that affect the anatomy and function of the kidneys, is particularly common in individuals with diabetes and hypertension and is a progressive condition associated with significant illness and death rates [1–4].

CKD is defined by persistent urinary abnormalities, structural changes in the kidneys, or a decline in excretory function, all of which indicate a progressive loss of functional nephrons. It is a worldwide health concern linked to considerable illness and death rates, primarily due to its strong link with cardiovascular

Address for correspondence: Leyla Cimen, Ph.D. Department of Medical Biochemistry, Gaziantep Islam Science and Technology University Faculty of Medicine, Gaziantep, Türkiye
Phone: +90 506 341 89 62 **E-mail:** cimenleyla@gmail.com **ORCID:** 0000-0002-4730-5595

Submitted: May 26, 2025 **Revised:** December 17, 2025 **Accepted:** December 18, 2025 **Available Online:** February 18, 2026

disease. A large group of CKD patients are more susceptible to cardiovascular complications and early fatality. As chronic kidney disease advances to end-stage renal disease, initiating renal replacement therapy becomes necessary. However, in many parts of the world, access to renal replacement therapy remains limited. Various risk factors play a role in both the initiation and progression of CKD. This includes having fewer nephrons at birth and the loss of nephrons due to aging, and exposure to nephrotoxic agents. Additionally, chronic conditions significantly lead to ongoing kidney damage. Effective management of CKD requires early detection, identification and treatment of the underlying cause, and careful attention to secondary mechanisms that perpetuate nephron loss. Primary treatment approaches involve tight regulation of blood pressure, suppression of the renin-angiotensin system, and targeted therapies designed to delay the progression of kidney dysfunction [5, 6].

Chronic renal failure (CRF) is characterized by a gradual and ongoing decline in kidney function, impairing fluid and solute regulation as well as metabolic and endocrine processes, due to reduced glomerular filtration rate (GFR). This condition usually occurs when GFR falls below 25 mL/min. When GFR is reduced by 75% of normal, the deterioration in kidney function continues even when the damage that caused it is removed [7].

Chronic kidney failure and dialysis treatment induce metabolic alterations that are not fully captured by routine biochemical parameters, but also involve changes in metabolic biomarkers and amino acid–related pathways [8].

The kidney's role in amino acid and protein metabolism, including the metabolic processes regulated by the kidney for dietary protein and the breakdown and secretion of protein metabolites, is important [9]. Amino acids are essential components that support life, growth, reproduction, development, and well-being in all organisms [10]. Measuring the levels of free amino acids present in bodily fluids and tissues provides nutritional insights that are valuable for diagnosing certain diseases, particularly those related to metabolic disorders. Particular irregularities in concentrations of amino acids have been linked to various diseases and conditions such as liver and kidney failure, cancer, diabetes, fatty liver, muscle dysfunction and protein malnutrition. The role of plasma free amino acids in disease risk assessment prediction has been seen as potential applications for monitoring nutrition [11].

The primary objective of this study was to assess and compare serum amino acid levels in patients diagnosed with chronic kidney failure before and after dialysis treatment. Additionally, the study aimed to investigate the potential impact of these amino acid levels on treatment strategies and clinical outcomes, thereby providing valuable insights into the role of amino acid metabolism in kidney disease management.

Materials and Methods

Experimental design

Ethical approval for this observational study was obtained from the Harran University Clinical Research Ethics Committee (No: 20, Date: 29/11/2021). Informed consent was obtained from all of the patients included in this study and the research was conducted according to the ethical principles the Declaration of Helsinki.

Plasma samples were collected from 46 patients diagnosed with chronic renal failure who presented to the Department of Nephrology and Dialysis Unit of Sanliurfa Harran University Faculty of Medicine Hospital, both before and after dialysis, between the years 2021 and 2022. We collected blood samples from patients with chronic kidney disease undergoing hemodialysis and those pre and post-dialysis. The type of dialysis we performed was hemodialysis (HD). The most common type of dialysis involves a dialyzer that filters waste, salt, and excess fluid from the blood. This was performed three times a week at the dialysis center of Harran University Hospital, and each visit lasted approximately four hours. A catheter was also used to create a vein in the patients. Blood is withdrawn from the body, filtered through the dialyzer, and returned. All patients underwent three four-hour hemodialysis sessions per week at the dialysis department of Harran University Hospital over a period of min 3 max 4 years. 21 of these patients were male and 25 were female. The total sample size was 46, and the mean age for both sexes was 35.4±15.6 years (Table 1). However, glomerulonephritis and polycystic kidney disease were found to be significant etiological factors for the disease. None of the patients receiving hemodialysis had diabetic nephropathy. Patients who had undergone kidney transplantation or peritoneal dialysis were excluded from the study. Baseline information, including age, sex, age at hemodialysis initiation, and cause of renal failure, was obtained from medical records at the study center. The urea reduction rate was used as an index of hemodialysis adequacy, and baseline information and other parameters were compared between the two groups to determine the effect of hemodialysis duration on these factors. Plasma samples from 46 healthy individuals were used as the control group. The healthy control group had a normal kidney function (serum creatinine and eGFR within reference ranges), no history of chronic or renal diseases, and not using medications affecting renal function. Amino acids were measured once for control group. Of the individuals in the control group, 26 were female and 20 were male, and the mean age was 33.4±12.6 years (Table 1). In the control group, creatinine and eGFR values were 0.72 (0.30) mg/dL and 105.4 (46.82) mL/min/1.73 m^2, respectively, reflecting normal kidney function (Table 1). In the patient group, creatinine and eGFR values were 7.15 (3.02) mg/dL and 7.05 (5.35) mL/min/1.73 m^2, respectively, representing end-stage chronic kidney disease patients undergoing hemodialysis (Table 1). There was no significant difference in age between the groups ($p=0.50$). However, the differences in creatinine and eGFR values were statistically significant ($p<0.001$). These findings indicate that the patient and control groups reflect the clinically expected profiles. Blood samples taken from the individuals were taken into EDTA tubes, centrifuged to obtain plasma, and stored at -80°C until analysis.

Table 1. Age, sex and clinical characteristics of the patient and control groups

Groups	Patient group (n=46)	Control group (n=46)	p
Age (year)	35.4±15.6	33.4±12.6	0.50
Creatinine (mg/dL)	7.15 (3.02)	0.72 (0.30)	<0.001
eGFR (mL/min/1.73 m^2)	7.05 (5.35)	105.4 (46.82)	<0.001
Sex, n (%)			
Female	25 (54.3)	26 (56.5)	0.84
Male	21 (45.7)	20 (43.5)	

An independent t-test was used for age, and the data were presented as mean±standard deviation (mean±SD). Mann–Whitney U test was used for creatinine and eGFR. Creatinine and eGFR values are presented as median (IQR, Interquartile Range). p-value for sex was determined by Chi-square (χ^2) test.

LC-MS/MS analysis

Analyses were conducted using a LC-MS/MS (Shimadzu 8045, Japan) device. For the patient group, two plasma samples (pre- and immediately after post-dialysis) were collected from each individual, resulting in a total of 92 samples. In the control group, a single sample was obtained from each subject, yielding a total of 46 samples. For amino acid studies, samples taken from -80ºC were kept until they reached room temperature. JASEM amino acid kit was used for analysis. The kit's working principle was followed for plasma samples from each patient. First, 50µl of patients' plasma was taken into numbered sterile Eppendorf tubes. 50µl of the Internal Standard solution in the amino acid kit was transferred to these tubes. Each tube was vortexed for 5 seconds. 700µl of the Reagent-1 solution in the kit was added to the vortexed tubes. The tubes were vortexed again for 15 seconds. The vortexed tubes were centrifuged at 3000 rpm for 5 minutes. The supernatant portion of the samples carefully taken from the centrifuge was transferred to HPLC vial tubes with the help of a sterile pipette. For analysis, vial tubes were placed in the tray compartment in the HPLC section of the LC-MS/MS device and read. Mobile Phase-A and Mobile Phase-B in the amino acid kit were used as mobile phase. Restek LC Columns were used as columns.

Statistical analysis

Kolmogorov-Smirnov and Shapiro-Wilk tests were applied to evaluate whether the data followed a normal distribution. Since the variables showed normal distribution, Independent Samples test was used to compare the average amino acid values of healthy individuals and patients before dialysis. Paired samples test was used to compare the amino acid values of patients before and after dialysis. Descriptive statistics for numerical variables were presented as mean ± standard deviation. Statistical analyses were performed using the SPSS software package (Windows version 24.0), with a $p<0.05$ considered statistically significant.

Results

The amino acid levels of the healthy group and the pre-dialysis and post-dialysis amino acid levels of patients diagnosed with chronic renal failure are given collectively in Table 2.

In patients with chronic renal failure, alanine, arginine, aspartic acid, citrulline, histidine, methionine, hydroxyproline, glycine, leucine, isoleucine, lysine, ornithine, phenylalanine, proline, serine, glutamic acid, glutamine, valine, taurine, alloisoleucine, gammaaminobutyric acid, 3-methylhistidine amino acid levels were found higher than in the control group ($p<0.05$). Tyrosine, alphaaminoadipic acid, anserine, 1-methylhistidine, 5-hydroxytryptophan amino acid levels were also found higher in patients with chronic renal failure compared to the control group, but this was not statistically significant. Phosphoethanolamine, cystine, alphaaminobutyric acid, betaaminoisobutyric acid and tryptophan amino acids were decreased in CRF patients relative to the control group ($p<0.05$).

After dialysis, compared to pre-dialysis, there were increases in citrulline, glycine, phosphoethanolamine, taurine, anserine and alphaaminobutyric acid amino acid levels ($p<0.05$). After dialysis, there were increases in alanine, arginine, aspartic acid, glutamic acid, cystine, isoleucine, proline, histidine, alloisoleucine, alphaaminoadipic acid, betaaminoisobutyric acid, beta alanine, 1-methylhistidine and 5-hydroxytryptophan amino acid levels compared to pre-dialysis, but this was not statistically significant. After dialysis, there were decreases in glutamine, leucine, lysine, ornithine, phenylalanine, serine, valine, asparagine, methionine, tryptophan, tyrosine, hydroxyproline, gammaaminobutyric acid and 3-methylhistidine amino acid levels compared to pre-dialysis.

Paired samples test was performed to evaluate the significance of the difference between the arithmetic means of the groups given in Table 2, and citrulline, glycine, anserine, alphaaminobutyric acid, gammaaminobutyric acid, phosphoethanolamine and taurine levels were found to be significant ($p<0.05$).

Discussion

The kidneys are fundamentally involved in protein metabolism, taking part in the synthesis, breakdown, filtration, reabsorption, and excretion of amino acids and peptides. They also contribute to several key metabolic pathways, including the conversion of phenylalanine to tyrosine, arginine metabolism, and transmethylation. In patients with chronic kidney disease, disruptions in these processes can occur due to metabolic acidosis, chronic inflammation, dietary restrictions and amino

Table 2. Amino acid levels of control, pre-dialysis and post-dialysis patients groups (µmol/L) (mean±SD)

Aminoacids	Control	Pre-dialysis	Post-dialysis	p (C-pre)	p (pre-post)
1-methylhistidine	1.30±0.37	1.35±2.06	5.81±12.10	0.927	0.128
3-methylhistidine	0.66±1.15	5.42±7.74	2.90±2.81	0.013*	0.107
5-hydroxytryptophan	0.04±0.09	0.40±0.89	0.82±1.25	0.087	0.146
Alanine	274.73±83.43	348.79±101.11	355.59±98.91	0.007*	0.802
Alloisoleucine	0.36±0.20	1.35±0.85	1.75±0.94	0.000*	0.197
Alphaaminoadipic acid	0.94±0.57	1.10±1.90	2.35±5.35	0.723	0.277
Alphaaminobutyric acid	13.32±6.12	0.38±0.16	0.82±0.87	0.000*	0.029**
Anserine	2.11±2.31	2.96±1.59	4.50±2.69	0.158	0.045**
Arginine	68.49±22.42	262.88±94.63	269.19±85.75	0.000*	0.817
Asparagine	43.93±11.42	61.09±43.31	40.03±25.48	0.098	0.073
Aspartic acid	10.49±10.83	156.45±38.16	172.78±75.13	0.000*	0.464
Beta alanine	3.04±1.05	2.22±1.34	3.63±5.59	0.019*	0.275
Betaaminoisobutyric acid	2.66±0.90	1.12±0.99	2.12±2.52	0.000*	0.137
Citrulline	19.04±7.21	31.74±10.99	40.26±13.67	0.000*	0.024**
Cystathionine	0.12±0.12	0.20±0.12	0.34±0.47	0.021*	0.189
Cystine	46.55±24.44	0.56±0.58	0.70±0.48	0.000*	0.416
Gammaaminobutyric acid	4.89±1.70	15.87±13.79	8.71±2.61	0.002*	0.042**
Glutamine	139.17±65.15	277.72±115.66	276.19±197.17	0.000*	0.975
Glutamic acid	78.31±47.00	400.64±126.12	409.59±157.74	0.000*	0.792
Glycine	198.01±50.47	337.48±50.64	404.20±75.75	0.000*	0.009**
Histidine	57.52±12.48	89.14±22.65	90.76±21.33	0.000*	0.828
Hydroxyproline	25.67±10.39	95.33±44.36	81.25±37.95	0.000*	0.289
Isoleucine	59.96±15.95	107.90±26.12	117.64±74.83	0.000*	0.590
Leucine	95.27±27.06	381.40±124.91	341.20±106.80	0.000*	0.251
Lysine	132.56±36.88	267.12±148.09	198.06±72.99	0.001*	0.054
Methionine	24.25±6.27	44.20±31.17	34.77±13.49	0.010*	0.246
Ornithine	67.51±22.88	148.12±107.29	141.74±89.76	0.003*	0.865
Phenylalanine	51.10±10.20	146.47±36.48	143.42±23.46	0.000*	0.783
Phosphoetanolamine	28.38±24.45	3.90±1.56	7.47±2.91	0.000*	0.000**
Proline	155.49±40.28	338.91±91.73	384.03±118.90	0.000*	0.146
Serine	130.52±31.19	246.53±62.05	233.32±55.63	0.000*	0.526
Taurine	78.29±37.28	193.30±18.46	227.04±23.25	0.000*	0.000**
Threonine	132.52±37.08	144.03±45.99	135.44±33.15	0.334	0.518
Tryptophan	56.44±14.93	42.11±16.15	38.26±13.82	0.002*	0.433
Tyrosine	68.62±16.83	76.36±31.81	72.44±20.71	0.268	0.638
Valine	174.70±47.57	236.04±63.30	227.09±58.11	0.000*	0.647

*: p<0.05, control group compared to pre-dialysis groups (C-pre); **: p<0.05, pre-dialysis group compared to post-dialysis groups (pre-post).

acid losses during dialysis. As a result, both the quantity and quality of protein intake become particularly important. While protein restriction is generally recommended for individuals not yet on dialysis, those undergoing dialysis typically require more protein to compensate for increased catabolism and losses through the treatment [12].

Nutritional status is closely tied to clinical outcomes in CKD. Although serum albumin is widely used as an indicator of nutritional health, plasma amino acid levels may offer additional insights. Previous studies have shown that amino acids such as glutamine, homocysteine, and glutamate are associated with nutritional status. For example, a study involving children with stage 4–5 CKD found significantly higher glutamine levels compared to healthy peers [13]. Similarly, our own findings revealed elevated plasma glutamine levels in patients with renal failure. Since the kidneys play a central role in glutamine metabolism, particularly in ammonia production for acid-base balance, these elevations may reflect impaired utilization in CKD. In support of our findings, Yardım et al. [8] demonstrated in their study that metabolic biomarker levels are altered in hemodialysis patients; this suggests that amino acid metabolism associated with diabetic and inflammatory processes may be affected in chronic kidney failure and during hemodialysis [8].

Branched-chain amino acids (BCAAs), including leucine and valine, are also considered markers of nutritional status. One study reported reduced levels of these amino acids in early-stage CKD patients compared to healthy controls [14]. In contrast, our findings showed higher concentrations of leucine and valine in CRF patients, which may be explained by decreased renal clearance, metabolic adaptations, or effects related to dialysis.

The impact of dialysis on BCAA levels is also noteworthy. Debnath et al. [15] observed a significant decrease in plasma BCAA concentrations following hemodialysis, and a negative correlation between post-dialysis BCAA levels and fatigue. In line with this, we found that leucine and valine levels declined after dialysis, while isoleucine levels remained stable. This may indicate selective removal of certain amino acids during treatment.

Aromatic amino acids such as phenylalanine, tyrosine, and tryptophan are known precursors of uremic toxins like p-cresol sulfate and indoxyl sulfate. An animal study by Barba et al. [16] showed that diets low in protein and aromatic amino acids reduced renal inflammation, fibrosis, and uremic toxin levels. These findings suggest that modifying amino acid intake may help slow CKD progression without worsening nutritional status.

It has also been reported that phenylalanine-to-tyrosine conversion is impaired in CKD, leading to elevated phenylalanine and potentially lower tyrosine levels [17]. Consistent with this, we observed increased phenylalanine levels in CRF patients. However, tyrosine concentrations remained similar between groups, which might reflect individual metabolic variability.

Tryptophan metabolism is also altered in CKD. A metabolomics-based study in the general population linked elevated levels of citrulline, kynurenine, and phenylalanine with CKD risk, and highlighted the kynurenine-to-tryptophan ratio as a relevant marker [18]. In agreement with these findings, our study showed lower tryptophan levels in CRF patients, both before and after dialysis, suggesting disrupted tryptophan metabolism.

As kidney function declines, changes in serum amino acid profiles become more evident. One study found that alanine, tyrosine, and valine levels decreased with renal dysfunction, whereas phenylalanine and citrulline increased [19]. Our data partially align with this, as we observed elevated levels of phenylalanine, citrulline, alanine, valine, and tyrosine. These discrepancies may stem from differences in patient populations, dietary habits, or treatment status.

In contrast to earlier reports that showed increased cystine levels in CKD [20], we found that cystine concentrations were lower in our patient group. This may be due to altered sulfur amino acid metabolism or increased utilization under oxidative stress, which is commonly observed in CKD.

Low-protein diets (LPDs) are often used to reduce the generation of uremic toxins. Ariyanopparut et al. [21] reported that combining LPDs with ketoanalog supplementation (LPD-KAs) delayed the progression of CKD and postponed the need for dialysis. Patients who adhered to higher doses of ketoanalogs saw more benefit, although no significant changes were seen in phosphate levels or albuminuria.

This study has several limitations that should be considered. First, the sample size was relatively small and the study was conducted at a single center, which may limit the generalizability of the findings. Dietary intake and nutritional status were not assessed, and inflammatory markers such as CRP and IL-6 were not measured, which could have provided additional context for amino acid changes. Adjustment for dialysis membrane type and dose was not performed, which may influence amino acid levels. Although dialysis adequacy was assessed using the urea reduction ratio (URR), individual URR values were not reported. This was considered acceptable because the study primarily focused on amino acid changes, and all patients met standard adequacy criteria, ensuring that dialysis efficiency was within acceptable ranges. Additionally, the study design involved single time-point sampling, which may not capture intra-individual variability. These limitations should be taken into account when interpreting the results and highlight areas for future research.

Conclusion

Chronic kidney disease has a high prevalence in the general population and is associated with increased mortality. Therefore, more reliable biomarkers are essential for accurate diagnosis, monitoring disease progression, and guiding treatment strategies. Plasma amino acid levels reflect metabolic alterations and correlate with renal function. In this study, we evaluated the changes in amino acid profiles in patients with renal failure before and after dialysis, comparing them to a healthy control group, with these results detailed in the findings section.

Once the diagnosis and underlying cause of CKD are established, amino acid analysis can provide critical insights into the metabolic disturbances associated with the disease. Detecting specific amino acid imbalances or deficiencies enables clinicians to customize nutritional interventions or supplementation, potentially improving patient outcomes and slowing disease progression.

However, a larger sample size is required to validate these findings. Current literature on the relationship between amino acid biomarkers and chronic renal failure remains limited, highlighting the need for further research in this area.

Disclosures

Ethics Committee Approval: The study was approved by the Harran University Clinical Research Ethics Committee (no: 20, date: 29/11/2021).

Informed Consent: Informed consent was obtained from all participants.

Conflict of Interest Statement: The authors have no conflicts of interest to declare.

Funding: The authors declared that this study has received no financial support.

Use of AI for Writing Assistance: No AI technologies utilized.

Authorship Contributions: Concept – N.B.; Design – N.B.; Supervision – N.B., M.B.; Funding – N.B.; Materials – N.B., A.A., I.K.; Data collection and/or processing – N.B., A.A., I.K., M.B.; Data analysis and/or interpretation – N.B., A.A., M.B., L.C.; Literature search – N.B., A.A., L.C.; Writing – N.B., A.A., L.C.; Critical review – N.B., M.B., L.C., I.K., A.A.

Peer-review: Externally peer-reviewed.

References

1. Levey AS, Coresh J. Chronic kidney disease. Lancet 2012;379(9811):165–80. [CrossRef]
2. Kalantar-Zadeh K, Jafar TH, Nitsch D, Neuen BL, Perkovic V. Chronic kidney disease. Lancet 2021;398(10302):786–802. [CrossRef]
3. Hui Y, Zhao J, Yu Z, Wang Y, Qin Y, Zhang Y, et al. The role of tryptophan metabolism in the occurrence and progression of acute and chronic kidney diseases. Mol Nutr Food Res 2023;67:2300218. [CrossRef]
4. Okyar G, Yılmaz DA, Yıldırım MS, Yıldız M. Central nervous system response to chronic kidney disease. KSU Med J 2022;17(3):198–209. [CrossRef]
5. Romagnani P, Remuzzi G, Glassock R, Levin A, Jager KJ, Tonelli M, et al. Chronic kidney disease. Nat Rev Dis Primers 2017;3:1–24. [CrossRef]
6. Kazancioğlu R. Risk factors for chronic kidney disease: An update. Kidney Int Suppl 2013;3(4):368–71. [CrossRef]
7. Tanrıverdi MH. Chronic kidney failure. Konuralp Med J 2010;2(2):27–32.
8. Yardım M, Deniz L, Saltabas MA, Kayalp D, Akkoc RF, Kuloglu T. Relationship between atherogenic index of plasma, asprosin, and metrnl levels in hemodialysis patients. Int J Med Biochem 2024;7(2):60–6. [CrossRef]
9. Ko GJ, Obi Y, Tortorici A, Kalantar-Zadeh K. Dietary protein intake and chronic kidney disease. Curr Opin Clin Nutr Metab Care 2017;20(1):77–85. [CrossRef]
10. Wu G, Wu Z, Dai Z, Yang Y, Wang W, Liu C, et al. Dietary requirements of "nutritionally non-essential amino acids" by animals and humans. Amino Acids 2013;44(4):1107–13. [CrossRef]
11. Nagao K, Kimura T. Use of plasma-free amino acids as biomarkers for detecting and predicting disease risk. Nutr Rev 2020;78(3):79–85. [CrossRef]
12. Yıldıran H, Gençer F. Kidney diseases and protein metabolism. J Nutr Diet 2018;46:7–12. [CrossRef]
13. Fadel FI, Elshamaa MF, Essam RG, Elghoroury EA, El-Saeed GSM, El-Toukhy SE, et al. Some amino acids levels: Glutamine, glutamate, and homocysteine, in plasma of children with chronic kidney disease. Int J Biomed Sci 2014;10(1):36–42. [CrossRef]
14. Kumar MA, Bitla ARR, Raju KVN, Manohar SM, Kumar VS, Narasimha SRPVL. Branched chain amino acid profile in early chronic kidney disease. Saudi J Kidney Dis Transpl 2012;23(6):1202–7.
15. Debnath S, Lorenzo C, Bansal S, Morales J, Rueda RO, Kasinath BS, et al. Branched-chain amino acids depletion during hemodialysis is associated with fatigue. Am J Nephrol 2020;51(7):565–71. [CrossRef]
16. Barba C, Benoit B, Bres E, Chanon S, Vieille-Marchiset A, Pinteur C, et al. A low aromatic amino acid diet improves renal function and prevent kidney fibrosis in mice with chronic kidney disease. Sci Rep 2021;11:19184. [CrossRef]
17. Kopple JD. Phenylalanine and tyrosine metabolism in chronic kidney failure. J Nutr 2007;137(6):1586S–90S. [CrossRef]
18. Lee H, Jang HB, Yoo MG, Park SI, Lee HJ. Amino acid metabolites associated with chronic kidney disease: An eight-year follow-up Korean epidemiology study. Biomedicines 2020;8(7):222. [CrossRef]
19. Li R, Dai J, Kang H. The construction of a panel of serum amino acids for the identification of early chronic kidney disease patients. J Clin Lab Anal 2018;32(3):e22282. [CrossRef]
20. Robins AJ, Milewczyk BK, Booth EM, Mallick NP. Plasma amino acid abnormalities in chronic renal failure. Clin Chim Acta 1972;42(1):215–7. [CrossRef]
21. Ariyanopparut S, Metta K, Avihingsanon Y, Eiam-Ong S, Kittiskulnam P. The role of a low protein diet supplemented with ketoanalogues on kidney progression in pre dialysis chronic kidney disease patients. Sci Rep 2023;13:15459. [CrossRef]

INTERNATIONAL JOURNAL OF
MEDICAL BIOCHEMISTRY

DOI: 10.14744/ijmb.2025.90958
Int J Med Biochem 2026;9(1):22–28

Research Article

Digital transformation in clinical biochemistry education: A comprehensive analysis through YouTube platform

Hakan Ayyildiz

Biochemistry Laboratory, Elazig Fethi Sekin City Hospital, Elazig, Türkiye

Abstract

Objectives: The proliferation of digital educational platforms has transformed medical education delivery, yet concerns regarding content quality persist. This study systematically evaluates clinical biochemistry educational content on YouTube and examines relationships between content characteristics and audience engagement.

Methods: A systematic YouTube search was conducted August 1–15, 2025, using standardized clinical biochemistry education terms. Videos were evaluated using a validated 10-point quality assessment framework encompassing scientific accuracy, educational structure, producer credibility, and technical accessibility. Statistical analyses included descriptive statistics, correlation analysis, and linear regression modeling.

Results: Of 152 identified videos, 69 met inclusion criteria (total views: 14,247,835; average of 206,491±167,420). Quality assessment revealed 65.2% (n=45) demonstrated high quality (8–10 points), 30.4% (n=21) moderate quality (5–7 points), and 4.4% (n=3) low quality (1–4 points). Pearson correlation identified robust positive association between quality scores and view counts ($r=0.782$, $p<0.001$), with quality accounting for 61.2% of viewership variance ($r^2=0.612$). Corporate training channels (34.8%) demonstrated highest mean viewership (n=247,825).

Conclusion: While YouTube is a valuable platform for clinical biochemistry education, quality standardization and accessibility improvements are needed. The analysis reveals the potential and diversity of digital educational tools in clinical biochemistry education.

Keywords: Biochemistry, biochemistry education, clinical chemistry, medical laboratory tests, laboratory

How to cite this article: Ayyildiz H. Digital transformation in clinical biochemistry education: A comprehensive analysis through YouTube platform. Int J Med Biochem 2026;9(1):22–28.

Clinical biochemistry is one of the cornerstones of modern medical diagnosis and treatment processes. Technological advances have transformed educational methodologies in this field and have established digital platforms as important educational resources [1]. Video-sharing platforms such as YouTube are emerged as educational tools of increasing importance for medical students and healthcare professionals [2, 3].

In recent years, the widespread adoption of distance education, influenced by the COVID-19 pandemic, has brought the quality and reliability of digital educational content to the forefront [4]. Particularly in fields such as clinical biochemistry, where accurate interpretation of laboratory results is vital, the quality standards of digital educational materials are crucial [5]. YouTube, with approximately 2.7 billion monthly active users, is the world's largest video-sharing platform and offers a rich source of medical education content [6]. The platform is also widely used by medical students, with approximately 9 out of every 10 medical students benefiting from it [7]. Additionally, 83% of healthcare organizations have official YouTube channels for sharing educational content [8]. However, there are concerns regarding quality control of user-generated content [9]. Therefore, videos to be used or considered for use in education should be selected in a controlled manner.

This study aims to: (1) systematically evaluate the quality of clinical biochemistry videos on YouTube, (2) examine the effects of technology integration in this field, and (3) analyze

Address for correspondence: Hakan Ayyildiz, MD. Biochemistry Laboratory, Elazig Fethi Sekin City Hospital, Elazig, Türkiye
Phone: +90 505 779 16 72 **E-mail:** hknayyildiz@hotmail.com **ORCID:** 0000-0002-3133-9862

Submitted: October 15, 2025 **Accepted:** December 18, 2025 **Available Online:** February 18, 2026

the accuracy of information shared on social media in the context of digital medical education.

Materials and Methods

Video selection and data collection

The systematic search was conducted on the YouTube platform between August 1–15, 2025. Videos were accessed using YouTube Data API v3 (API Endpoint: search.list method) with the following standardized search terms: " Biochemistry", "medical laboratory tests", " Medical Laboratory Personnel", " Automation, Laboratory", "lab results interpretation," and "biochemistry education." Order Parameter: relevance (default YouTube ranking), Type Filter: video, VideoDefinition: any (SD/HD), VideoDuration: any (no duration restriction), SafeSearch: none, MaxResults per query: 50 (API maximum), Language Filter: relevanceLanguage=en, PublishedAfter: 2015-08-15T00:00:00Z, PublishedBefore: 2025-08-15T23:59:59Z, Region Code: none (global search), Minimum View Count Filter: Applied post-retrieval (≥100 views).

Search parameters

- **Date range:** Videos published between August 15, 2015 – August 15, 2025 (last 10 years).
- **Language filter:** English language content only.
- **Geographic filter:** No geographic restrictions applied to ensure international representation.
- **Minimum view threshold:** ≥100 views.
- **Duplicate content elimination:** Duplicate or highly similar content was identified and eliminated through a three-step process:

Ethics committee approval for the study has been obtained from Elazığ Fethi Sekin City Hospital (No: 2025/14-28, Date:04/09/2025) and the study is conducted according to the Helsinki Declaration.

Inclusion criteria

Educational content related to clinical biochemistry, English language support, at least 100 views, published within the last 10 years, educational content for learning purposes.

Exclusion criteria

Content that contains only product advertising, Insufficient audio/video quality, Content containing scientific errors, Duplicate content.

Quality assessment criteria

Videos were evaluated using a 10-point system with objective, literature-based criteria. Five main criteria were assessed and scored: Scientific Content Quality, Educational Structure, Producer Credibility, and Accessibility/Visual Quality. The criteria and scoring were inspired by scoring systems found in the literature (Global Quality Scale (GQS), Modified DISCERN), scores were assigned according to the table below and Quality assessments were performed by a single investigator.

Scientific content quality (0–3 points): Scientific accuracy and currency, Quality of reference sources, Alignment with clinical practice.

Educational structure (0–2 points): Pedagogical organization, Clarity of learning objectives, Systematic presentation of the subject matter.

Producer credibility (0–2 points): Expert identity and qualifications, Institutional commitment, Transparency and openness.

Technical and accessibility (0–2 points): Audiovisual quality, Subtitles, and multilingual support

According to the scoring system above, video quality scores are considered as follows: High Quality (8–10 points), Medium Quality (5–7 points), Low Quality (1–4 points).

Statistical Analysis

All analyses were performed using Python (version 3.9) with scipy.stats, sklearn.linear_model, and statsmodels libraries. Visualizations were generated using Chart.js and Python WordCloud libraries. Lexical frequency analysis was performed on video titles using term frequency (TF) weighting, with the 50 most frequent terms visualized in a word cloud. Normality of continuous variables (view counts, quality scores) was assessed using the Shapiro-Wilk test ($p>0.05$ threshold) and visual inspection of Q-Q plots. For normally distributed data, independent samples t-tests compared mean view counts between quality categories. For non-normally distributed data, Mann-Whitney U tests were applied. Chi-square tests evaluated categorical associations (channel type vs. quality category). Pearson correlation coefficient (r) quantified the linear relationship between quality scores and view counts. Simple linear regression modeling assessed the predictive relationship, reporting unstandardized coefficients (β), 95% confidence intervals, R^2, and F-statistics. Model assumptions were verified through residual plots. Effect Size Calculation: Cohen's d was computed to quantify the magnitude of differences in view counts between quality categories, with interpretation thresholds: small (d=0.2), medium (d=0.5), large (d=0.8), and very large (d≥1.3) effects.

Results

The systematic search protocol yielded 152 candidate videos, of which 69 met the predetermined inclusion criteria and underwent comprehensive quality assessment. Collectively, these 69 videos accumulated 14,247,835 views as of August 15, 2025. Descriptive statistics of video viewership metrics are presented in Table 1 and the IDs, channel names, view counts, quality scores, categories, channel types, and content categories of the 10 most-viewed videos among the 69 analyzed (Appendix 1) are comprehensively displayed in Figure 1 and Figure 2. The relationship between video production volume and quality scores during the analyzed period is presented in Figure 3.

Content analysis word cloud visualization revealed that 'automated analyzer' technologies and 'clinical chemistry' applications are predominantly covered in medical laboratory

Table 1. Video viewing statistics

Statistics	Value
Total views	14,247,835
Average views	206,491
Standard deviation	167,420
Highest views	697,568
Lowest views	107
Median views	26,519

training materials. The most frequently used terms have been identified as 'Clinical Chemistry', 'Medical Laboratory', 'Chemistry', 'Lab', and 'Automated' (Appendix 2).

Application of the standardized quality assessment framework revealed a tripartite distribution of video quality. High-quality content constituted the majority of analyzed videos, with moderate-quality videos forming a substantial minority and low-quality videos representing a small portion of the sample. Cohen's d calculations between quality categories: High vs. Medium Quality, High vs. Low Quality, Medium vs. Low Quality (Table 2).

The analysis revealed that high-quality videos garnered substantially more views compared to medium-quality content, with this difference being statistically significant. Pearson correlation analysis demonstrated a robust positive association between video quality scores and viewership metrics, indicating that quality substantially accounts for the variance in view counts. Furthermore, simple linear regression modeling established a significant predictive relationship, demonstrating that incremental improvements in quality score corresponded to proportional increases in viewership (Table 3).

Taxonomic classification of video sources revealed a heterogeneous distribution across channel types. Individual educational content creators represented the largest proportion, followed by corporate training entities, medical institutions including hospitals and clinics, and academic institutions (Table 4). Video content categories, the most frequently covered topics were laboratory test interpretation, clinical laboratory specialist training, and hematology tests (Table 5). Analysis revealed that nearly half of the videos included subtitle support, and about one-third displayed verified channel badges. Video lengths varied considerably, from short segments to long presentations, with an average length of moderate. Furthermore, examination of creator credentials showed that the vast majority possessed identifiable expertise, while a small percentage came from sources with unclear professional backgrounds (Table 6). Video production volume increased markedly in the post-COVID period relative to pre-COVID years, while mean quality scores showed a modest improvement. However, this temporal difference in quality did not achieve statistical significance (Table 7).

Discussion

The present investigation demonstrates that 65.2% of systematically selected clinical biochemistry educational videos on YouTube meet rigorous quality criteria (score ≥8/10). This

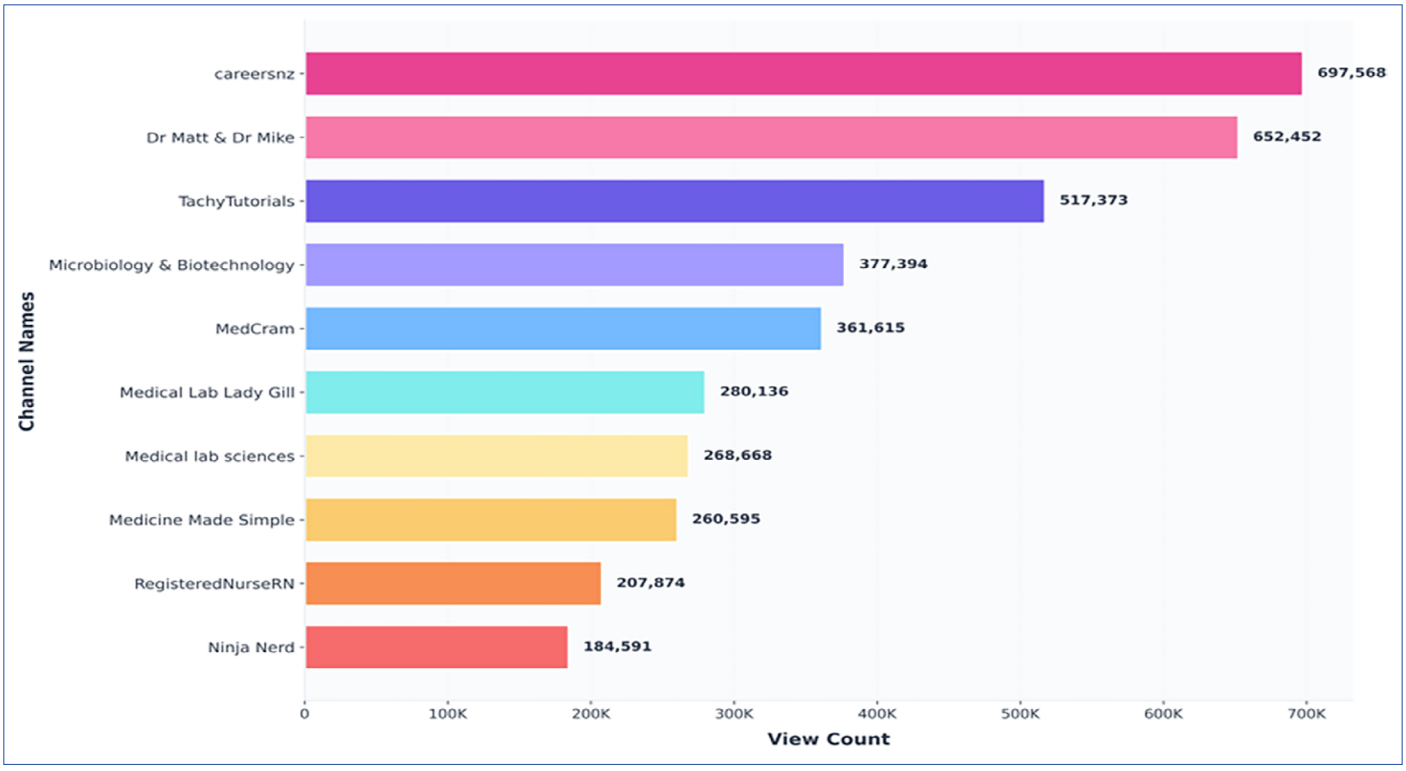

Figure 1. Top 10 most-viewed videos: Channel types and viewership metrics bar chart displaying view counts (in thousands, K=×1,000) for the ten highest-viewed videos (n=10/69).

Rank	Video ID	Title	Channel Name	Views	Quality Score	Category
1	YDWk-C8nN2Y	A day in the life of a Medical Laboratory Technician	careersnz	697,568	8/10	Career Introduction
2	6PTB254Kkbk	Urinalysis Explained	Dr Matt & Dr Mike	652,452	9/10	Test Interpretation
3	jjSinZsLdWY	ALT, AST, ALP & GGT (Liver Function Tests) - How to Interpret	TachyTutorials	517,373	8/10	Test Interpretation
4	E4a8g1o72AM	BIOCHEMICAL TEST | Bacterial Identification Technique	Microbiology & Biotechnology	377,394	7/10	Microbiology
5	57mvZvV3zpY	Liver Function Test Interpretation (LFTs) | Liver Enzymes	MedCram	361,615	9/10	Test Interpretation
6	DfLQizAR1VU	Hematology: How to interpret automated Complete Blood Count	Medical Lab Lady Gill	280,136	9/10	Automation
7	w8eCtpBbTa4	Enzymes and it's characters	Medical lab sciences	268,668	6/10	Basic Biochemistry
8	JVmPu8o2ycc	Full Blood Count (FBC/CBC) interpretation | COMPLETE GUIDE	Medicine Made Simple	260,595	8/10	Test Interpretation
9	2va2aT6lqrU	Metabolic Panel Explained: Basic (BMP) & Comprehensive	RegisteredNurseRN	207,874	8/10	Test Interpretation
10	JiaMJaA34Jg	Liver Function Tests (LFTs) | Clinical Medicine	Ninja Nerd	184,591	9/10	Test Interpretation

Figure 2. Detailed video analysis list displaying video ID, title, channel names, view counts, quality score, and content category for the top 10 most-viewed videos (n=10 of 69 total videos analyzed).

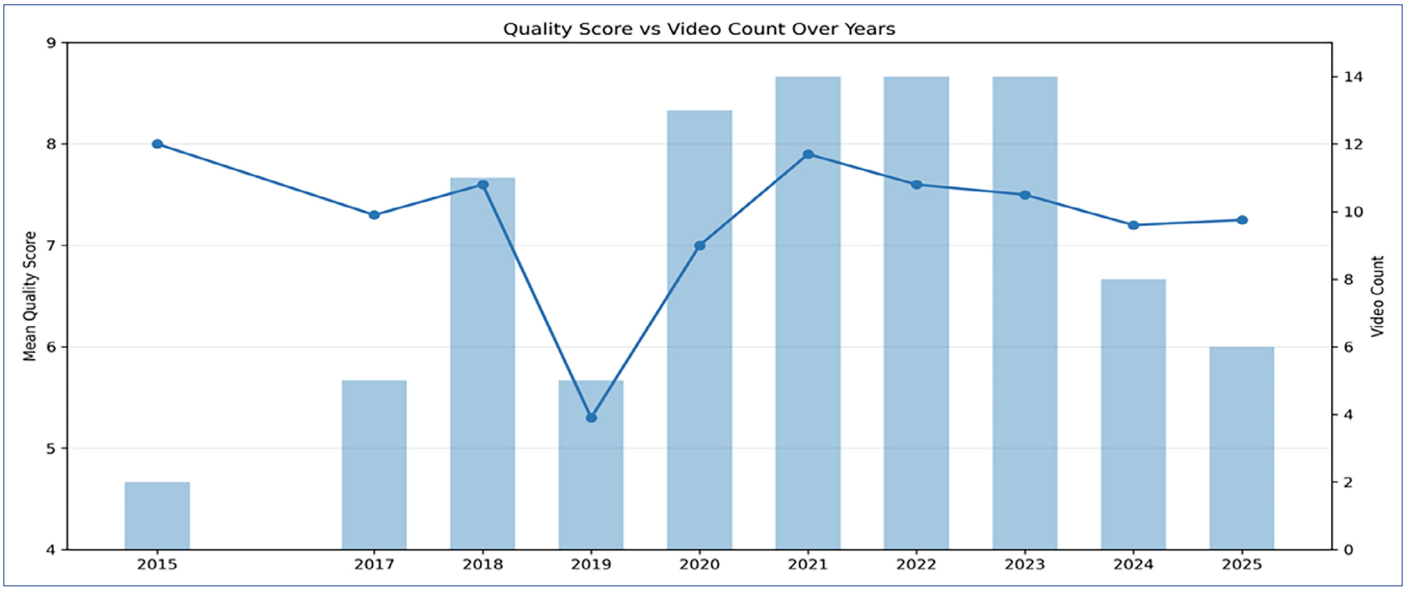

Figure 3. Quality score vs video count over years.

proportion substantially exceeds quality benchmarks documented in previous systematic reviews of medical content on the platform [10, 11]. The fact that high-quality content received statistically significantly more views (284,156 vs. 89,247, $p<0.001$) demonstrates that higher-quality content achieves greater visibility, which may be partially explained by platform algorithms favoring engagement metrics associated with quality ($r=0.782$, $p<0.001$). According to the linear regression model, for each 1-point increase in quality score, the videos receive an average of 40,267 additional views (95% CI: 32,450–48,084 [Table 3]). Effect size analysis, on the other hand, confirms that quality differences lead to significant differences in the number of viewers. These findings substantiate the hypothesis that content quality exerts a substantial influence on audience reach within the digital education ecosystem, with higher-quality educational content consistently attracting larger audiences [12].

In light of the data obtained from the analysis, the high representation of practical applications such as laboratory test interpretation (26.1%), Clinical laboratory specialist training

Table 2. Distribution of video quality categories and statistical comparisons (n=69)

Quality category	Video count (%)		Mean views ±SD	Cohen's d
	n	%		
High (8–10)	45	65.2	284,156±195,420	1.24†
Medium (5–7)	21	30.4	89,247±67,350	1.98‡
Low (1–4)	3	4.4	12,458±8,750	0.89§

†: High vs. Medium; ‡: High vs. Low; §: Medium vs. Low. SD: Standard deviation.

Table 3. Statistical analysis of video quality and viewership metrics

Metric	Value	Statistical significance
Descriptive statistics		
High-quality videos (mean views ±SD)	284,156±195,420	p<0.001
Medium-quality videos (mean views ±SD)	89,247±67,350	
Correlation analysis		
Pearson correlation coefficient®	0.782	p<0.001
95% Confidence Interval	[0.68, 0.86]	
Coefficient of determination (r^2)	0.612	
Variance explained by quality	61.2%	
Linear regression model		
Regression coefficient (β)	40,267	p<0.001
95% Confidence Interval for β	[32,450, 48,084]	
Intercept	-145,832	
Model R^2	0.612	
F-statistic	F(1.67)=104.83	p<0.001
Regression equation	Predicted View Count=-145,832+40,267×Quality Score	

Table 4. Channel types and viewership statistics

Channel type	Video count		Total views	Average views	Quality average
	n	%			
Corporate training	24	34.8	5,947,800	247,825	8.7/10
Individual education	31	44.9	4,682,550	151,050	7.3/10
Medical institutions	10	14.5	2,847,235	284,724	8.9/10
Universities	4	5.8	770,250	192,563	8.5/10

(17.4%) and hematology tests (11.6%) may indicate that digital education is evolving from theoretical knowledge transfer toward practical skill acquisition.

Word cloud analysis obtained from video transcripts reflects the technology-focused approach of modern laboratory education. The most frequently used terms were identified as "Clinical Chemistry," "Medical Laboratory," "Chemistry," "Lab," and "Automated." The word cloud (Appendix 2) shows that the graph is concentrated along the "clinical/medical laboratory" and "clinical chemistry" axes. The frequent appearance of device- and process-oriented terms ("analyzer," "automated") along with manufacturer names indicates a clear prominence of automation/equipment in the content and exhibits a trend aligned with the digital transformation process. Test-level terms (e.g., liver/thyroid function tests, urinalysis, blood count) and discipline names (hematology, microbiology, molecular) show that "laboratory diagnostics" subfields are represented in the corpus. Professional role/education terms ("technologist," "laboratory scientist," "training," "career") indicate that a portion of the texts focuses on education and careers. These observations highlighted three primary themes: (i) instrumentation/automation in clinical chemistry, (ii) routine biochemistry and hematology test panels, and (iii) professional training and roles. In summary, it can be inferred that technological developments, traditional and routine procedures, as well as specific test panels, are popular topics in clinical biochemistry for visual education and information access. Consequently, within the framework of educational transformation, emerg-

Table 5. Video content categories

Content category	Video count		Average views
	n	%	
Laboratory test interpretation	18	26.1	298,547
Clinical laboratory specialist training	12	17.4	156,892
Hematology tests	8	11.6	247,156
Liver Function tests	7	10.1	315,247
Laboratory automation systems	6	8.7	89,456
Kidney function tests	5	7.2	183,731
Thyroid function tests	4	5.8	68,307
Lipid profile tests	3	4.3	62,590
Metabolic panels	3	4.3	207,874
Biochemical tests (general)	3	4.3	251,548

ing and relevant topics should be systematically integrated into learning objectives, contingent upon their periodic evaluation and updating to ensure alignment with contemporary educational needs and evolving disciplinary knowledge.

The temporal analysis of content quality revealed a modest increase in mean quality scores from the pre-COVID period to the post-COVID era, though this difference did not reach statistical significance ($p>0.05$). This finding suggests that while the pandemic precipitated a substantial surge in video production volume, it did not significantly compromise the overall quality of educational content on the platform. The maintenance of quality standards during a period of rapid content expansion may reflect the progressive maturation of digital health education and the increasing engagement of credentialed professionals in online content creation. This model demonstrates a potential trade-off between quantity and quality, with the notable exception of 2021, when both high production volume and elevated quality scores were achieved concurrently. Moreover, the decline in both the number and quality of videos during the COVID-19 pandemic, followed by their subsequent recovery toward the end of the pandemic period, represents a significant factor in assessing the impact of this global health crisis on video-sharing platforms (Table 7; Fig. 3). This observation aligns with broader shifts in digital learning during the pandemic, when online education became essential for higher education institutions, fundamentally reshaping how educational content was created and consumed on digital platforms [13, 14].

The analyses conducted found that only 4.4% of videos fell into the low-quality category, which demonstrates the effectiveness of the selection criteria while also revealing that platform-wide quality control mechanisms need to be reviewed for educational purposes—in other words, there is a need for oversight of units that incorporate the platform into educational materials. The literature supports this need [7, 11]. Therefore, if educational clinics or institutions are considering or already obtaining educational support from digital platforms, it may be necessary to conduct video analyses under

Table 6. Video technical and source characteristics

Video characteristics	Count (%)		Mean±SD
	n	%	
Technical features			
Subtitle support	29	42.0	–
Verified channel	24	34.8	–
4K quality	18	26.1	–
Duration (minutes)	–	–	12.8±11.4
Expert identity			
Board certified	21	30.4	–
Corporate trainers	24	34.8	–
RMT (Registered Medical Technologist) / MLT (Medical Laboratory Technician)	15	21.7	–
Unverified	9	13.1	–

SD: Standard deviation.

Table 7. Distribution of video count and mean quality scores by publication period

Publication period	Video count (n)	Mean quality score ±SD	p
Pre-COVID (2015–19)	17	7.18±1.47	>0.05
Post-COVID (2020–25)	52	7.38±1.48	
Total	69	7.33±1.47	

expert supervision or establish digital education groups. The distribution of the analysis regarding expert identity verification is presented in Table 6. The determination that the uncertain identity rate is 13% validates the above finding.

The fact that 42% of videos include subtitle support (independent of automatic translation features) (Table 6) demonstrates that content on the platform can achieve global accessibility and serve educational purposes. The observation that 75.3% of videos experienced increased view counts after 2020 strongly confirms the pandemic's impact on rising demand for digital education. This suggests that the pandemic has become an irreversible aspect of global life. These findings indicate that clinical biochemistry education and professional collaboration have entered a more accessible era, making visual social media platforms increasingly vital to educational standards and emphasizing the importance of integrating them into conventional educational frameworks.

Limitations

This study has several important limitations that should be considered when interpreting the findings: Single Platform Analysis, Language Restriction, Single Rater Assessment, Quality Assessment Tool Limitations, Cross-Sectional Design, Selection Bias and Keyword Limitations, Lack of Learning Outcome Data, Technology Integration Assessment, Geographic and Temporal Context. These limitations suggest that findings

should be interpreted as: Specific to YouTube as a platform within the English-language educational landscape, Indicative of content quality potential rather than definitive learning effectiveness, Representative of 2015-2025 digital education trends rather than long-term stable patterns, Requiring validation through complementary research addressing learning outcomes, multi-platform analysis, and longitudinal follow-up

Conclusion

This study demonstrates that the YouTube platform is a valuable and important resource for clinical biochemistry education. The fact that 65.2% of the 69 analyzed videos meet high quality standards, with these videos reaching a total of 14.2 million views, reveals not only the outreach potential of digital education platforms in the field of clinical biochemistry but also the rich potential and diversity they offer for clinical biochemistry education. The findings obtained from the analysis of 69 videos strongly indicate that digital educational tools play a transformative role rather than merely a supplementary one to traditional education.

The high-quality performance and average viewership (247,825) of institutional channels underscores the critical importance of a reliable institutional identity in digital education. In conclusion, digital transformation in clinical biochemistry education is an inevitable process, and for this transformation to be successful, institutional approaches, quality assurance systems, continuous research and development activities, and global collaboration platforms are required. The analytical findings of this and similar studies can serve as a foundation for future research and policy development processes.

Disclosures

Online Appendix Files: https://jag.journalagent.com/ijmb/abs_files/IJMB-90958/IJMB-90958_(3)_IJMB-90958_Appendix.pdf

Ethics Committee Approval: The study was approved by the Elazığ Fethi Sekin City Hospital Ethics Committee (no: 2025/14-28, date: 04/09/2025).

Informed Consent: Informed consent was obtained from all participants.

Conflict of Interest Statement: The author declare that there are no competing interests associated with the manuscript.

Funding: No funding was received for this study.

Use of AI for Writing Assistance: No AI technologies utilized.

Peer-review: Externally peer-reviewed.

References

1. Ramos-Rodriguez C, Martinez Garcia A, Lopez Hernandez D, Silva Martinez E. Digital transformation in medical education: A systematic review of emerging technologies and pedagogical approaches. Med Teach 2023;45(8):789–98.
2. Barry DS, Marzouk F, ChulakOglu K, Bennett D, Tierney P, O'Keeffe GW. Anatomy education for the YouTube generation. Anat Sci Educ 2016;9(1):90–6. [CrossRef]
3. Topf JM, Sparks MA, Phelan PJ, Shah N, Lerma EV, Graham Brown MP, et al. The evolution of nephrology education: Perspectives on social media. Clin J Am Soc Nephrol 2016;11(7):1319–25.
4. Rose S. Medical student education in the time of COVID-19. JAMA 2020;323(21):2131–2. [CrossRef]
5. Garcia Betances RI, Arredondo Waldmeyer MT, Fico G, Cabrera Umpiérrez MF. A succinct overview of virtual reality technology use in Alzheimer's disease. Front Aging Neurosci 2021;7:80. [CrossRef]
6. Wikipedia. YouTube. Available at: https://en.wikipedia.org/wiki/YouTube. Accessed Feb 4, 2025.
7. Pearlman O, Konecny LT, Cole M. Information literacy skills of health professions students in assessing YouTube medical education content. Front Educ 2024;9:1354827. [CrossRef]
8. Market.us. Social media in healthcare statistics. Available at: https://media.market.us/social-media-in-healthcare-statistics/. Accessed Feb 4, 2025.
9. Osman W, Mohamed F, Elhassan M, Abdulhadi Shoufan. Is YouTube a reliable source of health-related information? A systematic review. BMC Med Educ 2022;22(1):382. [CrossRef]
10. Alfarhan AI, Alsubk A, Almohsen S, Alotaibi MM, Alshehri MA, Alsuhaibani MN. The content quality of YouTube videos for professional medical education. Acad Med 2021;96(10):1484–93. [CrossRef]
11. Drozd B, Couvillon E, Suarez A. Medical YouTube videos and methods of evaluation: Literature review. JMIR Med Educ 2018;4(1):e3. [CrossRef]
12. Szmuda T, Syed MT, Singh A, Ali S, Özdemir C, Słoniewski P. YouTube as a source of patient information for Coronavirus Disease (COVID-19): A content-quality and audience engagement analysis. Rev Med Virol 2020;30(5):e2132. [CrossRef]
13. Ali W. Online and remote learning in higher education institutes: A necessity in light of COVID-19 pandemic. High Educ Stud 2020;10(3):16–25. [CrossRef]
14. Ikanubun LE, Lidiah Tereda Iwo. Audience engagement in practice tests and instructional videos on YouTube. J Inov Teknol Pendidik 2025;12(1):27–39.

INTERNATIONAL JOURNAL OF
MEDICAL BIOCHEMISTRY

DOI: 10.14744/ijmb.2025.38981
Int J Med Biochem 2026;9(1):29–38

Research Article

Should HFE mutations be checked in polycythemic patients even at lower iron levels?

Seda Misirlioglu Sucan[1], Hatice Demet Kiper Unal[2], Asli Subasioglu[3], Bahriye Payzin[2]

[1]Department of Internal Medicine, Izmir Katip Celebi University Ataturk Research and Training Hospital, Izmir, Türkiye
[2]Department of Hematology, Izmir Katip Celebi University Ataturk Research and Training Hospital, Izmir, Türkiye
[3]Department of Medical Genetics, Izmir Katip Celebi University Ataturk Research and Training Hospital, Izmir, Türkiye

Abstract

Objectives: The relationship between polycythemia and hereditary hemochromatosis (HH) has been investigated in several studies. This study aimed to evaluate the association between iron parameters and Hemochromatosis Protein (HFE) gene mutations in patients with primary or secondary polycythemia, as well as in non-polycythemic patients with elevated iron parameters.

Methods: A total of 106 patients who were evaluated for polycythemia or underwent HFE mutation testing due to elevated transferrin saturation (TS) and ferritin levels in the hematology department between 2015 and 2022 were retrospectively reviewed.

Results: The median age of the 106 patients (77 male, 29 female) was 54 years (range, 19–83). HFE gene mutations were detected in 44 patients (41.5%; 31 male, 13 female). Thirty-seven patients (35%) with Myeloproliferative Neoplasms (MPNs) were classified as Group 1, 52 (49%) with secondary polycythemia as Group 2, and 17 (16%) who underwent HFE mutation testing due to elevated TS/ferritin levels without polycythemia as Group 3. The mean TS level in Group 1 was significantly higher than in Group 2 (p=0.032). Among HFE(+) patients, mean TS was significantly higher in Group 3 compared with Group 2 (p=0.023). When all polycythemic HFE(+) patients (primary + secondary) were compared with non-polycythemic HFE(+) patients, mean TS was significantly higher in non-polycythemic patients (p=0.026).

Conclusion: The relatively high frequency of HFE positivity in patients with secondary polycythemia, together with its association with lower TS levels, suggests that the possibility of HH should not be overlooked in secondary polycythemia, even at lower TS levels.

Keywords: Hemachromatosis, hemochromatosis protein (HFE), polycythemia, , transferrin

How to cite this article: Misirlioglu Sucan S, Kiper Unal HD, Subasioglu A, Payzin B. Should HFE mutations be checked in polycythemic patients even at lower iron levels?. Int J Med Biochem 2026;9(1):29–38.

Hereditary hemochromatosis (HH) is an autosomal recessive disease that disrupts iron metabolism and leads to iron accumulation in the parenchymal cells of tissues. It mainly affects the liver, heart, and pancreas. The HFE gene is located on the short arm of chromosome 6 (6p21.3). Typical HH patients carry two copies of the C282Y mutation in the HFE gene. The C282Y homozygous mutation is the most common genotype seen in HH, with a frequency of 80–85%. A minor HFE mutation is found in the H63D genotype, either in the homozygous form or as a compound heterozygous (C282Y/

This article is extracted from the first author, Seda Mısırlıoğlu Sücan's doctorate dissertation entitled "Evaluation of the Relationship between Transferrin Saturation and Ferritin Levels with HFE Mutation Status in Patients with Primary and Secondary Polycythemia" supervised by Hatice Demet Kiper Ünal (İzmir Katip Çelebi University, Ataturk Research and Training Hospital, İzmir, 2023; YOK national thesis center, no:821163).

Address for correspondence: Seda Misirlioglu Sucan, MD. Department of Internal Medicine, Izmir Katip Celebi University Ataturk Research and Training Hospital, Izmir, Türkiye
Phone: +90 506 573 06 79 **E-mail:** sedamisirlioglu95@gmail.com **ORCID:** 0000-0001-8088-2872

Submitted: May 21, 2025 **Revised:** November 05, 2025 **Accepted:** November 07, 2025 **Available Online:** February 18, 2026

H63D) variant. Most patients present with normal serum iron tests and only mild to moderate iron accumulation [1].

Ferritin is the most commonly used biomarker of systemic iron stores in clinical practice. If serum ferritin exceeds 300 ng/mL, systemic iron overload may be considered. However, ferritin expression can be influenced not only by serum iron, but also by inflammatory cytokines, hormones, and oxidative stress [2]. Therefore, professional societies recommend screening for transferrin saturation (TS=serum iron/TIBC × 100) in both asymptomatic and symptomatic patients with suspected hemochromatosis. If the TS is >45%, with or without hyperferritinemia, further testing for HFE gene mutations is recommended [3].

The World Health Organization (WHO) defines polycythemia as hemoglobin (Hgb) >16.5 g/dL and/or hematocrit (Hct) >49% in men, and Hgb >16 g/dL and/or Hct >48% in women [4]. Polycythemia vera (PV) is a Myeloproliferative Neoplasms (MPNs) characterized by clonal proliferation of myeloid cells, with 95% of patients harboring the JAK2 V617F mutation. Although no direct association has been established between PV and HH, the coexistence of the two disorders has been reported in a small number of case studies [4, 5].

Secondary polycythemia may occur due to elevated erythropoietin levels in conditions such as chronic obstructive pulmonary disease (COPD), cyanotic right-to-left cardiac shunts, sleep apnea, high altitude, chronic carbon monoxide intoxication, post-renal transplantation, polycystic kidney disease, hepatocellular carcinoma, renal cancer, and certain brain tumors [6].

Even when no cause for secondary polycythemia is identified, it has been suggested that the presence of erythrocytosis in HH patients with polycythemia may be secondary to increased iron uptake by erythroid precursors in the bone marrow, which may or may not be transferrin-dependent [7].

In this retrospective study, in contrast to previous reports, we aimed to investigate the relationship bƏetween transferrin saturation and serum ferritin levels in patients with primary or secondary polycythemia undergoing HFE mutation testing, as well as to evaluate iron kinetics and the presence of HFE gene mutations in patients without polycythemia.

Materials and Methods

The study was approved by the Local Ethics Committee for Clinical Research of Izmir Katip Çelebi University Atatürk Training and Research Hospital (Committee approval dated 21.03.2023 and decision number 0054). The research was conducted in accordance with the "WMA Declaration of Helsinki - Ethical Principles for Medical Research Involving Human Subjects".

We retrospectively reviewed the iron kinetic parameters and mutation results of patients who underwent HFE mutation testing between January 2015 and January 2022 at the Department of Hematology, İzmir Kâtip Çelebi University Faculty of Medicine Hospital.

For all patients, complete blood count (hemoglobin, hematocrit, white blood cell, neutrophil, and platelet counts) was performed using an automated hematology analyzer (XN-1000, Sysmex Corporation, Kobe, Japan). Serum ferritin levels were determined by chemiluminescence immunoassay (DxI 800, Beckman Coulter Inc., USA). Erythropoietin (EPO) levels were measured by chemiluminescence immunometric analysis on the Immulite 2000 system (Siemens Healthineers, Germany). Biochemical parameters including aspartate aminotransferase (AST), alanine aminotransferase (ALT), creatinine, serum iron, and total iron-binding capacity (TIBC) were analyzed using a fully automated biochemistry analyzer (AU5800, Beckman Coulter Inc., USA).

Genetic testing included analysis of HFE C282Y and H63D polymorphisms as well as JAK2 exon 14 and exon 12 mutations. Genomic DNA was extracted from peripheral blood leukocytes using a column-based purification kit (Qiagen, Hilden, Germany). Genotyping for HFE mutations was performed by real-time polymerase chain reaction (PCR) with allele-specific probes using commercial kits (Genvinset HFE H63D and Genvinset HFE C282Y, Qiagen). JAK2 mutation analysis was carried out by real-time PCR using the Ipsogen JAK2 MutaQuant Kit (Qiagen) according to the manufacturer's instructions.

Demographics, comorbidities, smoking history, presence of splenomegaly, and treatments received were also evaluated.

Statistical analysis

The data were analyzed using SPSS version 26.0 with a 95% confidence level. Frequency and percentage (n, %) were reported for categorical variables, whereas mean, standard deviation (mean±SD), minimum, maximum, and median (M) were reported for numerical variables.

For group comparisons, the independent samples t-test or Mann–Whitney U test was used for continuous variables, while the chi-square test was applied for associations between categorical variables. Logistic regression analysis was performed to identify factors associated with HFE mutation positivity. In addition, receiver operating characteristic (ROC) analysis was conducted to determine the cut-off values of hemoglobin, hematocrit, ferritin, and transferrin saturation (TS) for predicting HFE mutation status.

Results

Of 112 patients screened for HFE gene mutations, 106 were included in the analysis after exclusion criteria were applied. The cohort consisted of 77 males and 29 females (M/F ratio: 2.5/1), with a median age of 54 years (range, 19–83). Age at diagnosis was significantly higher in female patients compared with males (p=0.002). Overall, 44 patients (41.5%) were positive for an HFE mutation (31 males, 13 females), with no significant difference in prevalence by gender (p=0.67). The mean age did not differ between HFE-positive and HFE-negative patients (p=0.23); however, among mutation carriers, females had a significantly higher mean age at diagnosis than males (p<0.001).

Analysis of TS and serum ferritin levels showed that HFE mutation carriers had significantly higher mean TS compared

Table 1. Comparison of laboratory parameters by HFE mutation status

	HFE				p
	Negative		Positive		
	Min-max (M)	Mean±SD	Min-max (M)	Mean±SD	
Overall					
Age at diagnosis	20–83 (54)	52.76±15.41	19–77 (51.5)	49.34±16.63	**0.268**
Follow-up duration (months)	0–186.4 (18.3)	39.64±50.47	0.1–179.6 (31.5)	38.92±43.48	**0.939**
Platelets (10^9/L)	106–1067 (265.5)	368.57±231	123–1138 (284.5)	366.32±242.95	**0.961**
Leukocyte (10^9/L)	5.1–27.8 (7.9)	9.15±3.98	4–38.7 (7.6)	9.07±5.74	**0.331**
Neutrophil (10^9/L)	2.6–16.9 (4.7)	5.53±2.82	2.4–31.9 (4.2)	5.61±4.79	**0.364**
ALT	6–309 (21)	29.6±37.09	6–139 (21)	30.61±27.56	**0.849**
AST	8–220 (20)	25.63±26.98	9–101 (20.5)	24.86±17.99	**0.964**
Creatinine (mg/dL)	0.5–2.5 (0.9)	0.95±0.34	0.5–2.9 (0.9)	0.96±0.35	**0.460**
EPO (mU/mL)	1–25.9 (5.2)	7.14±6.31	1–46.8 (5.7)	8.84±9.77	**0.517**
TS (%)	18–83 (44.5)	44.96±15.21	22–91 (51.8)	51.41±16.49	**0.040***
Female					
Serum Iron (µg/dL)	20–307 (94)	98.58±58.23	67–234 (108)	124±48.57	**0.093**
TIBC (µg/dL)	225–521 (337)	334.16±70.53	188–350 (296)	285.91±55.94	**0.063**
Hgb (g/dL)	9.5–19.9 (16.1)	15.18±3	8.5–16.7 (14.7)	14.27±2.4	**0.380**
Hct (%)	29.6–61.5 (47.6)	45.6±8.7	26.1–51.8 (43.4)	42.7±7.5	**0.360**
Ferritin (ng/mL)	23–1650 (79)	382.43±509.18	64–347 (143)	172.3±89.26	**0.150**
TS (%)	24.1±78.62 (39.5)	41.85±15.81	25.7–79.05 (48.4)	48.65±15.77	**0.250**
Male					
Serum Iron (µg/dL)	25–311 (108)	112.9±44.07	57–299 (127)	131.06±52.82	**0.106**
TIBC (µg/dL)	174–467 (315)	313.08±70.86	208–410 (321)	319.58±52.88	**0.655**
Hgb (g/dL)	10.4–19.5 (17.2)	16.77±1.9	12.7–18.8 (17)	16.73±1.5	**0.920**
Hct (%)	33.1–67 (50.2)	50.68±6.2	38–56.5 (50.4)	40.06±4.3	**0.210**
Ferritin (ng/mL)	18–2607 (131)	271.87±432.40	30–1127 (153)	250.48±244.57	**0.810**
TS (%)	18–83.2 (46.2)	46.04±15.02	18.9–81.7 (54.4)	52.56±16.9	**0.080**

Values are expressed as mean±SD. *: $p<0.05$ was considered statistically significant (t-test or Mann–Whitney test). Hgb, Hct, and iron-related parameters were evaluated separately by gender. HFE: Hemochromatosis protein; SD: Standard deviation; ALT: Alanine transaminase; AST: Aspartate transaminase; EPO: Erythropoietin; TIBC: Serum total iron-binding capacity; Hgb: Hemoglobin; Hct: Hematocrit; TS: Transferrin saturation.

with non-carriers (p=0.04). When evaluated separately by sex, neither TS nor ferritin levels differed significantly between HFE-positive and HFE-negative patients (p=0.81 and p=0.15 for ferritin in males and females, respectively; non-significant for TS). Other hematologic and biochemical parameters, including hemoglobin, hematocrit, leukocyte count, platelet count, ALT, and AST, did not show significant differences according to HFE mutation status (Table 1).

Of the total cohort, 56 patients (52.8%) had TS >45%, 13 (12.7%) had TS between 40–45%, and 13 (12.7%) presented with elevated serum ferritin for sex. Twenty-four patients (22.6%) underwent HFE testing due to clinical suspicion of hereditary hemochromatosis (HH). There was no significant association between the indications for testing and the presence of an HFE mutation, either overall or by sex (p=0.35).

Regarding underlying diagnoses, 37 patients (35%) were classified as CMPN (n=28, polycythemia vera [PV], 7 essential thrombocythemia [ET], 2 primary myelofibrosis [PMF]), 52 patients (49%) as secondary polycythemia, and 17 patients (16%) as non-polycythemic with elevated iron parameters. In addition, two patients had diffuse large B-cell lymphoma (DLBCL), two had acute lymphoblastic leukemia (ALL), one had Hodgkin lymphoma (HL), and one had Ph-positive chronic myeloid leukemia (CML). Among comorbidities, hypertension was present in 30 (28.3%), diabetes mellitus in 19 (17.9%), and atherosclerotic cardiovascular disease in 13 (12.3%); other conditions were less frequent. For comparative analyses, patients were categorized into three groups: Group 1 included those with Myeloproliferative Neoplasms (MPNs; PV, ET, PMF), Group 2 comprised patients with secondary polycythemia, and Group 3 consisted of non-polycythemic patients presenting with elevated iron parameters.

Smoking status was available for all patients: 36 (34%) were current smokers, 16 (15.1%) were former smokers, and 54 (50.9%) never smoked. Including former smokers, half of the HFE-positive patients were ever-smokers, with no significant

Table 2. Transferrin saturation (TS, %) by clinical group and HFE status

A. Overall (all patients)	Mean±SD
Group	
Group 1 (CMPN)	52.7±14.2
Group 2 (Secondary polycythemia)	43.9±17.3
Group 3 (Non-polycythemic, elevated iron parameters)	50.8±15.2
Pairwise p: G1 vs G2=0.032*; G1 vs G3=0.86; G2 vs G3=0.12	
B. HFE-positive	
Group	
Group 1	53.8±14.2
Group 2	47.0±17.5
Group 3	63.9±10.4
Pairwise p: G1 vs G2=0.32; G1 vs G3=0.084; G2 vs G3=0.023* | Groups 1+2 (all polycythemic†) vs Group 3: 48.1±16.9 vs 60.8±12.9 → p=0.026*	
C. HFE-negative	
Group	
Group 1	50.7±12.7
Group 2	41.2±17.0
Group 3	43.7±12.7
Pairwise p: G1 vs G2=0.036*; G1 vs G3=0.13; G2 vs G3=0.63 | Groups 1+2 (all polycythemic†) vs Group 3: 44.22±16.0 vs 47.22±12.3 → p=0.52	

*: Values are mean±SD. Pairwise p values were calculated using t-test or Mann–Whitney test, as appropriate. p<0.05 was considered statistically significant. †: All polycythemic: polycythemic cases from Group 1 combined with all patients in Group 2.

Table 3. Distribution of HFE mutation genotypes across groups

HFE mutation type	Genotype	Group 1 (CMPN)	Group 2 (Secondary polycythemia)	Group 3 (Others‡)	Total (%)	p
C282Y	Homozygous	0	1	0	1 (0.9%)	0.82
	Heterozygous	1	1	1	3 (2.8%)†	
	Negative	33	50	19	102 (96.2%)	
H63D	Homozygous	1	1	1	3 (2.8%)	0.65
	Heterozygous	11	22	5	38 (35.8%)†	
	Negative	22	27	15	64 (60.4%)	
	No result	-	1	-	1 (0.9%)	

‡: Others: Non-polycythemic, elevated iron parameters; †: Compound C282Y and H63D mutation in one patient.

difference compared with HFE-negative patients (p=0.74). In Group 2 (secondary polycythemia), 22 patients (42%) were current smokers, while 7 (14%) had quit and 23 (44%) had never smoked. Notably, there were significantly more male patients in Group 2 compared with the other groups (p=0.014). Similarly, both HFE-positive and HFE-negative males were more common in Group 2 than in Groups 1 and 3 (p=0.031).

Group comparisons of TS (%) levels are summarized in Table 2. Patients with CMPN (Group 1) had significantly higher mean TS compared with those with secondary polycythemia (Group 2, p=0.032), while Group 3 values did not differ significantly from either group. In HFE-positive patients, TS was significantly higher in Group 3 compared with Group 2 (p=0.023), but there was no difference between Groups 1 and 2. Moreover, non-polycythemic HFE-positive patients had higher mean TS compared with polycythemic HFE-positive patients (p=0.026). Among HFE-negative patients, TS was higher in Group 1 than in Group 2 (p=0.036). Finally, within Group 3, HFE-positive patients had significantly higher TS compared with HFE-negative patients (p=0.002).

The distribution of HFE genotypes is presented in Table 3. Overall, the C282Y and H63D variants were detected in 4 (3.8%) and 41 (38.7%) patients, respectively, with one patient harboring a compound heterozygous genotype. There

Table 4. Clinical characteristics of patients with heterozygous/homozygous C282Y, compound C282Y/H63D, and homozygous H63D mutations

ID	Sex	Age (y)	Genotype	Dx/Notes	Hgb (g/dL)	Hct (%)	TS (%)	Ferritin (ng/mL)	FU (mounth)	Status
1 (GK)	M	45	C282Y homozygous	Sec. polycythemia; β-thal trait; NS	16.2	50.5	71	735	31	Alive
2 (AA)	M	35	C282Y/H63D compound het.	Sec. polycythemia; NS	17.1	47.9	47.9	241	55	Alive
3 (SB)	F	72	C282Y heterozygous	MPN–ET; DM; CKD	13.8	42.5	33.2	347	33	Alive
4 (SD)	F	77	C282Y heterozygous	MPN–PV; JAK2 V617F+; DM	15.2	46.8	48	64	34	Alive
5 (AÇ)	M	49	H63D homozygous	HT; splenomegaly	13.7	41.6	76	1127	3	Alive
6 (KA)	M	54	H63D homozygous	Renal cyst; BPH; HLD	14.3	40.6	60	489	6	Alive
7 (ÖA)	M	31	H63D homozygous	Sec. polycythemia; S	17.7	48.1	53.7	48	2	Alive

M: Male; F: Female; MPN: Myeloproliferative neoplasm; PV: Polycythemia vera; ET: Essential thrombocythemia; DM: Diabetes mellitus; CKD: Chronic kidney disease; HT: hypertension; HLD: Hyperlipidemia; BPH: Benign prostatic hyperplasia; TS: Transferrin saturation; FU: Follow-up; S: Smoker; NS: Non-smoker; het.: Heterozygous.

was no significant difference in the distribution of homozygous and heterozygous forms of either genotype across the groups. The heterozygous H63D mutation was the most common finding, detected in 38 patients (35.8%), with similar prevalence among groups.

Evaluation of genotypes according to the clinical indications for HFE testing showed that homozygous C282Y was observed in one patient with TS >45%, and homozygous H63D in three patients. A heterozygous C282Y variant was identified in one patient with elevated ferritin, and compound C282Y/H63D heterozygosity was found in one patient with TS >45%. The heterozygous H63D variant was represented across all testing indications. No significant association was found between genotype type and testing indication (p=0.78 for C282Y, p=0.45 for H63D).

Clinical characteristics of patients with heterozygous or homozygous C282Y and homozygous H63D mutations are shown in Table 4. Among heterozygous H63D carriers, no significant differences were observed in hemoglobin, hematocrit, serum ferritin, or TS levels compared with HFE-negative patients in both PV and secondary polycythemia subgroups. The only significant difference was seen in Group 3, where TS was higher in heterozygous H63D carriers compared with non-carriers (Table 5). In subgroup analyses, ferritin levels appeared paradoxically higher in some HFE wild-type patients compared with mutation carriers (Table 5). Although such a finding is not consistent with the expected pathophysiology, ferritin is an acute phase reactant and may be elevated in the context of occult inflammatory, immunologic, or metabolic conditions. Despite the exclusion of patients with overt infection or inflammatory disease at baseline, comorbidities such as diabetes mellitus, thalassemia minor, or yet undiagnosed immunologic/rheumatologic disorders could have contributed to this observation.

ROC analysis identified a TS cut-off of 51.7% for predicting polycythemia in HFE-positive patients. Figures 1 and 2 present the ROC curves with AUC, sensitivity, specificity, and 95% confidence intervals, but this threshold had limited diagnostic accuracy and was not clinically relevant.

Discussion

HFE hemochromatosis (type I hereditary hemochromatosis) represents the most common form of inherited iron overload. Polycythemia is defined as hemoglobin levels >16.5 g/dL in men and >16.0 g/dL in women and/or hematocrit levels >49% in men and >48% in women [4]. Previous studies have investigated the relationship between polycythemia and hereditary hemochromatosis. In one report, C282Y homozygous patients (n=60) exhibited significantly higher mean hemoglobin, hematocrit, MCV, and MCH values compared to 65 healthy controls without HFE mutations [8]. Similarly, in a series of 152 hereditary hemochromatosis patients (63.2% male), 44 (28.9%) carried the C282Y homozygous genotype, 10 (6.6%) the H63D homozygous genotype, and 27 (17.8%) the compound heterozygous C282Y/H63D genotype. Median hemoglobin and hematocrit values were 15.5 g/dL and 44.9% in C282Y homozygotes, 16.0 g/dL and 47% in H63D homozygotes, 15.8 g/dL and 46% in compound heterozygotes, 16.0 g/dL and 47% in C282Y heterozygotes, and 16.6 g/dL and 48% in H63D heterozygotes [9].

A retrospective analysis of 213 patients with hereditary hemochromatosis (mean age 53.6±15.2 years; 143 males, 67.1%) identified HFE mutations in all cases. Homozygous C282Y mutations were present in 108 patients (50.7%), while polycythemia was observed in 59 patients (27.6%) [10]. In a large population-based study of 10,198 Caucasians, the reported allele frequencies were 0.63% for C282Y and 1.52% for H63D. Notably, mean hemoglobin and MCV levels were significantly higher in mutation carriers compared with non-carriers [11].

In our retrospective cohort of 106 patients screened for HFE mutations, 77 (73%) were male. A total of 44 patients (41.5%)

Table 5. Laboratory parameters of patients carrying the H63D heterozygous mutation compared with HFE wild-type patients

Parameter	PV (Group 1 subset)	Group 1 (MPNs)	Group 2 (Secondary polycythemia)	Group 3 (Others‡)
Hemoglobin (Male, g/dL)	H63D(+): 16.9±0.73 WT: 17.52±0.79 p=0.22	H63D(+): 15.85±1.8 WT: 17.0±2.0 p=0.24	H63D(+): 17.58±0.70 WT: 17.49±0.66 p=0.69	H63D(+): 14.3±1.2 WT: 13.68±2.3 p=0.64
Hematocrit (Male, %)	H63D(+): 50.9±1.57 WT: 53.52±4.59 p=0.28	H63D(+): 47.8±5.4 WT: 52.0±7.0 p=0.20	H63D(+): 51.23±2.59 WT: 51.0±2.29 p=0.76	H63D(+): 42.8±3.9 WT: 41.8±6.2 p=0.77
Hemoglobin (Female, g/dL)	H63D(+): 15.7±1.1 WT: 17.3±1.6 p=0.15	H63D(+): 13.3±2.8 WT: 16.3±3.1 p=0.079	H63D(+): 16.3±0.17 WT: 17.1±1.45 p=0.37	H63D(+): 12.1±2.41 WT: 11.5±1.5 p=0.66
Hematocrit (Female, %)	H63D(+): 47.5±4.97 WT: 51.9±5.95 p=0.29	H63D(+): 40.0±9.0 WT: 49.1±9.6 p=0.084	H63D(+): 48.1±3.18 WT: 51.08±5.25 p=0.40	H63D(+): 35.9±6.8 WT: 35.5±4.7 p=0.91
Ferritin (Male, ng/mL)	H63D(+): 168±149.4 WT: 114.39±57 p=0.28	H63D(+): 198±169.2 WT: 170.1±45.4 p=0.63	H63D(+): 174.4±124.1 WT: 297.93±545 p=0.36	H63D(+): 329±219.6 WT: 465.3±467.9 p=0.64
Ferritin (Female, ng/mL)	H63D(+): 146±2.64 WT: 147.1±154.8 p=0.96	H63D(+): 152.8±39 WT: 137.1±144.0 p=0.78	H63D(+): 225.3±112.1 WT: 146±2.64 p=0.28	H63D(+): 143±57.84 WT: 897.5±556.1 p=0.015*
Transferrin saturation (%)	H63D(+): 50.64±14.53 WT: 48.8±13.46 p=0.76	H63D(+): 54.13±11.9 WT: 49.8±13.1 p=0.33	H63D(+): 45.5±17.8 WT: 41.42±17.3 p=0.42	H63D(+): 70.3±11.5 WT: 45.19±12.1 p=0.007*

*: p<0.05; WT: HFE wild-type; ‡: Others: Non-polycythemic, elevated iron parameters; MPNs: Myeloproliferative Neoplasms.

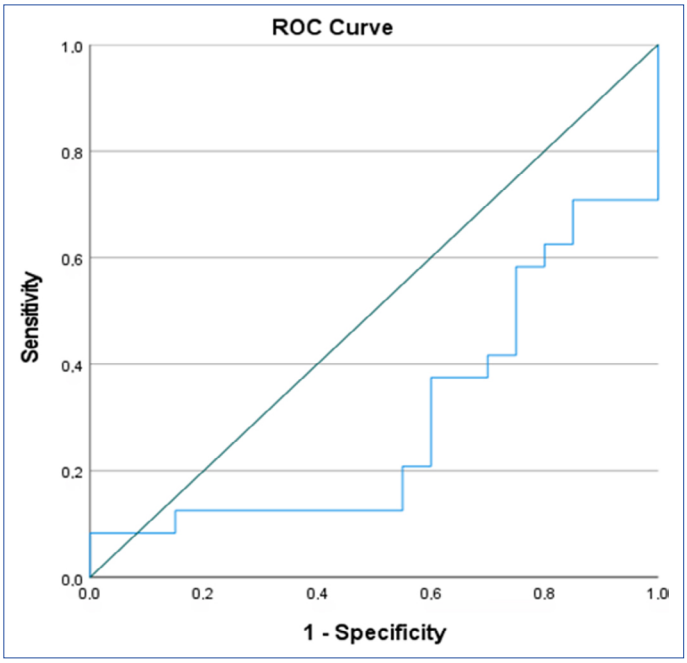

Figure 1. ROC curve for transferrin saturation (ST) in predicting HFE mutation positivity (Secondary polycythemia vs Myeloproliferative Neoplasms (MPNs)+Others). Receiver operating characteristic (ROC) curve for ST in predicting HFE mutation positivity in secondary polycythemia versus CMPN+Others. AUC=0.298 (95% CI: 0.140–0.456), p=0.02. Sensitivity/specificity were 37%/40% at the 51.7% cut-off, and 58%/25% at the 45.3% cut-off.

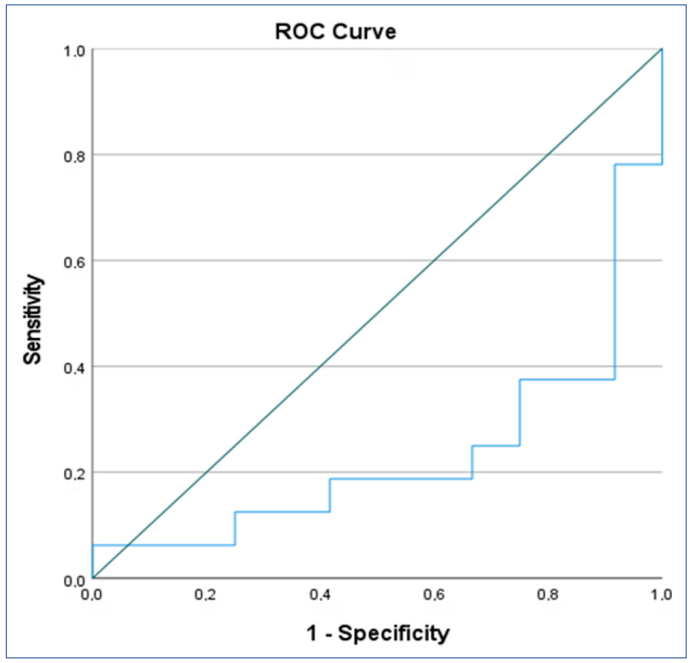

Figure 2. ROC curve for transferrin saturation (ST) in predicting HFE mutation positivity (Secondary polycythemia vs Myeloproliferative Neoplasms (MPNs)+Others). Receiver operating characteristic (ROC) curve for in predicting HFE mutation positivity in all polycythemias (including PV) versus non-polycythemias. AUC=0.232 (95% CI: 0.081–0.383), p=0.07. Sensitivity/specificity were 37%/25% at the 51.7% cut-off, and 56%/8% at the 45.3% cut-off.

tested positive for an HFE mutation (31 males, 13 females). The distribution of mutation positivity did not differ significantly between sexes (p=0.67). Although the absolute number of male carriers was more than twice that of females, this finding reflects the higher proportion of males in the cohort rather than a true male predominance in HFE mutation frequency.

There are only a limited number of studies on HFE gene mutations reported from our country. Most of these have identified the H63D variant, while the C282Y mutation has rarely been detected [12–17]. A large familial cluster carrying HFE mutations was described in the Diyarbakır region, where, among the relatives of a proband with a homozygous C282Y mutation, 17 were heterozygous for C282Y, 4 were heterozygous for H63D, and 2 carried a homozygous C282Y genotype [18]. In another national study that compared 86 patients with transferrin saturation (TS) above 45% to 57 controls with TS below 45%, no C282Y mutations were detected, while the H63D mutation was present in 27% of patients and 21% of controls, showing no significant association with the clinical phenotype [12]. More recently, a study published in 2021 investigated the frequency and distribution of HH-related mutations among 97 patients with elevated TS who were clinically suspected to have HH. Heterozygous H63D mutation was detected in 19 patients, 14 (20%) of whom had TS between 38–45% and 5 (18.5%) with TS >45% [17].

With the advent of genetic testing, the average age at diagnosis of HH has been reported to be similar in men and women, although disease manifestations tend to be milder in women [18]. In a large 12-year cohort of homozygous C282Y patients, clinical iron overload was observed in 28.4% of men but in only 1.2% of women [18]. In our study, the median age of patients with HFE mutations was in the fifth decade (51.5 years), consistent with previous reports. A significant age difference was observed between male and female carriers (median 45 years vs. 62 years, p=0.001). This may be attributed to the protective effect of menstruation, pregnancy, and childbirth, which tend to delay iron accumulation in women until the postmenopausal period.

When analyzed separately by sex, there was no significant difference in mean hemoglobin concentration or hematocrit levels between HFE mutation carriers and non-carriers (p=0.92 and 0.21 in males; p=0.38 and 0.36 in females). The predominance of heterozygous H63D carriers, along with only a single homozygous C282Y patient in our cohort, may partly explain these findings. We did not evaluate MCV in our study, as a substantial proportion of CMPN patients were receiving cytoreductive therapy such as hydroxyurea, and others were undergoing chemotherapy or radiotherapy for hematologic or solid malignancies, which could have confounded MCV measurements.

Initially, no relationship was thought to exist between polycythemia vera (PV) and hereditary hemochromatosis (HH). In 2002, a study screening 232 patients with various hematologic disorders for C282Y and H63D mutations found no significant association with PV [19]. Similarly, a 2004 study of 52 PV patients reported no evidence of a link with HFE mutations [5].

However, subsequent reports have suggested that coexistence may occur in rare cases. In 2016, a case report described a 75-year-old woman with concurrent HH and PV [6]. More recently, in 2021, a heterozygous C282Y mutation was identified in a 59-year-old PV patient presenting with elevated serum ferritin and transferrin saturation [18]. Although HH and PV generally appear to be unrelated conditions, these reports indicate that overlap is possible, and some authors recommend considering HH screening in PV patients, and vice versa.

In our retrospective series, one noteworthy case was a 77-year-old female patient who had been diagnosed with PV three years earlier. She was JAK2-positive, had low serum erythropoietin levels, and a history of type 2 diabetes mellitus. The patient was receiving hydroxyurea and acetylsalicylic acid (ASA) as part of her PV management. Iron metabolism in PV can be influenced by abnormal erythropoiesis, systemic inflammation, reduced iron availability, and hypoxia-driven regulation of intestinal iron absorption [18]. Moreover, gastrointestinal lesions such as erosions, ulcers, and Helicobacter pylori infection are reported more frequently in PV compared with the general population [18]. Most patients with PV exhibit iron deficiency at diagnosis, even prior to initiation of therapeutic phlebotomy, the standard treatment approach [20, 21]. Although thrombosis is the most serious complication in PV, bleeding also represents a clinically important risk. At diagnosis, the reported rates of major thrombosis and major bleeding were 24.3% and 4.3%, respectively, whereas at follow-up under cytoreductive therapy and ASA, these rates were 18.4% and 1.8% [22]. Interestingly, despite long-term ASA use and gastrointestinal complaints, this patient exhibited persistently elevated transferrin saturation (48%). HFE mutation analysis revealed heterozygous C282Y positivity.

Another case of interest in our cohort was a 72-year-old female patient with essential thrombocythemia (ET), also diagnosed with type 2 diabetes mellitus and chronic renal failure. She was negative for JAK2 V617F mutation but was receiving hydroxyurea and ASA. Although her transferrin saturation was 33%, her serum ferritin level was elevated in the absence of an inflammatory condition, with C-reactive protein values within the normal range. Genetic testing for HFE mutations was therefore performed, revealing heterozygous C282Y positivity.

In our study, two male patients carrying a homozygous C282Y mutation and one patient with a compound C282Y/H63D heterozygous mutation presented with secondary polycythemia. One of the C282Y homozygous patients was also a carrier of β-thalassemia. Despite a hemoglobin level of 16.2 g/dL, his hematocrit was 50.5%, leading to the diagnosis of secondary polycythemia. Leukocyte and platelet counts were within normal limits. Neither of the patients had a history of smoking, and no alternative cause for secondary polycythemia was identified. Additionally, a 31-year-old male patient with homozygous H63D mutation and a histo-

ry of smoking developed secondary polycythemia and required therapeutic phlebotomy. Asif et al. [9] reported that although previous studies primarily associated elevated hemoglobin levels with homozygous C282Y patients, their own findings also demonstrated increased hemoglobin levels in heterozygous carriers [11].

In a cohort of 152 patients with HFE mutations, polycythemia was observed in 33 individuals (27.7%). The authors argued that even carrier status for the HFE mutation could be associated with elevated hemoglobin and hematocrit levels, independent of serum ferritin concentration and secondary causes of polycythemia. In contrast, Khan et al. [10] reported a different perspective. Among 213 patients with HFE mutations, polycythemia was detected in 23 (10.8%) and 59 (27.6%) cases, respectively. They concluded that although hereditary hemochromatosis may confer relative protection against anemia, polycythemia does not develop in the majority of patients, and the limited available data on hemoglobin parameters do not support a high overall prevalence of polycythemia in this population. In our view, the polycythemia rates reported by the two groups appear broadly comparable.

In our study, secondary polycythemia was identified in three of seven patients with clinically significant C282Y or homozygous H63D mutations. In two of these cases, no secondary cause of polycythemia could be determined. Among the remaining patients with secondary polycythemia, heterozygous H63D mutations were detected in 21 individuals (18 males, 3 females). Overall, 24 of 106 patients screened for HFE mutations (23%) had secondary polycythemia associated with an HFE mutation. When considered in relation to mutation status, 24 of 44 patients with HFE mutations (55%) also had secondary polycythemia. We did not observe a significant difference in the distribution of patients with or without HFE mutations across the groups. It should be noted, however, that secondary polycythemia accounted for the majority of patients who underwent genetic testing due to transferrin saturation >40%, elevated ferritin relative to sex, or a clinical suspicion of HH, even though the absolute numbers were limited.

Within the secondary polycythemia group, 13 of 24 patients with HFE mutations and 16 of 28 patients without HFE mutations (including one case with undetectable H63D mutation) reported a history of smoking, with no significant difference between them (p=0.26). This finding suggests that smoking, although a well-established cause of secondary polycythemia, is not sufficient to exclude the presence of an HFE mutation Moreover, the mean transferrin saturation in Group 2 patients with secondary polycythemia was significantly lower than in Group 3 patients without polycythemia (47.0±17.5% vs. 63.9±10.4%, p=0.023). ROC analysis indicated a TS cut-off value of 51.7% for differentiating patients with and without HFE mutations and polycythemia. However, since current recommendations already use TS >45% as the threshold for HFE testing, this higher cut-off was not considered clinically useful.

Consistent with this, recent clinical guidelines for hereditary hemochromatosis emphasize that TS values above 45–50% are more diagnostically informative than hyperferritinemia [23]. In line with these recommendations, our analysis highlighted TS as a more meaningful parameter than serum ferritin when evaluating the relationship between HFE genotypes and polycythemia. While the most frequent genotypes associated with iron overload are C282Y homozygosity and C282Y/H63D compound heterozygosity, several reports have also documented iron overload and even polycythemia in patients with H63D heterozygosity. A recent case report described a patient carrying an H63D heterozygous variant who presented with iron overload and erythrocytosis [24]. Similarly, Sandnes et al. [25] demonstrated that patients with H63D heterozygosity (H63D/WT) had a median ferritin level of 711 ng/mL—comparable to homozygous variants—with ferritin >500 ng/mL observed in 91.3% and TSAT>45% in 17.4% of cases. These findings collectively suggest that H63D heterozygosity, although often considered clinically less relevant, may still contribute to increased iron burden and polycythemia in certain individuals.

Limitations

The clinical relevance of C282Y and homozygous H63D mutations in HH is well recognized. However, the relatively small number of patients carrying these mutations, as well as the overall limited number of HFE-positive cases compared with previous studies, represents a limitation of our study. Larger, prospective studies are warranted to better define these associations.

Conclusion

In this retrospective study, we demonstrated that patients with HFE mutations and polycythemia—particularly those with secondary polycythemia—exhibited significantly lower mean TS levels compared to mutation-positive patients without polycythemia. Importantly, our findings suggest that in polycythemic patients, iron parameters may appear deceptively low, likely due to increased erythrocyte mass consuming or "diluting" available iron. This phenomenon may mask underlying HFE positivity, meaning that HFE mutations can be present even at lower-than-expected TS values.

Secondary polycythemia is a common clinical condition, yet in many cases the underlying cause remains unexplained. In our cohort, the frequency of HFE positivity among patients with secondary polycythemia was relatively high, even though the difference across groups did not reach statistical significance. Taken together, these findings emphasize that measurement of TS and serum ferritin should not be overlooked in patients with secondary polycythemia, and that HFE genotyping may be considered even at lower TS thresholds when the etiology of polycythemia remains unclear. Recognizing this association is clinically relevant for patient management, particularly in guiding decisions about therapeutic phlebotomy.

Disclosures

Ethics Committee Approval: The study was approved by the Izmir Katip Çelebi University Atatürk Training and Research Hospital Clinical Research Clinical Research Ethics Committee (no: 0054, date: 21/03/2023).

Informed Consent: Informed consent was obtained from all participants.

Conflict of Interest Statement: The authors have no conflicts of interest to declare.

Funding: The authors declared that this study received no financial support.

Use of AI for Writing Assistance: No AI technologies utilized.

Authorship Contributions: Concept – S.M.S, H.D.K.U., A.S., B.P.; Design – S.M.S, H.D.K.U., A.S., B.P.; Supervision – S.M.S, H.D.K.U., A.S., B.P.; Funding – S.M.S, H.D.K.U., A.S., B.P.; Materials – S.M.S, H.D.K.U., A.S., B.P.; Data collection and/or processing – S.M.S.; Data analysis and/or interpretation – S.M.S, H.D.K.U., A.S., B.P.; Literature search – S.M.S, H.D.K.U.; Writing – S.M.S, H.D.K.U., A.S., B.P.; Critical review – S.M.S, H.D.K.U., A.S., B.P.

Peer-review: Externally peer-reviewed.

References

1. Burke W, Thomson E, Khoury MJ, McDonnell SM, Press N, et al. Consensus statement: Hereditary hemochromatosis gene discovery and its implications for population-based screening. JAMA 1998;280(2):172. [CrossRef]
2. Kawabata H. The mechanisms of systemic iron homeostasis and etiology, diagnosis, and treatment of hereditary hemochromatosis. Int J Hematol 2018;107(1):31–43. [CrossRef]
3. Fleming RE, Ponka P. Iron overload in human disease. N Engl J Med 2012;366(4):348–59. [CrossRef]
4. Swerdlow SH, Campo E, Pileri SA, Harris NL, Stein H, Siebert R, et al. The 2016 revision of the World Health Organization classification of lymphoid neoplasms. Blood 2016;127(20):2375–90. [CrossRef]
5. Franchini M, de Matteis G, Federici F, Solero P, Veneri D. Analysis of hemochromatosis gene mutations in 52 consecutive patients with polycythemia vera. Hematology 2004;9:413–4. [CrossRef]
6. Singh P, Toom S, Shrivastava MS, Solomon WB. A rare combination of genetic mutations in an elderly female: A diagnostic dilemma. Blood 2016;128(22):5487. [CrossRef]
7. Keohane C, McMullin MF, Harrison C. The diagnosis and management of erythrocytosis. BMJ 2013;347:f6667. [CrossRef]
8. Barton JC, Bertoli LF, Rothenberg BE. Peripheral blood erythrocyte parameters in hemochromatosis: Evidence for increased erythrocyte hemoglobin content. J Lab Clin Med 2000;135(1):96–104. [CrossRef]
9. Asif S, Begemann M, Raza S. Polycythemia in patients with hereditary hemochromatosis: Real or myth. J Clin Med Res 2019;11(6):422–7. [CrossRef]
10. Khan AA, Hadi Y, Hassan A, Kupec J. Polycythemia and anemia in hereditary hemochromatosis. Cureus 2020;12(4):e7607. [CrossRef]
11. Beutler E, Felitti V, Gelbart T, Ho N. The effect of HFE genotypes on measurements of iron overload in patients attending a health appraisal clinic. Ann Intern Med 2000;133(5):329–37. [CrossRef]
12. Simsek H, Sumer H, Yilmaz E, Balaban YH, Ozcebe O, Hascelik G, et al. Frequency of HFE mutations among Turkish blood donors according to transferrin saturation: Genotype screening for hereditary hemochromatosis among voluntary blood donors in Turkey. J Clin Gastroenterol 2004;38(8):671–5. [CrossRef]
13. Simsek H, Balaban YH, Yilmaz E, Sumer H, Buyukasik Y, Cengiz C, et al. Mutations of the HFE gene among Turkish hereditary hemochromatosis patients. Ann Hematol 2005;84(10):646–9. [CrossRef]
14. Yönal O, Hatirnaz O, Akyüz F, Ozbek U, Demir K, Kaymakoglu S, et al. HFE gene mutation, chronic liver disease, and iron overload in Turkey. Dig Dis Sci 2007;52(11):3298–302. [CrossRef]
15. Bozkaya H, Bektas M, Metin O, Erkan O, Ibrahimoglu D, Dalva K, et al. Screening for hemochromatosis in Turkey. Dig Dis Sci 2004;49(3):444–9. [CrossRef]
16. Yönal O, Hatirnaz O, Akyüz F, Köroğlu G, Ozbek U, Cefle K, et al. Definition of C282Y mutation in a hereditary hemochromatosis family from Turkey. Turk J Gastroenterol 2007;18(1):53–7.
17. Paşa S. Hereditary hemochromatosis gene mutations in the South Eastern Region of Turkey. Artuklu Int J Health Sci 2021;1(1):2–6. [Article in Turkish] [CrossRef]
18. Aydinol B, Yilmaz S, Genç S, Aydinol MM. Presentation of a case with C282Y mutation detected in HFE gene and research of gene mutation frequency in patient's family. Turk J Biochem 2014;39(2):150–4. [CrossRef]
19. Hannuksela J, Savolainen ER, Koistinen P, Parkkila S. Prevalence of HFE genotypes, C282Y and H63D, in patients with hematologic disorders. Haematologica 2002;87(2):131–5.
20. Thiele J, Kvasnicka HM, Muehlhausen K, Walter S, Zankovich R, Diehl V. Polycythemia rubra vera versus secondary polycythemias: A clinicopathological evaluation of distinctive features in 199 patients. Pathol Res Pract 2001;197(2):77–84. [CrossRef]
21. Gianelli U, Iurlo A, Vener C, Moro A, Fermo E, Bianchi P, et al. The significance of bone marrow biopsy and JAK2V617F mutation in the differential diagnosis between the early prepolycythemic phase of polycythemia vera and essential thrombocythemia. Am J Clin Pathol 2008;130(3):336–42. [CrossRef]
22. Passamonti F, Malabarba L, Orlandi E, Pascutto C, Brusamolino E, Astori C, et al. Pipobroman is safe and effective treatment for patients with essential thrombocythaemia at high risk of thrombosis. Br J Haematol 2002;116(4):855–61. [CrossRef]
23. Girelli D, Marchi G, Busti F. Diagnosis and management of hereditary hemochromatosis: Lifestyle modification, phlebotomy, and blood donation. Hematology Am Soc Hematol Educ Program 2024;2024(1):434–42. [CrossRef]

24. Abeyagunawardena I, Mayura S, Samarasingha P, Nawinne A, Karunatilake H. Iron overload in histidine-to-aspartic acid substitution at 63 (H63D) gene heterozygous hereditary hemochromatosis with erythrocytosis: A case report. Cureus 2024;16(12):e76335. [CrossRef]
25. Sandnes M, Vorland M, Ulvik RJ, Reikvam H. HFE genotype, ferritin levels and transferrin saturation in patients with suspected hereditary hemochromatosis. Genes 2021;12(8):1162. [CrossRef]

INTERNATIONAL JOURNAL OF
MEDICAL BIOCHEMISTRY

DOI: 10.14744/ijmb.2025.46503
Int J Med Biochem 2026;9(1):39–44

Research Article

Quercetin improves *in vitro* maturation of bovine oocytes after a post-mortem delay

Moath Abdul Munem[1], Hassan Muhdi[2], Sara Abou Baker[3], Ahmad Ayoubi[4], Dima Joujeh[1]

[1]Department of Biotechnology Engineering, University of Aleppo Faculty of Technical Engineering, Aleppo, Syria
[2]National Commission for Biotechnology (NCBT), Damascus, Syria
[3]Yashfeen Center for Assisted Fertilization and IVF at the New Arab Hospital, Damascus, Syria
[4]Department of Pharmacognosy, Ebla Private University Faculty of Pharmacy, Aleppo, Syria

Abstract

Objectives: Oocyte quality and maturation are critical factors determining successful fertilization and embryo development *in vitro*. However, delays in processing ovarian tissues after animal slaughter or collection can negatively impact oocyte viability and developmental potential. This study investigated the effect of Quercetin on the maturation of bovine oocytes subjected to a field-relevant post-mortem delay.

Methods: Oocytes were isolated from ovaries approximately six-hour delay post-collection, mimicking practical conditions encountered in tissue handling. Then, they were treated with hyaluronidase, mechanically denuded, and cultured with quercetin at concentration of 15 µg/mL, against a control group.

Results: The results demonstrated that quercetin improved the extrusion of polar bodies compared to the control group. Additionally, pH variations were noted among control and quercetin treated group, potentially influencing maturation outcomes.

Conclusion: These findings highlight that quercetin at 15 µg/mL significantly enhances the maturation of bovine oocytes, suggesting its potential to modulate oocyte quality *in vitro*.

Keywords: Bovine oocytes, *in vitro* maturation (IVM), polar body extrusion, post-mortem delay, quercetin

How to cite this article: Munem MA, Muhdi H, Baker SA, Ayoubi A, Joujeh D. Quercetin improves *in vitro* maturation of bovine oocytes after a post-mortem delay. Int J Med Biochem 2026;9(1):39–44.

High-quality mature oocytes are essential in both the livestock and biomedical fields [1]. *In vitro* maturation (IVM) has gained considerable interest as an alternative to *in vivo* maturation prior to fertilization, due to its practical advantages. Compared to conventional *in vitro* fertilization (IVF), IVM offers benefits such as shorter stimulation periods, reduced injection frequency, and lower overall costs associated with drugs and monitoring, making it valuable in medical treatments and livestock breeding programs [2]. This process is gaining popularity despite ongoing concerns about its inefficiency. Previous research has shown that oocytes matured under *in vitro* conditions are exposed to various cellular stressors, which contribute to a higher incidence of loss of competence in developed embryo compared to those developed *in vivo* [3].

In many livestock, oocytes obtained from slaughterhouse-derived ovaries serve as a primary source for large-scale *in vitro* embryo production. However, the quality of these oocytes can be adversely affected when ovaries are transported over long distances from the slaughterhouse to the laboratory. Factors such as insufficient oxygen and energy supply, along with disruptions to the endogenous antioxidant systems within the isolated ovaries, may impair the viability of follicular oocytes [4].

Address for correspondence: Dima Joujeh, MD. Department of Biotechnology Engineering, University of Aleppo Faculty of Technical Engineering, Aleppo, Syria
Phone: +963994046745 **E-mail:** dimajoujeh@gmail.com **ORCID:** 0000-0001-8240-9886
Submitted: June 10, 2025 **Revised:** October 07, 2025 **Accepted:** October 13, 2025 **Available Online:** February 18, 2025

In the natural process of *in vivo* oocyte maturation, reactive oxygen species (ROS) are effectively neutralized by antioxidant enzymes present in the follicular fluid, ensuring a controlled balance between ROS production and elimination. In contrast, oocytes matured *in vitro* lack this enzymatic defense system, leading to an imbalance that promotes the accumulation of ROS [5]. Elevated ROS levels can interfere with proper meiotic progression and impair embryonic development, ultimately reducing the overall quality of the oocytes [1].

Over recent decades, the *in vitro* production (IVP) of bovine embryos has become an increasingly important tool in the dissemination and commercialization of high-value dairy and beef genetics. In 2021 alone, more than 1.5 million IVP-derived bovine embryos were produced worldwide [6].

The objective of this study is to investigate the effect of quercetin on the *in vitro* maturation of bovine oocytes subjected to a field-relevant post-mortem delay, thereby assessing its potential to enhance oocyte quality under suboptimal collection conditions.

Materials and Methods

Ethics committee approval

Bovine ovarian tissues were collected as byproducts of routine commercial slaughter at a local abattoir. All procedures regarding tissue collection adhered strictly to local animal welfare regulations and commercial slaughter practices. Since the tissues were collected post-mortem and did not involve any *in vivo* animal sacrifice or experimental procedure, formal review and approval by an Institutional Animal Care and Use Committee (IACUC) was not required for this study.

This preliminary and exploratory study (proof-of-concept) was conducted at the laboratories of the General Commission for Biotechnology in Damascus and the Yashfeen Center for Assisted Fertilization and IVF at the New Arab Hospital. The primary objective was to evaluate the effect of quercetin on the *in vitro* maturation of bovine oocytes under delayed processing conditions.

Our experimental procedures for oocyte isolation and *in vitro* maturation were based on previously established and validated protocols, with necessary adaptations implemented to suit the specific requirements and logistical constraints of this study [7, 8].

Ovarian tissue collection and handling

Ovaries were collected from slaughtered cows at a local abattoir. They were transported to the laboratory in a sterile physiological saline solution (0.9% NaCl) at a controlled temperature of 30–35°C. A 6-hour post-mortem delay was deliberately maintained to simulate the field-relevant conditions under which ovarian tissues are typically collected and handled.

Oocyte isolation and preparation

Cumulus–oocyte complexes (COCs) were isolated from the transported ovaries using a combined approach of slicing and aspiration, as illustrated in Figure 1.

Aspiration: An 18-gauge needle attached to a 10 mL syringe was used to aspirate oocytes from visible surface follicles with diameters ranging between 2–6 mm.

Slicing: The remaining small follicles (<2 mm) were recovered by slicing the ovarian cortex tissue.

The retrieved COCs (total of 20 suitable COCs were collected and utilized across the entire study) were washed three times in a phosphate-buffered saline (PBS) solution to remove any blood or tissue debris. Subsequently, the eight (8) morphologically best-quality COCs were selected and used for immediate culture and experimentation. Following isolation, COCs were treated with a 0.1% hyaluronidase enzyme solution at 37°C for 30 seconds to enzymatically disperse the surrounding cumulus cells. This was followed by three washes in maturation medium to remove residual enzyme. Mechanical denudation was then performed by gently pipetting the oocytes through a stripper pipette with a progressively smaller bore size (170 µm) to ensure the complete removal of all cumulus cells.

In vitro maturation and experimental groups

The experiment was performed as one biological run, with the retrieved oocytes distributed into two experimental groups for direct qualitative comparison:

- **Control group:** Four (4) denuded oocytes were cultured in the maturation medium (DMEM supplemented with 10% FBS, 2 mM Glutamine and 1% penicillin/streptomycin). The medium utilized a bicarbonate buffering system and was overlaid with a layer of mineral oil to prevent evaporation and stabilize the pH.
- **Quercetin-treated group (Q15):** Four (4) denuded oocytes were cultured in the DMEM supplemented with 10% FBS, 2 mM Glutamine and 1% penicillin/streptomycin). The medium utilized a bicarbonate buffering system and was overlaid with a layer of mineral oil to prevent evaporation and stabilize the pH. The medium utilized a bicarbonate buffering system and was overlaid with a layer of mineral oil to prevent evaporation and stabilize the pH.

The quercetin stock solution was prepared by dissolving Quercetin in DMSO; the final concentration of the solvent DMSO in the culture medium did not exceed 0.1% (v/v) to ensure non-cytotoxicity. To ensure stability and bioavailability, the concentrated Quercetin stock solution was prepared fresh prior to the experiment and was subsequently stored in light-protected containers at −20°C when not in immediate use.

The culture was carried out in a humidified atmosphere at 37°C and 6% CO_2 in air (Normoxic conditions with approximately 20% O_2) for a period of 48 hours. No medium changes were performed during the 48-hour culture period. The entire procedure was performed under a strict sterile environment.

Evaluation

After the 48-hour culture period, oocytes from both groups were evaluated under an inverted microscope to assess

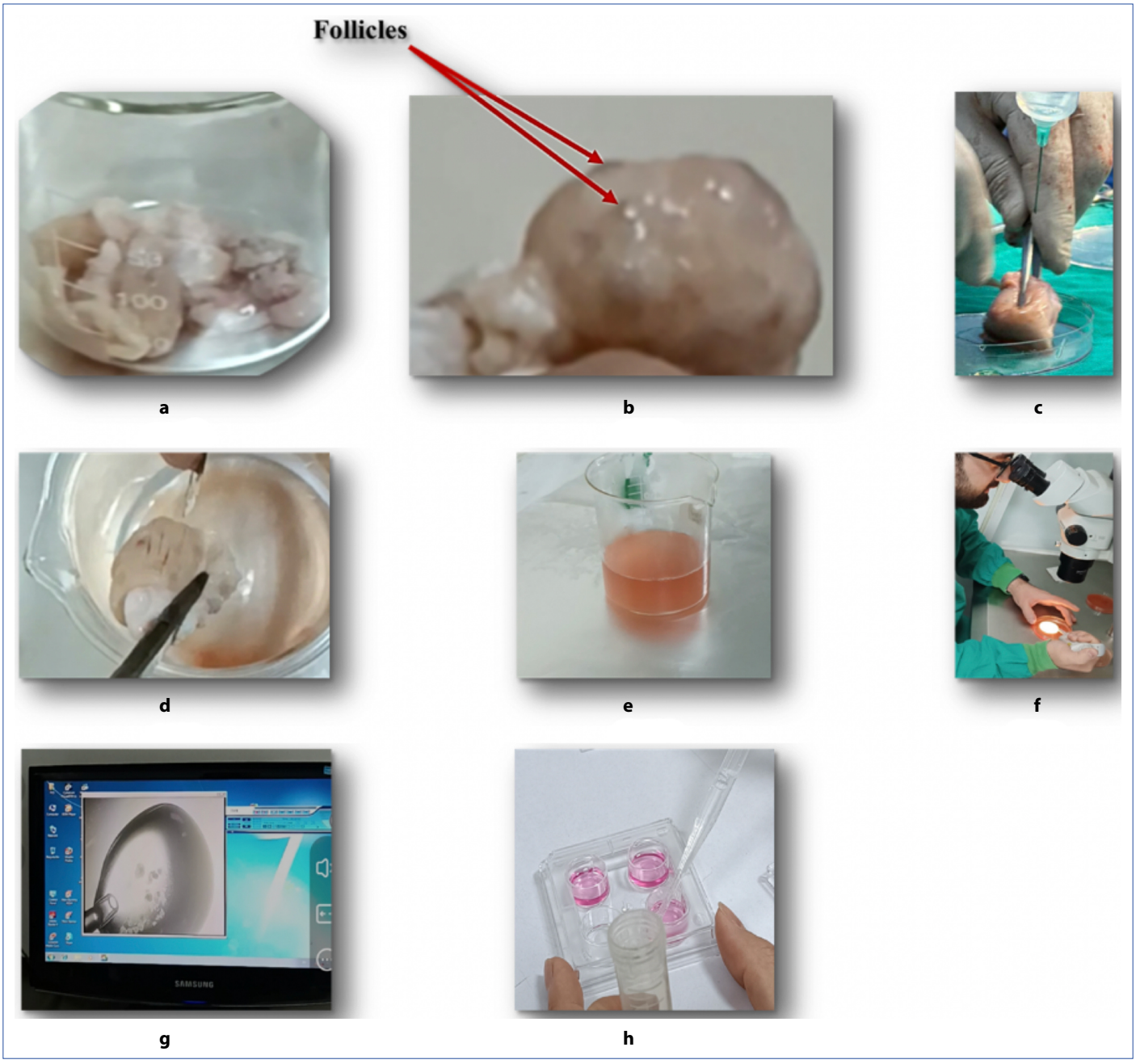

Figure 1. Bovine oocyte recovery method (Aspiration followed by slicing). (a) Collecting ovaries from the slaughterhouse, (b) bovine ovary showing visible surface follicles (indicated by arrows), (c) aspirating follicular fluid using a syringe, (d) slicing Ovaries to Recover Small Follicles and Remaining Oocytes, (e) collecting follicular fluid, (f) microscopic examination for oocytes, (g) mechanical denudation of oocytes, (h) preparing oocytes for in vitro maturation.

their maturation based on the presence and morphology of the first polar body. The pH of the maturation media was also measured.

Due to the constraints mentioned, data were analyzed as qualitative observations and comparative ratios. We acknowledge that this small sample size is insufficient for robust statistical inference. The findings are intended to establish a proof-of-concept and identify clear trends for future statistically powered studies.

Results

After 48 hours of *in vitro* culture, polar body extrusion was observed in both the control and quercetin-treated groups. In the control group, one out of four oocytes showed a polar body; however, it appeared abnormally enlarged, flat, and irregular in shape, which may indicate incomplete maturation and abnormal progression through meiosis. In contrast, in the group treated with 15 µg/mL of quercetin, three out of four oocytes exhibited normal-sized and round (normal shaped)

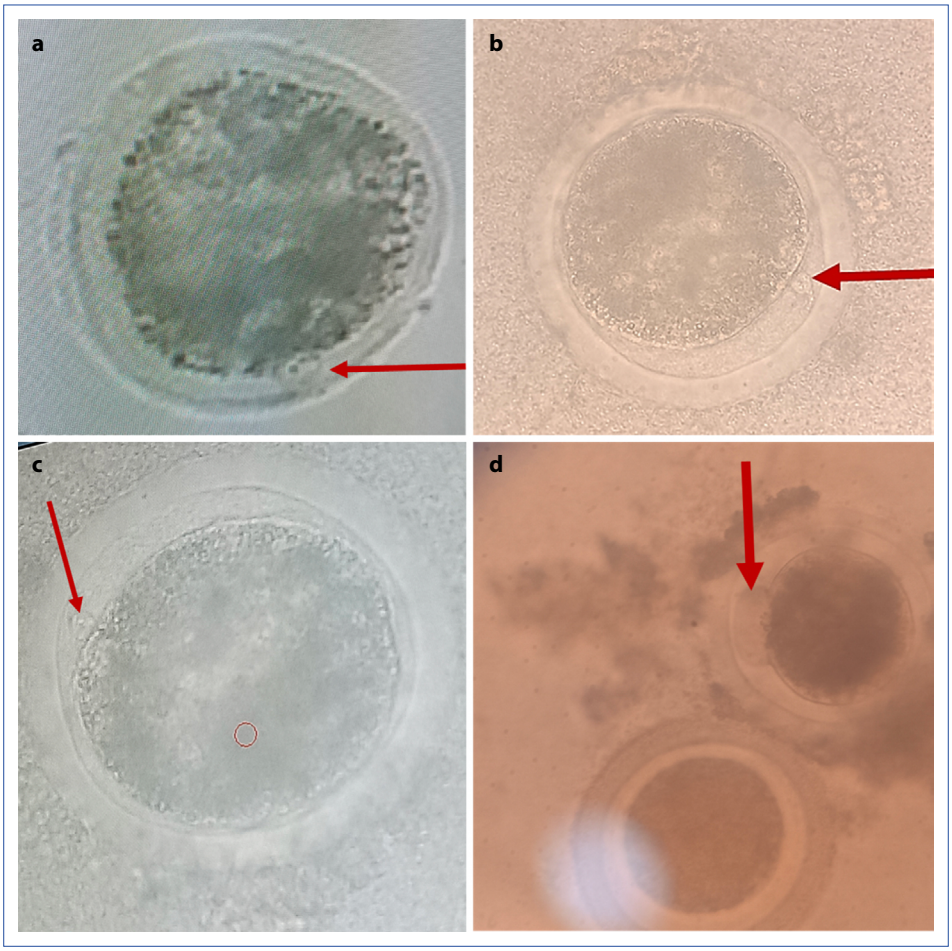

Figure 2. Bovine oocyte after 48 hours of *in vitro* culture. (a-c) Quercetin group: clearly visible first polar bodies (indicated by the arrows), suggesting completion of the first meiotic division and likely progression to the metaphase II stage. (d) Control group: A single polar body is visible (indicated by the arrow), although it appeared abnormally enlarged, flat, and irregular in shape which may reflect suboptimal maturation possibly influenced by post-mortem handling conditions.

polar bodies (Fig. 2), suggesting completion of the first meiotic division and likely progression to the metaphase II stage. These observations visually support the potential role of quercetin in enhancing oocyte maturation quality under the applied culture conditions.

The pH of the maturation media was measured after the completion of the *in vitro* culture period. The control well exhibited the highest pH value of 9.0. In comparison, the well containing quercetin at 15 µg/mL showed a slightly lower pH of 8.3. The mildly acidic shift in the quercetin-treated wells may reflect changes in the metabolic activity during culture.

Discussion

In vitro embryo production (IVP) is gaining increasing popularity despite persistent concerns about its inefficiency. This inefficiency is likely due to the inability to perfectly replicate the complex processes of oocyte maturation, fertilization, and embryo development that occur within the *in vivo* environment [6]. Consequently, exploring factors that can improve the success rates of this technology, particularly under suboptimal collection conditions, is of paramount importance.

This study was designed to investigate the effect of Quercetin, a potent natural flavonoid antioxidant, on the maturation of bovine oocytes subjected to a field-relevant post-mortem delay. The dose of 15 µg/mL of quercetin was selected based on a thorough review of existing literature, which has shown this concentration to be effective in mitigating oxidative stress and improving developmental outcomes in similar *in vitro* culture systems. This dose falls within the optimal range (10–25 µg/mL) identified by previous studies as being non-toxic and beneficial for mammalian oocytes and embryos [9].

Context, methodology, and biological constraints

Our methodology intentionally created a stress-intensive, low-support environment to clearly isolate the test compound's effect. This design involved:

Severe biological stress: Simulating a 6-hour post-mortem delay, which is known to drastically compromise oocyte viability.

Low exogenous support: The intentional omission of hormonal supplements (FSH/LH/Estradiol) ensured that the oocytes relied primarily on their intrinsic competence and the protective agent (Quercetin).

Stressful atmospheric conditions: Performing the culture under normoxic conditions (≈20% O_2) further amplified the oxidative stress, as the *in vivo* ovarian environment is naturally hypoxic (≈5% O_2).

We note that the sample size (n=4 per group) is limited. This is a direct consequence of the biological constraint—the 6-hour delay drastically reduced the pool of suitable oocytes—and establishes the context for our qualitative data analysis in this preliminary report.

The impact of stress on meiotic progression

Our findings indicate that oocytes in both groups suffered significant stress upon entry into culture, evidenced by the fact that polar body extrusion did not occur within the standard 24-hour period, instead requiring a prolonged 48-hour culture period. This delay highlights the severity of the damage inflicted by the prolonged tissue processing interval. The extended 6-hour interval between ovary collection and the start of oocyte culture is a significant source of cellular stress. During this period, oocytes are deprived of essential oxygen and nutrients, leading to a shift toward anaerobic metabolism. This shift not only depletes vital energy reserves but also promotes the accumulation of harmful reactive oxygen species (ROS), which can disrupt critical cellular structures like the meiotic spindle and impair mitochondrial function. Furthermore, these stressful conditions can induce morphological abnormalities such as cytoplasmic granulation and abnormal polar body formation, ultimately compromising oocyte viability and developmental competence. Our observations are consistent with previous reports indicating that the yield of intact, cumulus cell-enclosed oocytes decreases as the time between animal death and ovary collection increases [10].

Quercetin's role in enhancing meiotic competence

Despite the challenging conditions, our results show a clear qualitative difference driven by Quercetin:

Morphological failure: The control group extruded a polar body that appeared abnormally enlarged, flat, and irregular in shape. This highly specific morphological defect is a strong indicator of aberrant cytoplasmic division and severe meiotic spindle dysfunction, often linked to oxidative stress.

Morphological success: In stark contrast, the Quercetin-treated oocytes produced polar bodies that were normal in size and possessed the characteristic spherical, regular shape. This confirms that Quercetin enabled the oocytes to complete the first meiotic division (Meiosis I) correctly.

This significant improvement is attributable to Quercetin's potent antioxidant properties. It successfully neutralized accumulating ROS and helped preserve the integrity of the meiotic spindle, thereby maintaining the cellular architecture essential for accurate chromosome segregation.

Metabolic health and pH analysis

The measurement of the culture medium's pH provides further evidence of Quercetin's protective function:

- **Control group (pH=9.0):** The excessively high pH suggests severely compromised cellular metabolism and the inability to produce stabilizing acidic byproducts.
- **Quercetin group (pH=8.3):** The significantly lower pH indicates that Quercetin supported a more physiologically active and balanced metabolic state. This pH stabilization confirms that Quercetin enhanced the oocyte's intrinsic metabolic resilience, allowing it to better regulate its internal environment despite the imposed stress.

Conclusion

This preliminary study provides compelling, non-random qualitative evidence that Quercetin significantly improves key indicators of oocyte quality (normal polar body morphology and metabolic stabilization) under severe stress conditions.

These strong qualitative findings form the essential foundation for a future, larger-scale study that will incorporate numerous biological replicates and power analysis to quantitatively confirm these beneficial effects and definitively validate Quercetin's role as a resilience-enhancing agent in *in vitro* maturation protocols.

Informed Consent: Informed consent was obtained from all participants.

Conflict of Interest Statement: The authors have no conflicts of interest to declare.

Funding: University of Aleppo, National Commission for Biotechnology (NCBT), Damascus, Syria, and New Arab hospital, Damascus, Syria.

Use of AI for Writing Assistance: No AI technologies utilized.

Authorship Contributions: Concept – M.A.M., D.J.; Design – M.A.M., D.J.; Supervision – M.A.M., D.J.; Data collection and/or processing – M.A.M., H.M., S.A.B., A.A., D.J.; Data analysis and/or interpretation – M.A.M., H.M., S.A.B., A.A., D.J.; Literature search – D.J.; Writing – D.J.; Critical review – M.A.M., H.M., S.A.B., A.A., D.J.

Peer-review: Externally peer-reviewed.

References

1. Shi W, Qin C, Yang Y, Yang X, Fang Y, Zhang B, et al. Urolithin A protects porcine oocytes from artificially induced oxidative stress damage to enhance oocyte maturation and subsequent embryo development. Int J Mol Sci 2025;26(7):3037. [CrossRef]
2. Zhao Y, Zhiqiang E, Jiao A, Sun Z, Zhang H, Wang H, et al. Dendrobine enhances bovine oocyte maturation and subsequent embryonic development and quality. Theriogenology 2023;203:53–60. [CrossRef]
3. Pioltine EM, Costa CB, Barbosa Latorraca L, Franchi FF, Dos Santos PH, Mingoti GZ, et al. Treatment of *in vitro*-matured bovine oocytes with tauroursodeoxycholic acid modulates the oxidative stress signaling pathway. Front Cell Dev Biol 2021;9:623852. [CrossRef]

4. Sun WS, Jang H, Park MR, Oh KB, Lee H, Hwang S, et al. N-acetyl-L-cysteine improves the developmental competence of bovine oocytes and embryos cultured *in vitro* by attenuating oxidative damage and apoptosis. Antioxidants 2021;10(6):860. [CrossRef]
5. Wang Y, Qi JJ, Yin YJ, Jiang H, Zhang JB, Liang S, et al. Ferulic acid enhances oocyte maturation and the subsequent development of bovine oocytes. Int J Mol Sci 2023;24(19):14804. [CrossRef]
6. Keane JA, Ealy AD. An overview of reactive oxygen species damage occurring during *in vitro* bovine oocyte and embryo development and the efficacy of antioxidant use to limit these adverse effects. Animals 2024;14(2):330. [CrossRef]
7. Takada L, Junior A, Mingoti G, Balieiro J, Coelho L. Melatonin in maturation media fails to improve oocyte maturation, embryo development rates and DNA damage of bovine embryos. Sci Agric (Piracicaba, Braz) 2010;67(4):393–8. [CrossRef]
8. Blancas-Alvarez LA, Alvarez-Guerrero AL, Alcantar-Rodriguez A, Medrano A. Effects of melatonin on *in vitro* oocyte maturation and embryo development in pigs. Vet World 2025;18(5):1234. [CrossRef]
9. Kang JT, Kwon DK, Park SJ, Kim SJ, Moon JH, Koo OJ, et al. Quercetin improves the *in vitro* development of porcine oocytes by decreasing reactive oxygen species levels. J Vet Sci 2013;14(1):15. [CrossRef]
10. Schroeder AC, Johnston D, Eppig JJ. Reversal of postmortem degeneration of mouse oocytes during meiotic maturation *in vitro*. J Exp Zool 1991;258(2):240–5. [CrossRef]

INTERNATIONAL JOURNAL OF
MEDICAL BIOCHEMISTRY

DOI: 10.14744/ijmb.2025.02693
Int J Med Biochem 2026;9(1):45–54

Research Article

C-reactive protein/albumin ratio in non-ST elevation myocardial infarction: Determining its predictive value for mortality

Mine Busra Bozkurk[1], **Veysel Ozan Tanik**[2]

[1]Department of Biochemistry, Etlik City Hospital, Ankara, Türkiye
[2]Department of Cardiology, Etlik City Hospital, Ankara, Türkiye

Abstract

Objectives: Although the C-reactive protein/albumin ratio is accepted as a current biomarker in many diseases, such as myocardial infarction, studies on its clinical relevance in patients diagnosed with non-ST elevation myocardial infarction (NSTEMI) are limited. This study aimed to evaluate the prognostic significance of the C-reactive protein/albumin ratio in patients with NSTEMI.

Methods: This retrospective study included 300 patients diagnosed with NSTEMI. All patients were compared in terms of survival status and clinical, biochemical, and inflammatory markers. Logistic regression and receiver operating characteristic (ROC) curve analyses were used to determine the predictive value of CRP, albumin, and the CRP/albumin ratio.

Results: The CRP/ALB ratio was significantly higher in the mortality group than in the survivor group (p=0.001), whereas albumin levels were significantly lower (p=0.001). This ratio had a strong positive correlation with the CHA_2DS_2–VASc score (ρ=0.711, p<0.001) and independently predicted in-hospital mortality (OR=1.485, p=0.046). ROC analysis revealed an area under the curve (AUC) of 0.891 for the CRP/albumin ratio, which was significantly better than that of CRP or albumin alone (p<0.001). Although the combined CRP-albumin model had a slightly higher AUC (0.894), it was not significantly different from the C-reactive protein/albumin ratio.

Conclusion: The CRP/ALB ratio is a strong and independent predictor of in-hospital mortality in patients with NSTEMI. As an easily accessible and cost-effective biomarker, it provides valuable prognostic information and may improve early risk stratification and treatment strategies in clinical settings.

Keywords: Albumin, c-reactive protein, CRP/albumin ratio, inflammation, non-ST elevation myocardial infarction

How to cite this article: Bozkurk MB, Tanik VO. C-reactive protein/albumin ratio in non-ST elevation myocardial infarction: Determining its predictive value for mortality. Int J Med Biochem 2026;9(1):45–54

Non-ST-segment elevation myocardial infarction (NSTEMI) is a dangerous form of acute coronary syndrome (ACS) and remains one of the leading causes of morbidity and mortality. Although the specific changes on the electrocardiogram are less pronounced than those seen in ST-segment elevation myocardial infarction (STEMI), patients diagnosed with NSTEMI experience worse post-discharge outcomes than those with STEMI on their ECG [1]. For all these reasons, the urgent need for NSTEMI diagnosis, evidence-based risk stratification, and implementation of patient-specific treatment decisions is essential.

Risk stratification is crucial for NSTEMI treatment. Patients at high risk undergo invasive procedures earlier [2]. Therefore, risk stratification is highly effective in prognosis, and early and accurate implementation reduces mortality and morbidity [2, 3]. In recent years, the number of studies on inflammatory markers for risk assessment in patients with ACS has increased significantly [4–6]. Potentially useful biomarkers, such as C-reactive protein (CRP) and the CRP/albumin ratio (CAR), are available for measuring the clinical severity and predicting the prognosis of this group of diseases.

Address for correspondence: Mine Busra Bozkurk, MD. Department of Biochemistry, Etlik City Hospital, Ankara, Türkiye
Phone: +90 537 403 96 88 **E-mail:** drminebusra@gmail.com **ORCID:** 0000-0002-9329-3513
Submitted: August 15, 2025 **Revised:** October 07, 2025 **Accepted:** October 08, 2025 **Available Online:** February 18, 2025

CAR has been associated with thrombus burden and poor outcomes in patients [6–8]. Although some studies have been conducted on patients with NSTEMI, the results are more limited [9–12]. These studies have found a correlation between CAR and contrast-induced nephropathy, arterial occlusion, and hospital mortality in patients with STEMI elevation myocardial infarction. All studies and emerging evidence suggest that inflammation plays a direct or indirect role in the pathophysiology of NSTEMI.

Recent evidence supports the prognostic relevance of the CAR in cardiovascular diseases. A large prospective analysis from the UK Biobank demonstrated its association with cardiovascular outcomes and mortality [13]. A meta-analysis published in 2023 confirmed that an elevated CAR predicts adverse outcomes and mortality in different populations [14]. Furthermore, the CAR has been shown to be a useful prognostic biomarker in heart failure [15].

Therefore, this study aimed to investigate the prognostic value of the C-reactive protein/albumin ratio in patients diagnosed with NSTEMI. Unlike previous studies that mainly focused on STEMI populations, our study uniquely evaluated this biomarker specifically in NSTEMI patients, providing novel insights into its role in predicting in-hospital mortality.

Materials and Methods

The study protocol was approved by the Ankara Etlik City Hospital Ethics Committee (Date: 30/04/2025, No: 2025-0285) and conducted according to the Helsinki Declaration.

Study setting and study population

Our study evaluated patients aged 18–80 years who presented to the Etlik City Hospital with NSTEMI between January 2023 and December 2024. Three hundred patients with NSTEMI were retrospectively analyzed and divided into patient and control groups based on morbidity and mortality. Patients younger than 18 years, those diagnosed with MI other than NSTEMI, those with incomplete medical data, those with a previous diagnosis of AF, those with a history of antiarrhythmic therapy, those with end-stage renal disease, those with acute or chronic infections, and those with chronic inflammatory diseases were excluded from the study.Clinical characteristics, including a history of hypertension, diabetes mellitus, and heart failure, as well as medication use (β-blockers, ACE inhibitors or angiotensin receptor blockers, and statins), were recorded from the hospital electronic records. Patients with acute or chronic infections, chronic inflammatory or dermatologic diseases, malignancy, or those receiving corticosteroid or immunosuppressive therapy were excluded to minimize potential confounding effects on the inflammatory and biochemical parameters. CRP, albumin, mortality, length of hospital stay, CHA_2DS_2–VASc score, age, sex, blood pressure, body mass index, complete blood count parameters, biochemical parameters, and troponin parameters of the study population were retrospectively analyzed. The CHA_2DS_2–VASc score, which incorporates congestive heart failure, hypertension, age, diabetes mellitus, prior stroke or transient ischemic attack, vascular disease, and sex category, was calculated for each patient to assess the overall cardiovascular risk burden.

Venous blood samples were collected from all patients within the first 24 h after admission, prior to the initiation of specific medical therapy. Samples were obtained from the antecubital vein after at least 8 h of fasting and drawn into serum separator tubes. After centrifugation at 3500 rpm for 10 min, the serum was promptly separated and analyzed.

All biochemical and cardiac parameters were measured using a Roche Cobas 8000 modular analyzer (Roche Diagnostics, Mannheim, Germany). Serum CRP levels were determined using an immunoturbidimetric method, while albumin concentrations and other routine biochemical parameters were measured using enzymatic colorimetric methods on the same system.

High-sensitivity troponin T (HsTropT) was analyzed using the Roche Cobas 8000 e801 module employing the electrochemiluminescence immunoassay (ECLIA) principle. Complete blood count (CBC) parameters were measured using a Sysmex XN-1000 automated hematology analyzer (Sysmex Corporation, Kobe, Japan).

Statistical analysis

All statistical analyses were performed using SPSS version 23 (IBM Corp., Armonk, NY, USA), MedCalc version 23.2.8 (MedCalc Software Ltd., Ostend, Belgium), the Analyze-it add-in for Microsoft Excel (Analyze-it Software, Ltd., Leeds, UK), and R version 4.3.1 (R Foundation for Statistical Computing, Vienna, Austria). Data visualization and multivariate modeling in R were conducted using the mixOmics and ggplot2 packages.

The normality of the distribution was assessed using the Shapiro–Wilk test. As most continuous variables did not follow a normal distribution, they were summarized using median and interquartile ranges (25^{th}–75^{th} percentiles) and compared between groups using the Mann–Whitney U test. Categorical variables are presented as counts and percentages and were compared using the chi-square test or Fisher's exact test, where appropriate.

To evaluate the strength and direction of associations between inflammatory markers (CRP, albumin, and CRP/albumin ratio) and clinical variables (e.g., CHA_2DS_2–VASc score, length of hospital stay, and age), Spearman's rank correlation coefficient (ρ) was used because of the nonparametric nature of the data. The complete correlation matrix was visualized as a heatmap using R.

The diagnostic performance of albumin, CRP, and the CRP-to-albumin ratio in predicting in-hospital mortality was assessed using Receiver Operating Characteristic (ROC) curve analysis. The area Under the Curve (AUC) values and their 95% confidence intervals were calculated and compared using the DeLong test for correlated ROC curves. Pairwise AUC comparisons were performed using MedCalc, and the optimal cutoff values for each biomarker were determined based on the Youden index.

Table 1. Distribution of CRP/albumin ratio and related clinical parameters in NSTEMI patients

	Median (25/75%)	95% CI of median	Min-max
Gender, n (%)			
Female	93 (31)		
Male	207 (69)		
Mortality, n (%)			
Alive	271 (90.3)		
Deceased	29 (9.76)		
Age (year)	64 (55–74)	63–66	32–100
CHA_2DS_2–VASc	3.5 (1–6)	3–4	0–7
Length of Hospital stay	19 (11–26)	18–22	2–39
WBC ($\times 10^9$/L)	12.1 (10.1–14)	11.7–12.7	8.3–15.9
HGB (g/dL)	13.6 (12.2–15)	13.3–14	11.2–16.2
Neutrophil ($\times 10^9$/L)	4.9 (3.4–6.4)	4.5–5.2	1.7–8.5
Lymphocyte ($\times 10^9$/L)	2.3 (1.4–3.3)	2.2–2.5	0.7–4.1
HsTropT (pg/mL)	41 (24–61.5)	38–47	7–81
HbA1c (%)	6.7 (6–7.4)	6.6–6.9	5.3–8.1
Glucose (mg/dL)	121 (85–155.5)	115–129	54–189
Total cholesterol (mg/dL)	196.5 (150.5–246)	189–208	95–291
HDL (mg/dL)	45 (37–51)	44–47	29–59
LDL (mg/dL)	143 (120–167)	141–148	94–191
ALT (U/L)	52 (43–61.5)	51–54	34–71
TG (mg/dL)	140 (107–172)	133–148	74–211
Albumin (g/dL)	3.3 (2.7–4)	3.2–3.5	2.1–4.5
CRP (mg/L)	49.5 (30–68.5)	45–55	4–93
CRP/albumin ratio	14.8 (8.86–20.7)	14.1–15.85	1.16–40.4

CRP: C-reactive protein; NSTEMI: non-ST elevation myocardial infarction; CI: Confidence interval; WBC: White blood cells; HGB: hemoglobin, HsTropT: High-sensitivity troponin T; HbA1c: Hemoglobin A1c, HDL: High-density lipoprotein; LDL: low-density lipoprotein, ALT: Alanine aminotransferase; TG: Triglyceride; CRP: C-reactive protein.

A binary logistic regression model was constructed to identify independent predictors of in-hospital mortality. The model included demographic, hematological, metabolic, hepatic, and inflammatory variables of the patients. The enter method was used, and odds ratios (OR) with 95% confidence intervals were reported for the results. Multicollinearity was checked using variance inflation factors (VIFs), and model calibration was evaluated using the Hosmer–Lemeshow goodness-of-fit test.

For multivariate class discrimination between alive and deceased patients, Partial Least Squares Discriminant Analysis (PLS-DA) was performed using the mixOmics::plsda() function in R. This supervised multivariate technique was selected because of its robustness in handling collinearity and its ability to model small sample sizes. The analysis focused on three variables: CRP, albumin, and the CRP/albumin ratio. The model was validated using leave-one-out cross-validation (LOOCV), and the variance explained by each component was reported as follows: Visualization included pairwise component scatter plots, biplots, and 2D/3D score plots to illustrate class separation.

Multiple hypothesis testing was adjusted using the Bonferroni correction, where appropriate, especially for post hoc comparisons after the univariate analyses. Statistical significance was set at $p<0.05$.

Results

A total of 300 patients diagnosed with NSTEMI were included in the study. The majority of the study population was male (69%), and the median age was 64 years (IQR, 55–74). The overall in-hospital mortality rate was 9.7%. The distributions of the biochemical and inflammatory parameters are summarized in Table 1.

Hepatic enzyme (ALT) levels and triglyceride values also showed a wide distribution, which may have been influenced by comorbid metabolic conditions. In terms of inflammation and nutritional status, CRP and albumin levels varied significantly among individuals. In particular, the CRP/albumin ratio showed a wide range and interquartile range, suggesting significant differences in systemic inflammation and nutritional reserves among the patients. Cardiac injury markers, including Hs-TropT, showed elevated values consistent with acute myocardial injury, further supporting the diagnosis.

A significant and strong positive correlation was found between the CAR and the CHA_2DS_2–VASc score ($\rho=0.711$, $p<0.001$), whereas serum albumin showed a moderate negative correlation ($\rho=-0.307$, $p<0.001$) (Table 2, Fig. 1). This indicates that patients with higher systemic inflammation exhibit higher cardiovascular risk profiles.

Table 2. Spearman correlation heatmap of CRP, albumin, and composite ratio with selected clinical variables

Spearman's rs	Age	CHA_2DS_2–VASc	Length of Hospital stay	Albumin	CRP	CRP/albumin ratio
Age	–	-0.121	-0.123	-0.004	-0.076	-0.077
CHA_2DS_2–VASc	-0.121	–	0.114	-0.307	0.689	0.711
Length of Hospital stay	-0.123	0.114	–	-0.066	0.115	0.142
Albumin	-0.004	-0.307	-0.066	–	-0.124	-0.430
CRP	-0.076	0.689	0.115	-0.124	–	0.930
CRP/albumin ratio	-0.077	0.711	0.142	-0.430	0.930	–
HsTropT	-0.096	0.073	0.086	-0.043	0.037	0.057
Neutrophil (×10^9/L)	-0.019	-0.028	-0.008	-0.021	-0.011	-0.020
Lymphocyte (×10^9/L)	-0.028	-0.011	-0.064	0.036	0.018	-0.003
Total cholesterol	0.092	-0.061	-0.070	0.080	-0.052	-0.076
HDL	0.062	0.086	0.003	-0.147	-0.025	0.026
LDL	-0.030	-0.008	0.046	-0.023	0.019	0.031
TG	-0.051	0.052	0.029	-0.012	0.053	0.056

CRP: C-reactive protein; HsTropT: high-sensitivity troponin T; HDL: High-density lipoprotein; LDL: Low-density lipoprotein; TG: Triglyceride

Additionally, albumin levels exhibited a moderate inverse correlation with the CHA_2DS_2–VASc score (ρ=-0.307, p<0.001), further supporting the value of combining inflammatory and nutritional markers. The complete correlation matrix is presented in Appendix 1, which includes extended relationships among hematologic, metabolic, and inflammatory parameters.

These findings highlight the potential utility of the CAR as a composite biomarker that reflects both inflammatory status and cardiovascular risk, particularly in elderly patients with NSTEMI.

When patients were categorized according to in-hospital mortality status, 271 (90.3%) were survivors and 29 (9.7%) were non-survivors. As summarized in Table 3, patients in the deceased group had significantly higher CRP (p=0.001) and CRP/albumin ratio values (p=0.001), whereas albumin levels were significantly lower (p=0.001) compared with survivors. No statistically significant differences were observed between the two groups in terms of age (p=0.415), sex (p=0.676), glucose (p=0.952), or lipid profile parameters (p>0.05 for all).

These findings suggest that the CRP-to-albumin ratio may serve as a strong discriminator of in-hospital mortality in patients with NSTEMI, likely reflecting the combined impact of systemic inflammation and nutritional status on clinical outcomes.

In the multivariate logistic regression analysis, only the CAR remained an independent predictor of in-hospital mortality (OR=1.485, 95% CI=1.007–2.190, p=0.046), whereas CRP, albumin, and other biochemical markers were not statistically significant (Table 4).

This reinforces the utility of the CAR as a practical and independent biomarker for identifying patients at a higher risk of adverse outcomes during hospitalization.

Receiver operating characteristic (ROC) analysis demonstrated an AUC of 0.891 (95% CI: 0.850–0.924, p<0.001) for the CRP/albumin ratio, which was significantly higher than for CRP (p<0.0001) or albumin alone (p=0.0028). These results confirm the superior discriminative power of the CAR in predicting in-hospital mortality among patients with NSTEMI (Table 5, Fig. 2).

Pairwise comparisons of AUCs confirmed that the CAR was significantly better than albumin (p=0.0028) and CRP (p<0.0001). In contrast, there was no significant difference between the predictive abilities of albumin and CRP alone (p=0.8296), suggesting comparable but individually limited prognostic utilities. The combined model (CRP + albumin) yielded a slightly higher AUC than the CRP/albumin ratio alone (0.894 vs. 0.891), but this difference was not

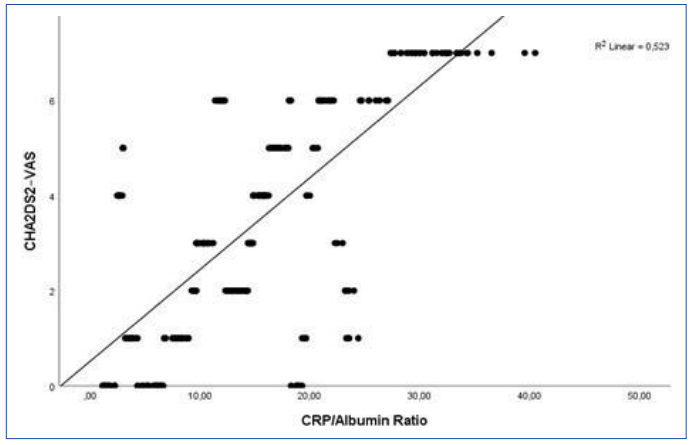

Figure 1. Scatter Plot depicting the association between systemic inflammation (CRP/albumin ratio) and cardiovascular risk burden (CHA_2DS_2–VASc).

CRP: C-reactive protein.

Table 3. Comparison of demographic, haematological, biochemical, and inflammatory parameters between alive and deceased NSTEMI patients

	Alive (n=271)	Deceased (n=29)	p
Gender, n (%)			
Female	85 (91.4)	8 (8.6)	0.676
Male	186 (89.8)	21 (10.3)	
Age (year)	64 (55–74)	64 (54–72)	0.415
CHA_2DS_2–VASc	3 (1–5)	7 (6–7)	0.001
Length of Hospital stay	18 (10–26)	27 (22–30)	0.001
WBC ($\times 10^9$/L)	12.1 (10.1–14.1)	12 (10.1–13.4)	0.803
HGB (g/dL)	13.6 (12.2–15.1)	13.4 (12.3–14.6)	0.506
Neutrophil ($\times 10^9$/L)	5.00 (3.50–6.40)	4.61 (3.12–5.21)	0.127
Lymphocyte ($\times 10^9$/L)	2.4 (1.4–3.3)	2 (1.5–2.8)	0.678
HsTropT (pg/mL)	40 (23–61)	50 (31–67)	0.082
HbA1c (%)	6.60 (5.90–7.40)	6.9 (6.2–7.3)	0.593
Glucose (mg/dL)	121 (87–154)	126 (82–163)	0.952
Total Cholesterol (mg/dL)	198(155–250)	185 (143–221)	0.293
HDL (mg/dL)	44 (37–50)	48 (42–54)	0.069
LDL (mg/dL)	144 (121–169)	142 (116–160)	0.560
ALT (U/L)	52 (43–62)	48 (41–56)	0.111
TG (mg/dL)	140 (106–171)	163 (112–182)	0.427
Albumin (g/dL)	3.4 (2.8–4)	2.6 (2.4–2.8)	0.001
CRP (mg/L)	46 (27–65)	75 (64–82)	0.001
CRP/albumin ratio	14.3 (8.25–18.29)	29.5 (21.79–33.3)	0.001

The results were expressed as Median (25–75%). Gender was expressed as count and %. NSTEMI: Non-ST elevation myocardial infarction; WBC: White blood cells; HGB: Hemoglobin; HsTropT: High-sensitivity troponin T; HbA1c: Hemoglobin A1c; HDL: High-density lipoprotein; LDL: Low-density lipoprotein; ALT: Alanine aminotransferase; TG: Triglyceride; CRP: C-reactive protein.

statistically significant, indicating that the ratio itself may encapsulate much of the predictive value of the two parameters (Fig. 3).

The optimal threshold for the combined logistic model was calculated as 0.085, based on Youden's index. This cutoff provided a sensitivity of 89% (73–98%) and specificity of 79% (74–84%), indicating strong discriminatory performance.

Taken together, these results support the use of the CRP-to-albumin ratio as a single, practical, and statistically superior biomarker for risk stratification in patients with NSTEMI, with a performance comparable to that of a multivariate logistic model combining CRP and albumin.

PLS-DA was applied to assess the discriminative ability of albumin, CRP, and the CRP/albumin ratio in differentiating between patients who survived and those who died during hospitalization. The model was constructed using these three variables as predictors, with mortality as the outcome variable.

The pairwise scatter plot matrix (Fig. 4a) indicates that Component 1 alone captured the majority of the variance (100%) relevant for class discrimination, whereas Components 2 and 3 contributed minimally (0%). The dominance of Component 1 suggests that the combination of CRP and albumin-based variables contains strong discriminatory information.

The biplot (Fig. 4b) revealed distinct clustering of alive versus deceased patients along Component 1, with the CRP/albumin ratio emerging as the most influential variable in the model. This finding is consistent with previous ROC analyses, which showed the highest AUC for the CRP-to-albumin ratio.

In the 2D score plot (Fig. 4c), a clear separation between the alive (green) and deceased (red) groups was observed, despite some overlap between the groups. The 3D score plot (Fig. 4d) further confirmed this separation, suggesting that these biomarkers, when used in combination, provide a meaningful projection space for classifying mortality risk.

Overall, the PLS-DA model supports the hypothesis that combining CRP and albumin levels and their ratio enhances the ability to distinguish patients with poor in-hospital outcomes, underscoring their clinical relevance in early mortality risk stratification.

Panel A presents a pairwise scatter plot matrix that illustrates the distribution and relationships between the components extracted using PLS-DA. Notably, Component 1 accounted for 100% of the explained variance, indicating that it captured the most substantial discriminative information between patient groups. Panel B shows the biplot, where a distinct separation between deceased (red) and alive (green) patients is evident along the first principal component (PC1) axis. Among the

Table 4. Multivariate logistic regression analysis of demographic, hematologic, biochemical, and inflammatory variables for predicting in-hospital mortality in NSTEMI patients

	B	Wald	Significance	Odds ratio Exp(B)	95% CI for Exp(B)	
					Lower	Upper
Age	-0.004	0.037	0.848	0.996	0.955	1.038
CHA_2DS_2–VASc	-0.016	0.009	0.926	0.984	0.706	1.372
WBC	-0.002	0.000	0.988	0.998	0.780	1.278
HGB	-0.094	0.314	0.575	0.910	0.655	1.265
Neutrophil	-0.117	0.592	0.441	0.889	0.660	1.199
Lymphocyte	-0.107	0.191	0.662	0.899	0.557	1.450
HsTropT	0.013	1.045	0.307	1.013	0.988	1.039
HbA1c	0.534	2.234	0.135	1.705	0.847	3.434
Glucose	-0.007	1.079	0.299	0.993	0.979	1.006
Total cholesterol	0.002	0.188	0.665	1.002	0.993	1.012
HDL	0.028	0.734	0.392	1.028	0.965	1.096
LDL	-0.015	2.371	0.124	0.985	0.967	1.004
ALT	0.000	0.000	0.990	1.000	0.953	1.051
TG	-0.001	0.042	0.837	0.999	0.986	1.012
Albumin	0.501	0.134	0.715	1.650	0.112	24.244
CRP	-0.071	1.107	0.293	0.932	0.817	1.063
CRP/albumin ratio	0.395	3.974	0.046	1.485	1.007	2.190
Constant	-8.086	1.504	0.220	0.000		

NSTEMI: Non-ST elevation myocardial infarction; WBC: White blood cells; HGB: Hemoglobin; HsTropT: High-sensitivity troponin T; HbA1c: Hemoglobin A1c; HDL: High-density lipoprotein; LDL: Low-density lipoprotein; ALT: Alanine aminotransferase; TG: Triglyceride; CRP: C-reactive protein.

Table 5. Diagnostic performance of albumin, CRP, CRP/albumin ratio, and CRP-albumin combination in predicting in-hospital mortality

Variable	Cut-off	Sensitivity	Specificity	AUC
Albumin	≤3.1	90 (72–93)	58 (52–64)	0.808[a] (0.756–0.851
CRP	>60	86 (62–96)	67 (61–73)	0.817[a] (0.768–0.859)
CRP/albumin ratio	>20.28	89 (72–98)	80 (75–85)	0.891[b] (0.85–0.924)
CRP-albumin combination	>0.085	89 (73–98)	79 (74–84)	0.894[b] (0.85–0.931)

Different letters in the same column indicate statistically significant differences. CRP: C-reactive protein; AUC: Area under the curve.

variables, the CRP/Albumin Ratio appeared to be the most influential in driving this separation. Panel C displays the two-dimensional scores plot, which reveals a partial overlap between groups but also demonstrates a discernible clustering pattern, suggesting meaningful group differentiation along Component 1. Panel D illustrates the three-dimensional scores plot, offering a spatial view of the component distribution and further emphasizing the separation between alive and deceased patients in the multivariate space defined by the first three components.

Discussion

In our study, we demonstrated that the CRP-to-albumin ratio is a significant and independent predictor of mortality during hospitalization in patients with NSTEMI. This biomarker is important and clinically relevant because it indicates systemic inflammation and malnutrition. Both factors are essential for understanding the clinical outcomes of acute coronary syndromes. In acute myocardial infarction, the body's physiological stress response can be determined much more accurately using this ratio than using CRP or albumin alone.

Patients who died had significantly higher CRP/albumin ratios and significantly lower albumin levels than those who survived did. This association has also been found in some NSTEMI cohort studies in 2022 and 2020, which reported that patients in these cohorts had significantly higher CRP/albumin ratios and significantly lower albumin levels than those without NSTEMI. [9, 16]. One of the many striking results of our study is that the correlation between the CRP/albumin ratio and the CHA_2DS_2–VASc score was stronger

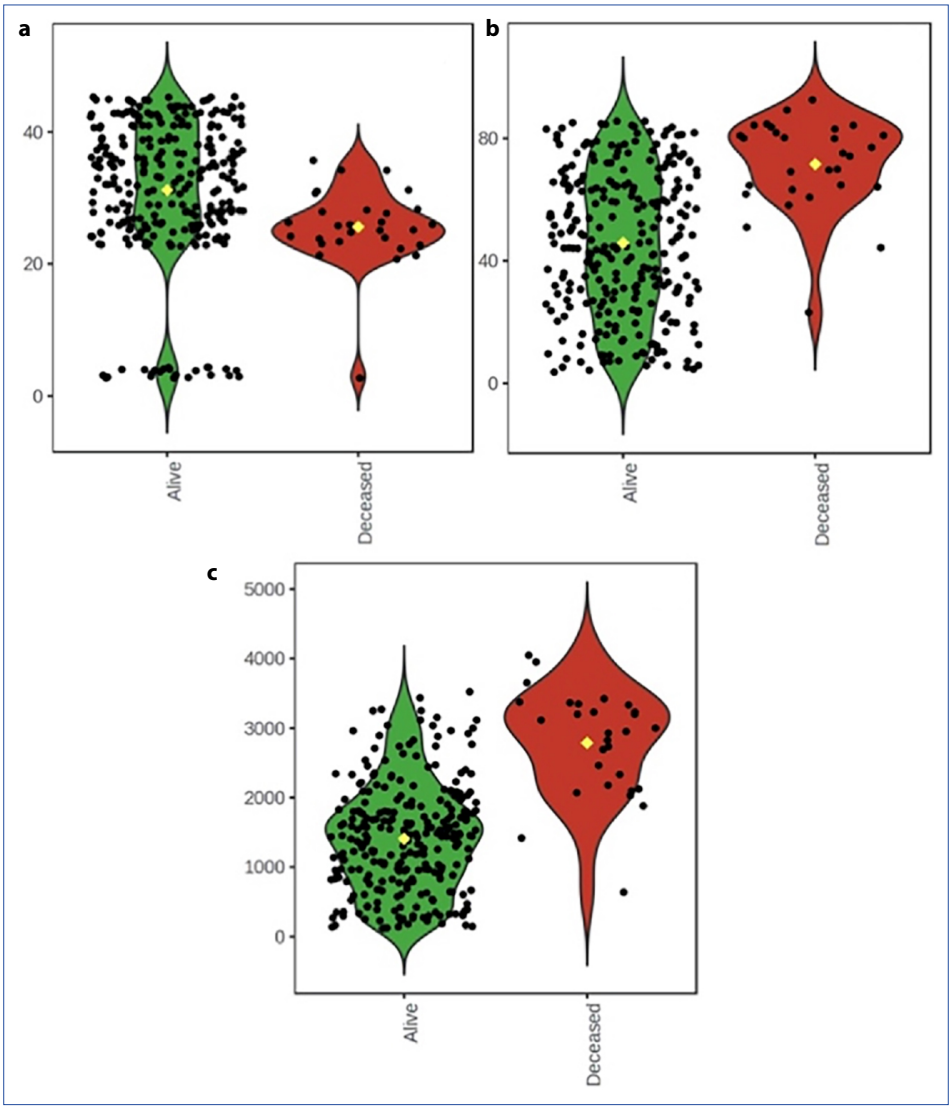

Figure 2. Violin plot comparison of albumin, CRP, and CRP/albumin ratio between alive and deceased non-survivors in NSTEMI patients.

CRP: C-reactive protein; NSTEMI: Non-ST elevation myocardial infarction.

than that between CRP and the CHA_2DS_2–VASc score. Although the CHA_2DS_2–VASc score has long been used to assess the risk of thromboembolic events in patients with atrial fibrillation, it is gaining increasing acceptance for the risk stratification of cardiovascular events. Consequently, the close correlation of a simple inflammatory ratio with a score increasingly accepted by the American College of Cardiology guidelines further highlights the potential utility of this test in clinical practice. Furthermore, although the high-sensitivity troponin T test plays a key role in the diagnosis of various types of myocardial injury, it was not found to be a strong predictor of in-hospital mortality in the patients included in our study.

Our ROC analysis provides additional support for the clinical utility of the CRP: ALB ratio. With an AUC value approaching 0.90, the ratio was found to be a significantly superior biomarker compared to CRP or albumin alone. Although a logistic model including both CRP and albumin yielded a slightly higher AUC, the difference was not significant. Our findings support the conclusion of a similar report in STEMI patients that the CRP/albumin ratio is a current and accepted marker of poor prognosis in the ACS spectrum [7]. Additionally, the distinction between the neutrophil percentage/albumin ratio (NPAR), a newer marker, appears to be more similar to CRP and MCV than to CRP or albumin. Moreover, a comparison with CRP and albumin does not reflect the clinically desirable properties of parameters such as CRP and albumin.

Our findings further support the concept that systemic inflammation and hypoalbuminemia reflect the combined metabolic and immune responses in acute myocardial injury. The CRP/albumin ratio, which integrates these two processes, ap-

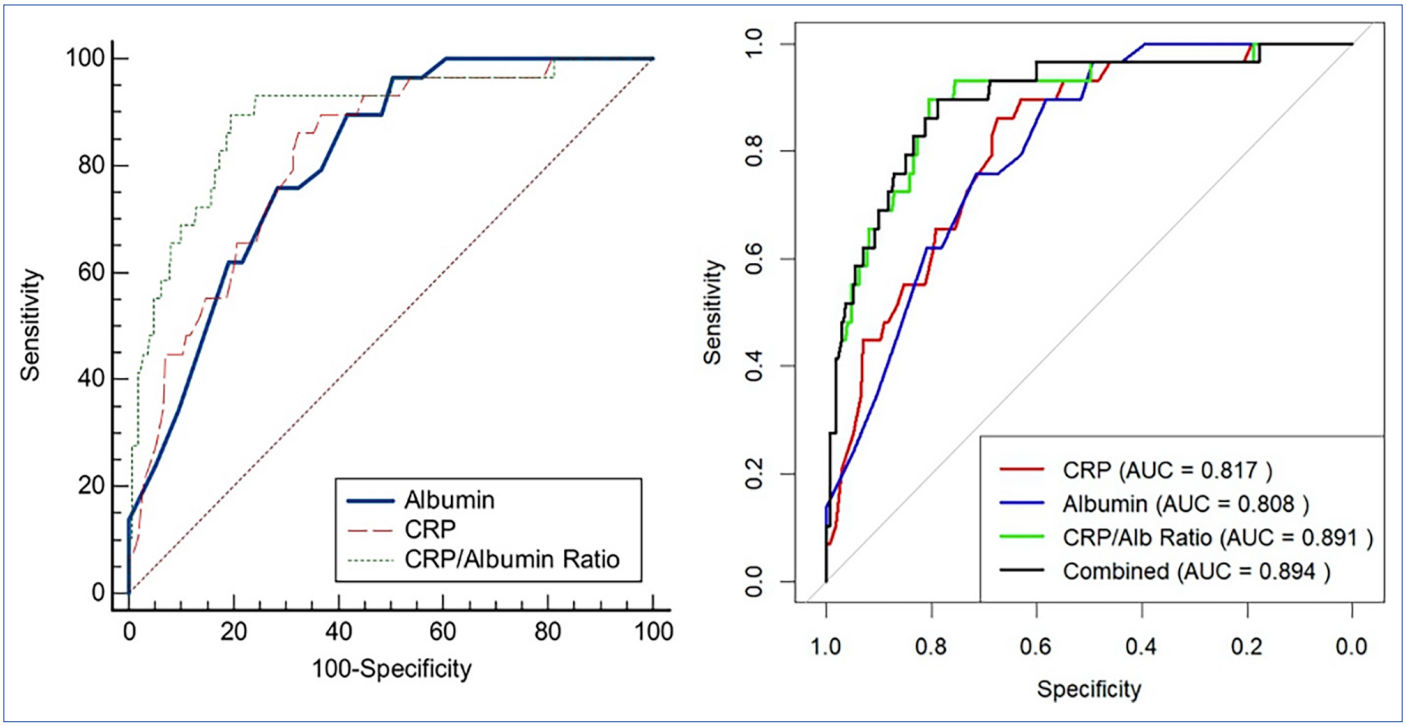

Figure 3. ROC curves comparing the predictive accuracy of albumin, CRP, CRP/albumin ratio, and combined logistic regression model for ın-hospital mortality in NSTEMI patients.

AUC: Area under the curve; CRP: C-reactive protein; ROC: Receiver operating characteristic; NSTEMI: Non-ST elevation myocardial infarction.

pears to provide a more stable indicator of patient prognosis than either marker alone. This is consistent with recent reports in both STEMI and NSTEMI populations showing that higher CRP/albumin ratios predict increased in-hospital mortality and adverse cardiovascular events [9, 10, 16]. The present study strengthens this evidence by demonstrating that this ratio remains an independent predictor even after adjusting for conventional risk factors.

These results are consistent with the pathophysiological mechanisms. Plaque rupture alone does not cause NSTEMI. It is now more widely accepted that the body's inflammatory response, which also causes damage to the blood vessel wall, is linked to endothelial dysfunction. Metabolic stress associated with strenuous physical training and resting conditions plays a significant role [8].

In this study and similar publications, the CRP-to-albumin ratio was considered an important predictor of prognosis in patients with MI. It appears particularly useful in identifying high-risk patients who initially appear stable and may therefore be easily overlooked for intensive care or other types of interventions.

The CRP-to-albumin ratio can be easily calculated using routine laboratory test results. This could provide a risk assessment method that can be easily and conveniently integrated into resource-limited emergency departments and small hospitals. This ratio could be integrated into risk scoring systems, such as TIMI or GRACE, to reduce mortality and morbidity.

From a clinical perspective, the CRP/albumin ratio may be particularly useful in identifying high-risk subgroups of patients who initially present with stable features but are at an increased risk of systemic inflammation and impaired nutritional reserves. Such patients could benefit from close monitoring and early intervention. Moreover, it should be emphasized that low albumin levels may not only reflect inflammation but can also be influenced by malnutrition and liver dysfunction. This multifactorial nature should be considered when interpreting the CRP-to-albumin ratio in clinical settings.

Conclusion

Our study demonstrated that the CRP-to-albumin ratio is a strong and independent predictor of mortality in patients with NSTEMI. This ratio is associated with complex mechanisms related to inflammation and nutritional status, which are often overlooked in routine assessments of cardiovascular risk factors. As a simple, accessible, and effective marker, this ratio is a promising parameter for improving rapid risk stratification in patients with NSTEMI.

Study Limitations: Our study had several limitations. The single-center, retrospective design and relatively small mortality subgroup (n=29) limit the generalizability and statistical power of our findings. Although the overall cohort size (n=300) was adequate, we did not perform detailed subgroup analyses by sex, diabetes, hypertension, or other comorbidities. Moreover, patients aged ≥80 years and those

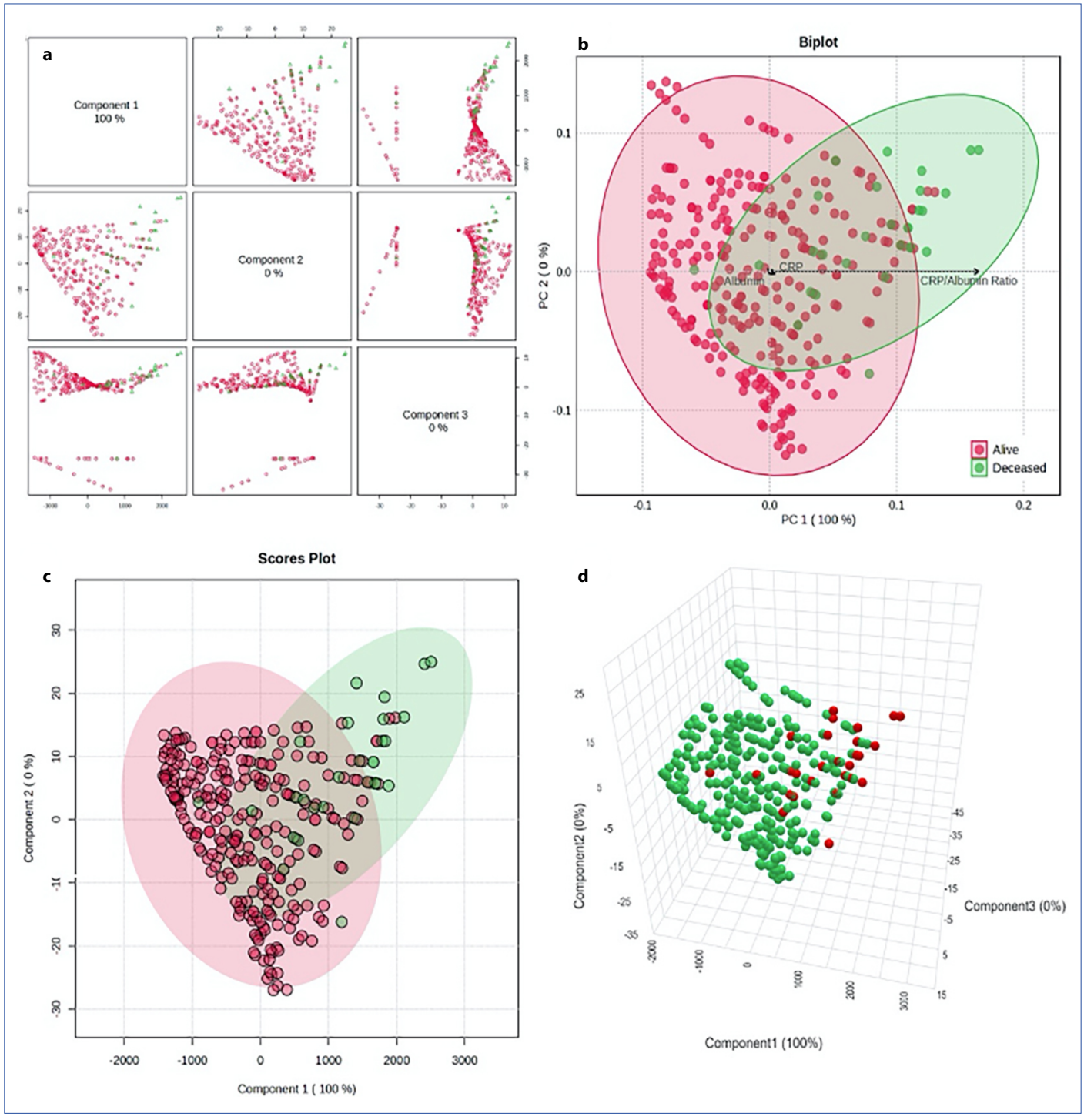

Figure 4. Partial least squares discriminant analysis (PLS-DA) plots based on albumin, CRP, and CRP/albumin ratio levels in relation to in-hospital mortality.

CRP: C-reactive protein.

with multiple comorbidities were excluded, which may reduce the representativeness of the real-world NSTEMI population in this study. Another limitation is that we focused primarily on CRP and albumin, without including additional inflammatory biomarkers such as IL-6, TNF-α, or high-sensitivity CRP, which could have provided a broader understanding of the underlying mechanisms of sarcopenia. Finally, our comparisons were limited to the CHA_2DS_2–VASc score and did not extend to other established prognostic tools such as GRACE or TIMI. Therefore, large-scale, multicenter, prospective studies are needed to validate our results and explore these aspects in greater depth.

Online Appendix Files: https://jag.journalagent.com/ijmb/abs_files/IJMB-02693/IJMB-02693_(4)_IJMB-02693_Appendix_1.pdf

Ethics Committee Approval: The study was approved by the Ankara Etlik City Hospital Ethics Committee (no: 2025-0285, date: 30/04/2025).

Informed Consent: Because our study was retrospective in design, informed consent was not obtained.

Conflict of Interest Statement: The authors have no conflicts of interest to declare.

Funding: The authors declared that this study received no financial support.

Use of AI for Writing Assistance: No AI technologies utilized.

Authorship Contributions: Concept – M.B.B., V.O.T.; Design – M.B.B., V.O.T.; Supervision – M.B.B., V.O.T.; Funding – M.B.B.; Materials – M.B.B.; Data collection and/or processing – M.B.B.; Data analysis and/or interpretation – M.B.B.; Literature search – M.B.B., V.O.T.; Writing – M.B.B.; Critical review – M.B.B., V.O.T.

Peer-review: Externally peer-reviewed.

References

1. Martínez MJ, Rueda F, Labata C, Oliveras T, Montero S, Ferrer M, et al. Non-STEMI vs. STEMI cardiogenic shock: Clinical profile and long-term outcomes. J Clin Med 2022;11:3558. [CrossRef]
2. Sami S, Willerson JT. Contemporary treatment of unstable angina and non-ST-segment-elevation myocardial infarction (part 1). Tex Heart Inst J 2010;37:141-8.
3. Sami S, Willerson JT. Contemporary treatment of unstable angina and non-ST-segment-elevation myocardial infarction (part 2). Tex Heart Inst J 2010;37:262–75.
4. Karaca M, Gumusdag A. Prognostic role of neutrophil percentage-to-albumin ratio in patients with non-ST-elevation myocardial ınfarction. Medicina (Kaunas) 2024 22;60:2101. [CrossRef]
5. Kaplangoray M, Toprak K, Aslan R, Deveci E, Gunes A, Ardahanli, I. High CRP-albumin ratio is associated high thrombus burden in patients with newly diagnosed STEMI. Medicine (Baltimore) 2023;102:e35363. [CrossRef]
6. Tanrıverdi Z, Fedai H. The association between C-reactive protein to albumin ratio and infarct location in patients with ST-segment elevation myocardial infarction. Cukurova Med J 2024;49(1):141–9. [CrossRef]
7. Askin L, Tanriverdi O, Tibilli H, Turkmen S. Prognostic value of C-reactive protein/albumin ratio in ST-segment elevation myocardial infarction. Interv Med Appl Sci 2019;11:168–71. [CrossRef]
8. Kaski JC, Cruz-Fernández JM, Fernández-Bergés D, García-Moll X, Martín Jadraque L, Mostaza J, et al. Systemic inflammation evaluation in patients with non-ST segment elevaton acute coronary syndromes. Rev Esp Cardiol 2003;56:389–95. [Article in Spanish] [CrossRef]
9. Kalyoncuoglu M, Durmus G. Relationship between C-reactive protein-to-albumin ratio and the extent of coronary artery disease in patients with non-ST-elevated myocardial infarction. Coron Artery Dis 2020;31:130–6. [CrossRef]
10. Menekşe TS, Kaçer İ, Hacımustafaoğlu M, Gül M, Ateş C. C-reactive protein to albumin ratio may predict in-hospital mortality in non-ST elevation myocardial infarction. Biomark Med 2024;18(3):103–13. [CrossRef]
11. Özkan C, Karayiğit O. Relationship between high sensitivity C-reactive protein to albumin ratio with infarct-related artery patency in patients with non-ST-segment elevation myocardial ınfarction. Angiology 2024;75(7):682–8. [CrossRef]
12. Satilmis S, Karabulut A. Value of C-reactive protein/albumin ratio in predicting the development of contrast-induced nephropathy in patients with non-ST elevation myocardial ınfarction. Angiology 2020;71(4):366–71. [CrossRef]
13. Wändell P, Carlsson AC, Li X, Sundquist J, Sundquist K. The predictive value of cardiovascular outcomes and mortality assessed by the C-reactive protein to albumin ratio in the UK Biobank. BMC Cardiovasc Disord 2024;24(1):495. [CrossRef]
14. Liu Y, Chen X, Zhang M, Zhao Y, Li J. Prognostic value of C-reactive protein to albumin ratio: A systematic review and meta-analysis. Expert Rev Mol Diagn 2023;23(10):1007–18.
15. Kurniawan RB, Pranata R, Kusumawardhani L, Huang I. The roles of C-reactive protein-albumin ratio as a novel biomarker in acute and chronic heart failure. Heart Lung 2024;64:108–14.
16. Rodi Tosu A, Çinar T, Kalyoncuoğlu M, Biter Hİ, Çakal S, Çakal B, et al. Predictive value of C-reactive protein/albumin ratio for no-reflow in patients with non-ST-elevation myocardial infarction. J Cardiovasc Thorac Res 2022;14:214–9. [CrossRef]

INTERNATIONAL JOURNAL OF
MEDICAL BIOCHEMISTRY

DOI: 10.14744/ijmb.2025.23281
Int J Med Biochem 2026;9(1):55–68

Review

Clinical and laboratory integration in Alzheimer's disease: From biological biomarkers to diagnostic implementation

Dildar Konukoglu

Department of Medical Biochemistry, Istanbul University-Cerrahpasa, Cerrahpasa Faculty of Medicine, Istanbul, Türkiye

Abstract

Alzheimer's disease (AD) is a progressive neurodegenerative disorder and the most common cause of dementia worldwide. Traditionally diagnosed based on clinical syndromes, AD is now increasingly defined as a biologically identifiable disease, reflecting advances in fluid and imaging biomarkers. Contemporary diagnostic frameworks emphasize the integration of clinical assessment with biological confirmation and staging, primarily through biomarkers of amyloid-β deposition, tau pathology, and neurodegeneration. This review provides a structured overview of current clinical staging systems and biomarker-based diagnostic approaches in Alzheimer's disease, with particular emphasis on analytical standardization, interpretive frameworks, and methodological limitations relevant to routine clinical practice. The revised 2024 Alzheimer's Association criteria are discussed, including the numeric clinical staging model and the AT(N) biomarker classification, which together enable biologically grounded diagnosis independent of symptom severity. Core biomarkers are categorized into Core 1 biomarkers, used for biological confirmation of AD pathology, and Core 2 biomarkers, which characterize disease burden, neurodegeneration, and progression. Cerebrospinal fluid (CSF) biomarkers remain the reference standard for *in vivo* biological diagnosis, while blood-based biomarkers—enabled by ultrasensitive analytical platforms—have emerged as scalable and minimally invasive tools for screening, risk stratification, and longitudinal monitoring. Multimodal biomarker profiling further supports the identification of mixed or non-Alzheimer comorbid pathologies, which are common in older populations and critically influence clinical interpretation and therapeutic decision-making. Despite their clinical utility, significant challenges remain. Measurement variability related to pre-analytical handling, assay performance, inter-laboratory differences, and lot-to-lot reagent effects continues to limit universal cut-off definition and broad clinical implementation. International standardization initiatives, reference materials, external quality control programs, and automation-ready assays have substantially improved analytical performance, yet pre-analytical variability—particularly for amyloid-β—remains a key unresolved issue. In conclusion, Alzheimer's disease biomarkers provide a powerful framework for biological diagnosis and staging, but their clinical value increasingly depends on rigorous standardization, harmonization, and context-aware interpretation rather than on the discovery of new markers alone.

Keywords: Alzheimer's disease, biomarkers, biological diagnosis, diagnostic staging, pre-analytical variability

How to cite this article: Konukoğlu D. Clinical and laboratory integration in Alzheimer's disease: From biological biomarkers to diagnostic implementation. Int J Med Biochem 2026;9(1):55–68.

Alzheimer's disease (AD) is a neurodegenerative disorder characterized by progressive cognitive decline and represents the most common cause of dementia in the elderly population. Pathophysiologically, it is defined by amyloid-β accumulation, hyperphosphorylation of tau protein, and the accompanying widespread neurodegeneration [1, 2].

For many years, the diagnosis of AD relied predominantly on the definition of a clinical syndrome, with underlying biological processes regarded as secondary, supportive elements. However, over the past decade—particularly within the last five years—the development and clinical validation of disease-specific biomarkers have led to a paradigm shift, whereby AD is increasingly approached as a biologically definable disorder [3, 4].

In contemporary practice, the diagnostic approach to AD begins with a comprehensive clinical evaluation, followed by biological confirmation and staging using laboratory and

Address for correspondence: Dildar Konukoglu, MD. Department of Medical Biochemistry, Istanbul University-Cerrahpasa, Cerrahpasa Faculty of Medicine, Istanbul, Türkiye
Phone: +90 532 547 50 54 **E-mail:** dkonuk@yahoo.com **ORCID:** 0000-0002-6095-264X

Submitted: December 22, 2025 **Accepted:** December 22, 2025 **Available Online:** February 18, 2026

imaging biomarkers. In 2011, the National Institute on Aging and the Alzheimer's Association (NIA-AA) convened three separate workgroups to develop diagnostic and evaluative recommendations for the preclinical, mild cognitive impairment (MCI), and dementia stages of Alzheimer's disease [5]. In 2018, a single workgroup was convened to update these earlier recommendations, resulting in the publication of a "research framework" intended to be revised over time in response to scientific advances [6]. The most recent revision, coordinated by the Alzheimer's Association and published in 2024, aimed to update the 2018 framework while preserving the core conceptual principles established by earlier NIA-AA workgroups [7]. These foundational principles continue to form the basis of the revised diagnostic criteria. In this chapter, the diagnostic approach to AD is first discussed within the framework of clinical criteria, followed by a detailed presentation of biomarker-based laboratory evaluation.

Accordingly, this review aims to integrate current clinical staging systems with biomarker-based laboratory diagnostics and limitations of the biological markers for AD into routine clinical practice.

Clinical Staging System in Alzheimer's Disease

The revised 2024 framework maintains the six-stage numeric clinical staging system introduced in 2018, with minor refinements [6,7]. This system applies exclusively to individuals within the AD pathophysiologic continuum, spanning from asymptomatic stages to severe dementia (Table 1):

- **Stage 1:** Biomarker-positive, asymptomatic.
- **Stage 2:** Subtle cognitive or neurobehavioral changes.
- **Stage 3:** Objective cognitive impairment without loss of independence.
- **Stages 4–6:** Progressive loss of independence (mild, moderate, and severe dementia).

This numeric model parallels both the Global Deterioration Scale and FDA guidance for early AD trials, while uniquely anchoring clinical severity to AD-specific biomarker evidence [7]. An important conceptual refinement is the introduction of stage 0, which represents genetically determined AD—such as autosomal dominant AD or Down syndrome–associated AD—in biomarker-negative, clinically asymptomatic individuals. This distinction is essential to avoid conflating genetic determinism with biomarker-defined disease biology in both clinical practice and trial design. In contrast, genetic risk alleles such as APOE ε4 are not incorporated into the staging scheme, as they indicate susceptibility rather than established disease. Nonetheless, APOE genotyping has gained clinical importance in the context of anti–amyloid-β immunotherapy because of its association with treatment-related risks [7–11]. This staging model emphasizes the severity of cognitive and functional decline, not the phenotypic subtype. It accounts for the heterogeneous and progressive nature of AD, which often involves overlapping cognitive phenotypes and mixed pathologies. Thus, numeric staging provides a biologically grounded complement to traditional syndromic labels like MCI and dementia, clarifying that biomarker-positive individuals already have AD, not merely "at risk" status [6–8].

Clinical Diagnostic Criteria in Alzheimer's Disease

The diagnostic process in AD is fundamentally based on clinical evaluation. Clinical diagnosis relies on a detailed assessment of the patient's cognitive complaints, objective confirmation of these complaints through standardized cognitive testing, and evaluation of the impact of cognitive impairment on activities of daily living. Clinical assessment represents a critical step, as it determines in which patient populations and for what purposes biomarkers should be used [7, 12].

In the diagnostic process, the nature of the cognitive complaint is evaluated first. Cognitive concerns reported solely by the individual, without objective confirmation on neuropsychological testing, are defined as *subjective cognitive decline*. This stage may correspond to the preclinical phase of AD. Conditions in which impairment in memory or other cognitive domains is objectively demonstrated, while activities of daily living remain largely preserved, are classified as *mild cognitive impairment* (MCI). Cognitive impairment that affects multiple domains and significantly interferes with daily functioning is considered to be at the dementia level [12].

The typical clinical presentation of AD is characterized by early and predominant involvement of episodic memory. However, atypical clinical phenotypes may also occur, including logopenic primary progressive aphasia, posterior cortical atrophy, or presentations dominated by frontal executive dysfunction. During clinical evaluation, the presence of features such as prominent hallucinations, cognitive fluctuations, early parkinsonism, or rapid disease progression should raise suspicion for non-Alzheimer neurodegenerative disorders in the differential diagnosis [7, 12].

Structural brain imaging is an essential component of the clinical diagnostic workup. Magnetic resonance imaging allows exclusion of vascular pathology and secondary causes of cognitive impairment, while also enabling assessment of Alzheimer-compatible structural changes, such as medial temporal lobe atrophy. Once clinical and imaging findings have been integrated, the diagnostic process proceeds to the stage of biomarker-based biological confirmation [13–15].

Biomarkers in Alzheimer's Disease

The biologically based diagnosis of AD is intended to complement—not replace—a comprehensive clinical evaluation. Advances in fluid-based biomarkers, particularly blood-based assays, together with the emergence of amyloid-β–targeted therapies for early symptomatic AD, have substantially increased the clinical relevance of biomarker-guided diagnosis [14, 15].

Table 1. Clinical staging of individuals on the Alzheimer's disease continuum

Stage	Definition	Cognitive status	Activities of daily living (ADLs)
Stage 0	Asymptomatic, deterministic gene carrier	No clinical change; cognitive testing within normal range	Fully independent
Stage 1	Asymptomatic, biomarker evidence only	Objective cognitive tests within expected range; no reported decline	Fully independent
Stage 2	Transitional decline	Cognitive performance within normal range; subtle cognitive or neurobehavioral decline from prior baseline lasting ≥6 months	Fully independent; no or minimal impact on ADLs
Stage 3	Cognitive impairment with early functional impact	Objective cognitive impairment on testing; decline documented by self, informant, or longitudinal testing	Independent, but reduced efficiency in complex ADLs
Stage 4	Dementia with mild functional impairment	Progressive cognitive decline	Dependence in instrumental ADLs; basic ADLs preserved
Stage 5	Dementia with moderate functional impairment	Advanced cognitive decline	Assistance required for basic ADLs
Stage 6	Dementia with severe functional impairment	Severe cognitive and functional decline	Complete dependence for basic ADLs

Table 2. AT(N) biomarker classification in Alzheimer's disease

Component	Pathophysiological process	Core biomarkers	Clinical significance
A	Amyloid-β deposition	CSF Aβ42 ↓ CSF Aβ42/40 ratio ↓ Amyloid PET (+)	Presence of Alzheimer's disease biology
T	Tau hyperphosphorylation	CSF p-tau181 p-tau217 Tau PET (+)	Alzheimer-specific pathology
N	Neuronal injury/neurodegeneration	CSF total tau, Neurofilament light chain MRI atrophy FDG-PET	Disease severity and prognosis

At present, biomarker testing is recommended for symptomatic individuals, rather than cognitively unimpaired persons, despite the technical capability to detect disease biology in preclinical stages. While abnormal biomarkers are often sufficient to confirm AD pathology in symptomatic patients, coexisting pathologies must always be considered, as mixed etiologies are common [14, 15].

Higher biological stages, particularly those reflecting tau pathology, increase the likelihood that clinical symptoms are attributable to AD and provide valuable prognostic information. Overall, AD biomarkers constitute essential tools for accurate diagnosis, biological staging, treatment eligibility assessment, and patient counseling. The flexible application of core biomarker categories allows clinicians to tailor diagnostic strategies according to clinical context, biomarker availability, and therapeutic decision-making [16, 17].

Recent advances in ultrasensitive immunoassay technologies have fundamentally transformed the diagnostic landscape by enabling reliable detection of AD-related biomarkers in blood. Traditionally, *in vivo* biological diagnosis relied on cerebrospinal fluid (CSF) biomarkers and positron emission tomography (PET) to demonstrate amyloid-β and tau pathology. Although analytically robust and biologically validated, these approaches are limited by invasiveness, cost, and accessibility. Blood-based biomarkers have therefore emerged as a practical and scalable complement—and in selected contexts, a partial alternative—to CSF- and PET-based diagnostics [8, 13, 18, 19].

Standardization for The Clinical Use of Biomarkers

The contemporary understanding of AD diagnosis conceptualizes the disorder not merely as a clinical syndrome, but as a biological continuum defined by specific underlying pathophysiological processes. The foundation of this approach is the AT(N) classification system, which comprises amyloid pathology (A), tau pathology (T), and neurodegeneration (N) (Table 2). In the AT(N) classification, the "A" component reflects amyloid-β deposition, the "T" component represents tau protein pathology, and the "N" component indicates neuronal injury and neurodegeneration. In clinical practice, the presence

Table 3. Interpretation of AT(N) biomarker notation

Notation	Interpretation	Typical findings
A–	No biomarker evidence of amyloid pathology	Normal CSF Aβ42 or Aβ42/40 ratio; negative amyloid PET
A+	Amyloid pathology present	Decreased CSF Aβ42 or Aβ42/40 ratio; positive amyloid PET
T1–	No evidence of AD-specific tau abnormality	Normal p-tau levels
T1+	Alzheimer-specific tau abnormality present	Elevated p-tau217, p-tau181, or p-tau231
T2–	No evidence of advanced tau deposition	Normal tau PET; normal MTBR-tau243
T2+	Cortical tau deposition present	Positive tau PET; elevated MTBR-tau243, p-tau205
N–	No evidence of active neuronal injury	Normal NfL, MRI, FDG-PET
N+	Neurodegeneration or neuronal injury present	Elevated NfL; cortical atrophy; FDG hypometabolism

of AD biology is primarily defined by positivity for A and T biomarkers, while the N component provides information regarding disease severity and progression [7, 8, 20].

Amyloid beta biomarkers (A component) are measured using both fluid-based methods (CSF, plasma) and PET, and they show a high degree of concordance. Aβ42 levels in fluids may exhibit detectable changes slightly earlier than amyloid PET. In contrast, tau biomarkers display a more complex temporal profile [7, 8, 20, 21].

The tau (T) component is no longer considered a single entity but is divided into two biologically and clinically distinct stages, referred to as **T1** and **T2. T1 biomarkers** represent early, amyloid-related tau dysregulation and consist of phosphorylated and secreted tau species that are released into CSF and plasma in response to amyloid-β pathology. These biomarkers, including p-tau217, p-tau181, and p-tau231, become abnormal very early in the disease course, often years before the onset of clinical symptoms, and demonstrate high specificity for Alzheimer's disease; therefore, they are considered suitable for establishing a biological diagnosis. In contrast, **T2 biomarkers** reflect established cortical tau proteinopathy characterized by the accumulation of neurofibrillary tangles within brain tissue. This stage is typically observed in individuals who already have amyloid pathology and is associated with disease severity, anatomical spread, and clinical progression rather than initial diagnosis. Biomarkers such as MTBR-tau243, p-tau205, and tau PET imaging fall into this category and are primarily used for disease staging and prognostic assessment. Thus, T1 biomarkers answer the question of whether AD biology is present, whereas T2 biomarkers inform how advanced and spatially distributed tau pathology has become [6–8, 20, 21].

Within the AT(N) framework, individuals can be grouped into three broad biomarker categories: Those with normal AD biomarkers; those within the Alzheimer' continuum, encompassing both Alzheimer's pathologic change and biologically defined AD; and c. those with normal amyloid biomarkers but abnormal tau and/or neurodegeneration markers. This latter category reflects evidence of one or more non–Alzheimer neuropathologic processes and has been termed suspected non–Alzheimer's pathophysiology (SNAP) [22]. Importantly, AT(N) biomarker classification is independent of clinical symptoms, and the term *biomarker profile* is preferred over stage, as it does not imply a fixed temporal sequence or causality [7]. Applying normal/abnormal thresholds to each AT(N) biomarker group yields a set of distinct AT(N) biomarker profiles (e.g., A+T–(N)–, A+T+(N)+), which allow individuals to be classified according to underlying biological patterns rather than solely clinical presentation [8] (Table 3).

Core Biomarkers in Alzheimer's Disease: Plasma and CSF-Based Approaches

Core biomarkers are a predefined subset of biological markers that directly reflect the defining molecular and cellular pathology of AD and form the basis of a biologically grounded diagnosis. In contemporary diagnostic frameworks, core biomarkers serve two complementary but distinct purposes: Biological confirmation of AD pathology and characterization of disease stage, pathological burden, and progression. Accordingly, core biomarkers are conceptually and operationally divided into Core 1 and Core 2 categories [7, 17, 23].

Core 1 biomarkers are disease-defining markers used to establish the presence or absence of AD biology, independent of clinical stage or symptom severity. In contrast, Core 2 biomarkers are disease-characterizing markers that provide information on the extent of tau pathology, neurodegeneration, and disease dynamics after AD biology has been confirmed [7, 21]. This hierarchical classification ensures a clear separation between biomarkers that answer the fundamental diagnostic question "Is AD biology present?" and those that address "How advanced and active is the disease, and to what extent is neurodegeneration occurring?" Such separation is critical for accurate etiologic interpretation, clinical decision-making, and integration of biomarkers into multimodal diagnostic profiles [7, 21, 24] (Table 4).

Core 1 Biomarkers: Biological Confirmation of Alzheimer's Disease: Core 1 biomarkers establish the presence of AD biology and constitute the first-line biological tools once clinical suspicion has been raised (Fig. 1). These biomarkers primarily reflect cerebral amyloid-β deposition and early amyloid-driven tau dysregulation and are applicable across the AD continuum, including presymptomatic stages [7] (Table 5).

Table 4. Summary of biomarkers used in the biological diagnosis, staging, and evaluation of Alzheimer's disease

Biomarker category	Pathophysiological process	Representative biomarkers	Primary clinical use
Core 1 biomarkers	Amyloid-β proteinopathy (A)	CSF Aβ42 ↓ CSF Aβ42/40 ↓ Amyloid PET (+)	Biological diagnosis
	Phosphorylated and secreted AD tau (T1)	Plasma/CSF p-tau217 p-tau181 p-tau231	Biological diagnosis
	Hybrid amyloid–tau indices	p-tau181/Aβ42, t-tau/Aβ42, Aβ42/40 %p-tau217	Diagnostic accuracy enhancement
Core 2 biomarkers	Established AD tau proteinopathy (T2)	MTBR-tau243, p-tau205 Tau PET	Staging, progression
Neurodegeneration (N)	Neuronal injury and degeneration	NfL (CSF,plasma) MRI atrophy FDG-PET hypometabolism	Severity, prognosis
Inflammation (I)	Astroglial activation	GFAP (CSF, plasma)	Supportive / early change
Vascular copathology (V)	Vascular brain injury	MRI/CT infarcts, white matter hyperintensities	Differential diagnosis
Synucleinopathy (S)	α-synuclein aggregation	αSyn-SAA	Copathology identification

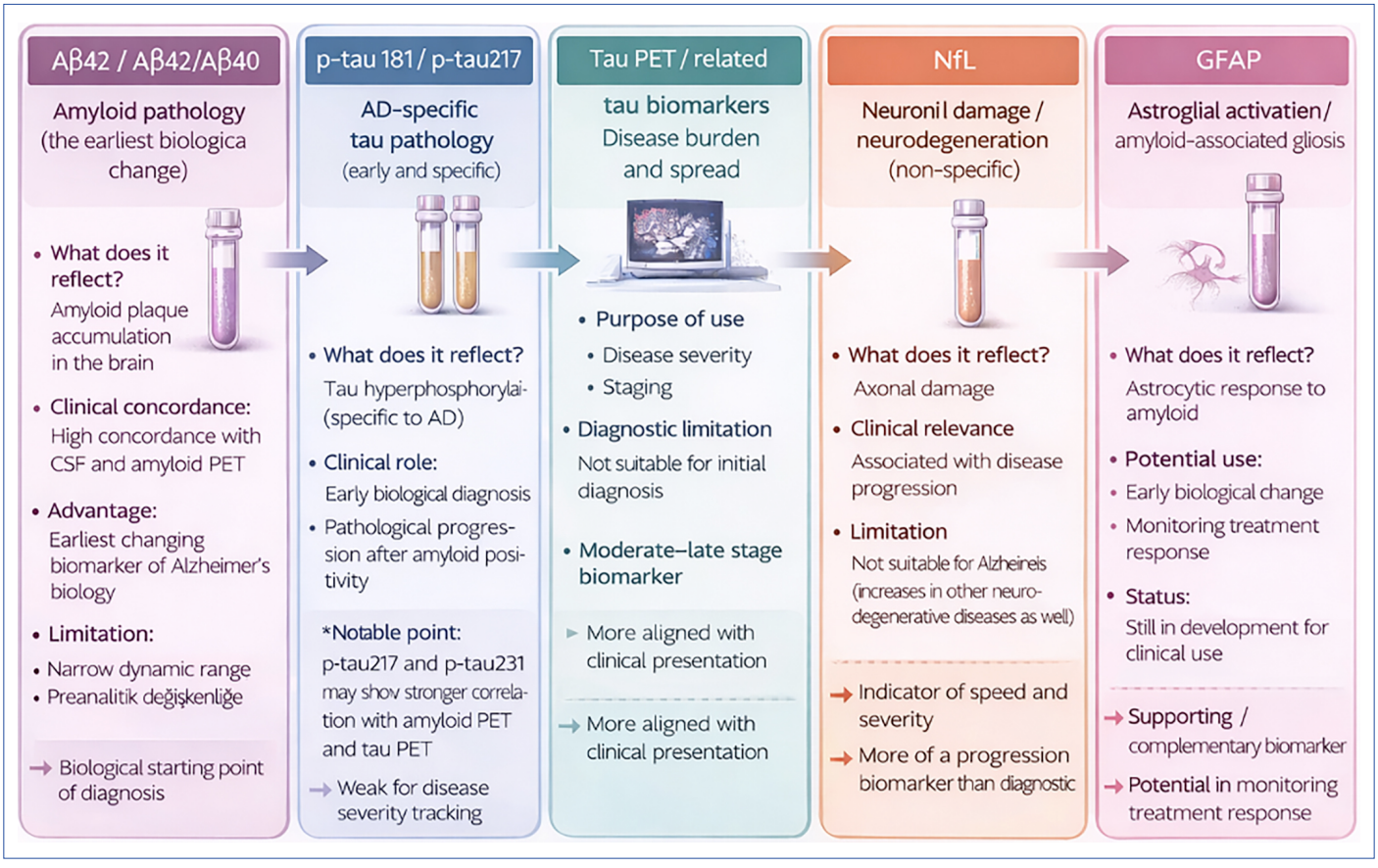

Figure 1. Biological biomarkers in Alzheimer's disease.

Table 5. Comparative overview of biomarkers in Alzheimer's disease

Biological target	CSF biomarkers	Plasma biomarkers	PET imaging	Clinical role
Amyloid-β (A)	Aβ42 ↓ Aβ42/40 ↓	Aβ42/40 ↓	Amyloid PET (+)	Biological diagnosis of AD
Tau pathology – early (T1)	p-tau181 p-tau217 p-tau231	p-tau217 p-tau181	—	AD-specific tau dysregulation
Tau pathology – established (T2)	MTBR-tau243 p-tau205	MTBR-tau243 p-tau205	Tau PET (+)	Disease staging and progression
Neurodegeneration (N)	Total tau NfL	NfL	MRI atrophy FDG-PET hypometabolism	Severity and prognosis
Inflammation (I)	GFAP	GFAP	—	Supportive, early biological change
Copathology – vascular (V)	—	—	MRI/CT infarcts, WMH	Mixed / vascular pathology
Copathology – synuclein (S)	αSyn-SAA	αSyn-SAA	—	Lewy body–related pathology

CSF biomarkers provide high analytical sensitivity and established diagnostic validity. Plasma biomarkers offer scalable, minimally invasive screening and longitudinal monitoring. PET imaging provides spatial localization and in vivo visualization of pathological burden but is limited by cost and accessibility. CSF: Cerebrospinal Fluid; AD: Alzheimer's Disease; MTBR: Microtubule-binding region; NLF: Neurofilament light chain; GFAB: Glial fibrillary acidic protein; αSyn-SAA: Alpha-synuclein seed amplification assay; FDG-PET: Fluorodeoxyglucose positron emission tomography; MRI: Magnetic resonance imaging; CT: Computed tomography; WMH: White matter hyperintensities.

a. Plasma Amyloid-β Biomarkers -A Biomarkers

Plasma Aβ biomarkers, particularly Aβ42 concentration and the Aβ42/Aβ40 ratio, reflect cerebral amyloid deposition and demonstrate concordance with CSF measures and amyloid PET positivity. The development of highly sensitive analytical platforms—including single molecule array (Simoa), electrochemiluminescence assays, and immunoprecipitation mass spectrometry—has enabled reproducible detection of reduced plasma Aβ42/Aβ40 across the AD continuum [25, 26].

Notably, alterations in plasma Aβ42/Aβ40 often occur early, in some cases preceding amyloid PET positivity, highlighting their potential utility for early biological screening and risk stratification. However, compared with CSF, plasma Aβ biomarkers exhibit a relatively narrow dynamic range, making them more susceptible to analytical variability and preanalytical confounders. Peripheral production, clearance mechanisms, and pharmacologic influences may further affect plasma Aβ levels. Consequently, plasma Aβ42/Aβ40 is best regarded as a biologically informative but analytically fragile Core 1 biomarker, suitable primarily for screening and enrichment strategies rather than standalone diagnostic use in routine clinical practice [7, 26–28].

b. Plasma Phosphorylated Tau Biomarkers -T1 Biomarkers

Complementing amyloid markers, plasma phosphorylated tau (p-tau) biomarkers represent the most robust blood-based indicators of AD-specific tau pathology and form a central component of Core 1 biomarkers. Among currently available epitopes, p-tau181, p-tau217, and p-tau231 consistently discriminate between amyloid-positive and amyloid-negative individuals, with elevations observed in both symptomatic and presymptomatic stages. Notably, p-tau217 and p-tau231 demonstrate larger fold-changes and higher disease specificity than p-tau181. From a pathophysiological perspective, plasma p-tau reflects amyloid-driven tau dysregulation and secretion rather than established neurofibrillary tangle deposition. Accordingly, these biomarkers align with the T1 category of the updated AT(N) framework and are particularly valuable for identifying AD biology prior to overt neurodegeneration or dementia [29–31].

Core 2 Biomarkers: Disease Burden, Neurodegeneration, and Progression: Once AD biology has been established using Core 1 biomarkers, Core 2 biomarkers assume a central role in disease staging, assessment of pathological extent, and prognostic evaluation. These biomarkers reflect more advanced and established stages of tau pathology and neurodegeneration and are therefore more closely associated with clinical severity and disease progression than Core 1 markers [7, 21] (Table 5).

a. Advanced Tau and Neurodegeneration Markers -T2 and N Biomarkers 3,11

While plasma p-tau reflects early tau dysregulation, biomarkers of advanced tau aggregation and neurodegeneration are more challenging to assess in blood. The microtubule-binding region (MTBR) of tau—particularly MTBR-tau243—has emerged as a promising plasma marker of established tau proteinopathy, showing closer associations with neurofibrillary tangle burden and tau PET findings. These markers are best classified within the T2 category, reflecting advanced tau pathology [14, 23, 32].

Neurofilament light chain (NfL) is the most widely adopted blood-based marker of neuroaxonal injury and constitutes a

core N biomarker. Plasma NfL levels correlate with CSF concentrations and increase with disease severity and progression but lack disease specificity, as elevations are observed in numerous neurological conditions. Accordingly, NfL reflects neurodegenerative burden rather than AD biology per se [7, 20, 33, 34].

b. Astrocytic and Inflammatory Biomarkers -I Biomarkers

Glial fibrillary acidic protein (GFAP) has emerged as a clinically relevant blood-based marker of astrocytic activation. Plasma GFAP levels are closely associated with cerebral amyloid pathology and often increase early in the AD continuum, sometimes preceding overt tau abnormalities. Although GFAP is not specific to AD, the magnitude of elevation is typically greater in AD than in many non-AD neurodegenerative diseases. Notably, reductions in plasma GFAP following anti-amyloid therapy suggest potential utility as a treatment-response biomarker, supporting its classification within the I category [7, 20, 35, 36].

c. Synaptic Injury Biomarkers and Emerging Blood-Based Candidates

Synaptic dysfunction is a central correlate of cognitive decline in AD. While several synaptic proteins, such as neurogranin, perform well in CSF, their translation to blood has been limited by peripheral expression and weak central–peripheral correlations. More recently, β-synuclein and synaptosomal-associated protein 25 (SNAP-25) have shown promise as blood-based indicators of synaptic injury, with associations to cortical atrophy and cognitive impairment. These biomarkers remain investigational but represent an important future direction in refining biological characterization and monitoring disease progression [37, 38].

d. Cerebrospinal Fluid Core Biomarkers

CSF biomarkers remain the reference standard for biological diagnosis of AD. Within the AT(N) classification, the A category includes CSF Aβ1–42 or the Aβ1–42/Aβ1–40 ratio, the T category comprises CSF phosphorylated tau, and the **N category** reflects neurodegeneration or neuronal injury, as indicated by CSF NfL or total tau (t-tau) [7, 21].

Reduced CSF Aβ1–42 concentrations are strongly associated with cerebral amyloid deposition, whereas elevated CSF p-tau levels are characteristic of AD and correlate with cortical neurofibrillary tangle burden. In contrast, increased CSF t-tau reflects neuronal injury or neurodegeneration more broadly and is not specific to AD, as elevations may also be observed in conditions such as traumatic brain injury, stroke, and Creutzfeldt–Jakob disease [7, 27–30].

Clinical-to-Biological Diagnostic Workflow in Alzheimer's Disease

This section presents a clinical-to-biological diagnostic workflow for AD from a laboratory and analytical perspective, emphasizing the stepwise use of validated biomarkers and their interpretive integration. The framework illustrates how analytical performance, biomarker categorization, and multimodal profiling collectively support biological confirmation, disease characterization, and the identification of comorbid pathologic processes across clinical and research settings.

Clinical–Laboratory Decision Pathway for Alzheimer's Disease Diagnosis

In clinical practice, the diagnostic process begins with the evaluation of cognitive complaints and the objective confirmation of impairment through standardized neuropsychological testing. Once clinical suspicion of AD is established, laboratory-based biological confirmation is pursued using **Core 1 biomarkers** as the first-line analytical approach. Positivity in Core 1 biomarkers provides evidence of underlying AD biology and supports a biologically defined diagnosis. Following biological confirmation, further laboratory and imaging-based assessment of disease stage, pathological extent, and progression is performed using **Core 2 biomarkers** and neuroimaging findings. These markers provide complementary information regarding tau pathology, neurodegenerative burden, and disease dynamics. In cases of discordance between clinical presentation and biomarker results, additional laboratory and imaging markers of **vascular pathology** or **synucleinopathies** should be considered to evaluate the presence of potential copathologies [6, 7].

An expanded representation of this clinical–laboratory diagnostic workflow, detailing the analytical rationale and interpretive integration of biomarkers across diagnostic stages, is provided in the supplementary material (Fig. 2). As illustrated, the workflow incorporates CSF or blood-based amyloid-β measures (Aβ42 or Aβ42/40 ratio), phosphorylated tau species, tau PET–related markers, NfL, and supportive biomarkers such as GFAP. Integration of core and non-core biomarkers enables the identification of mixed or alternative pathologies and supports refined etiologic interpretation, prognostic stratification, and informed therapeutic decision-making, including assessment of eligibility for disease-modifying interventions [6, 7, 17, 23–25, 39].

Multimodal Biomarker Profiles and Identification of Comorbid Pathologic Change

Following biological confirmation and initial disease characterization, further refinement of the diagnostic interpretation often requires evaluation beyond core AD pathology. In this context, multimodal biomarker profiles are conceptually distinct from the biological staging of AD. While biological staging applies exclusively to individuals in whom AD pathology has been established using core biomarkers, multimodal profiles are applicable to all individuals and are designed to characterize the overall neuropathophysiological state, either in conjunction with or independent of AD pathology [5, 7].

Within this extended framework, biomarkers are used not only to define AD biology but also to identify coexisting pathological processes that frequently contribute to cognitive impairment, particularly in older populations. Mul-

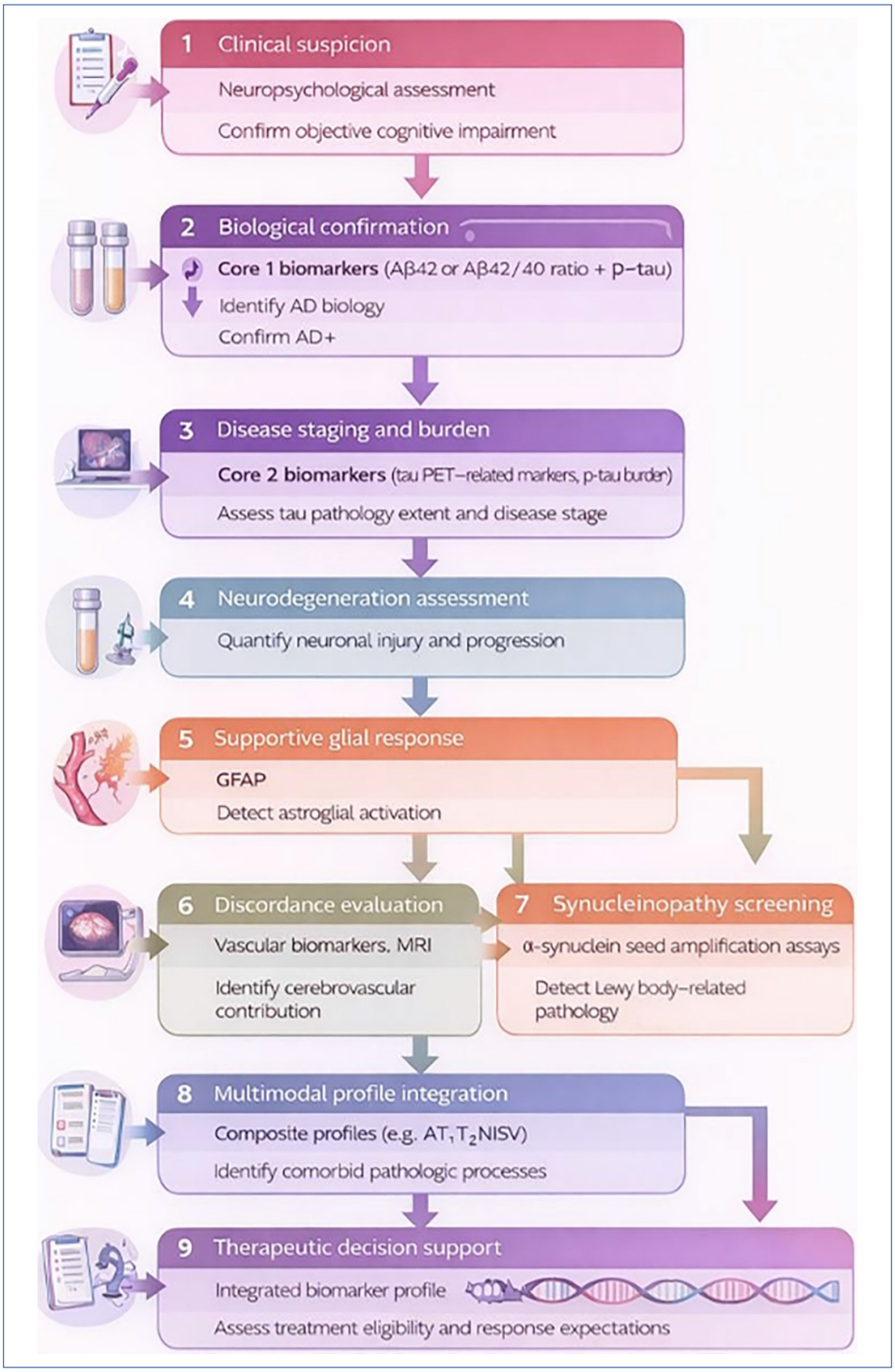

Figure 2. Clinical-laboratory decision framework for Alzheimer's disease diagnosis.

timodal biomarker profiling therefore extends beyond the traditional AT(N) system by integrating both core and non-core biomarkers into composite profiles (e.g., AT_1T_2NISV), with each component expressed either dichotomously or on a quantitative scale [23].

Although comprehensive profiling requires extensive biomarker assessment, partial profiles are often sufficient and clinically informative. This is particularly relevant given that isolated AD pathology is uncommon with advancing age; cognitive impairment is frequently shaped by multiple coexisting processes, including cerebrovascular disease, α-synuclein–related disorders, and limbic-predominant age-related TDP-43 encephalopathy (LATE). Multimodal profiles facilitate the identification of both **direct** and **indirect indicators of comorbidity**. Direct indicators include positive α-synuclein seed amplification assays or neuroimaging evi-

dence of multiple cerebral infarctions. Indirect indicators include biomarker mismatches, such as a **T2–N+** profile, suggesting that neurodegeneration or neuronal injury is driven by a pathology other than AD. For example, an individual with an **A+T2–N+** profile may have biologically defined AD accompanied by an additional neurodegenerative process, such as LATE, contributing independently to neuronal injury and cognitive decline [7, 40, 41].

Clinically, recognition of comorbid pathological change through multimodal biomarker profiling is essential for accurate etiologic interpretation, prognosis estimation, and individualized treatment planning. Such profiles may also influence expectations regarding response to disease-modifying therapies, particularly anti–amyloid-β treatments.In research settings, multimodal biomarker profiles support the definition of biologically homogeneous cohorts in early-phase trials and enable stratified or subgroup analyses in later-phase studies, thereby improving the assessment of therapeutic efficacy across heterogeneous patient populations [7, 17, 42–44]

Laboratory Reporting and Interpretation in Biomarker-Guided Diagnosis

Laboratory reports should present biomarker results not merely as numerical values but within a clearly defined pathophysiological and clinical context. For Core 1 biomarkers, reports should explicitly state whether findings are consistent with or not consistent with AD biology and include relevant methodological details, analytical performance characteristics, and validated cut-off values [7, 17, 18, 20].

Reports for Core 2 biomarkers and NfL should incorporate interpretive comments related to disease stage, neurodegenerative burden, and progression dynamics. GFAP and other inflammatory or glial markers should be presented as supportive findings rather than standalone diagnostic indicators, while the detection of biomarkers suggestive of vascular pathology or α-synuclein–related disease should prompt consideration of mixed or alternative etiologies [33–38, 45].

Pre-analytical Variability of Alzheimer's Biomarkers

Despite their central role in the biological diagnosis and staging of AD, currently available biomarkers have important limitations that must be acknowledged in both clinical and research settings.

Blood-Based Alzheimer's Biomarkers

Experience gained from CSF biomarkers in AD has clearly demonstrated that not only analytical, but also pre-analytical standardization is a critical determinant of biomarker reliability. Proteins that are prone to aggregation, particularly amyloid-β, may adhere to certain plastic materials or undergo *in vitro* aggregation, leading to substantial measurement variability. These observations have prompted systematic investigations into the effects of pre-analytical variables and the development of standardized protocols for blood, plasma, and serum samples [46, 47].

In a large multicenter study, commonly encountered pre-analytical variations across existing cohorts were systematically evaluated, including blood collection tube type, time from blood draw to centrifugation, centrifugation parameters, time from centrifugation to freezing, sample temperature during processing, aliquot volume, and number of freeze–thaw cycles [10]. Based on analyses of Aβ42/Aβ40, phosphorylated tau (p-tau181), total tau, GFAP, and NfL, a simple and standardized plasma handling protocol was proposed [46–48].

Systematic inventories of pre-analytical practices across multiple cohorts further revealed pronounced heterogeneity in critical handling steps. While factors such as needle size, blood draw location, tube filling volume, tube inversion, and freeze–thaw cycles showed little variation, substantial differences were observed in delays from blood draw to centrifugation and from centrifugation to freezing, with some studies reporting delays of up to 30 hours and 4 hours, respectively. These variables were therefore ranked as high priority for experimental evaluation [46–49].

Compared with EDTA plasma, values were generally lower in sodium-citrate tubes and higher in lithium-heparin tubes, while serum showed variable effects depending on the assay. Delayed centrifugation or delayed freezing for 24 hours at room temperature resulted in substantial reductions in Aβ42 and Aβ40 levels, whereas refrigeration largely mitigated these effects [10]. Prolonged intermittent storage at 4 °C prior to freezing caused pronounced declines in both peptides, while storage at −20 °C did not. In contrast, centrifugation temperature, aliquot volume, and repeated freeze–thaw cycles had minimal effects on Aβ42 and Aβ40 [9]. Although the Aβ42/40 ratio partially attenuated pre-analytical variability, this mitigating effect was assay- and condition-dependent and not universally reliable [48, 49].

Other blood-based biomarkers exhibited distinct pre-analytical sensitivity profiles. GFAP, NfL, p-tau181, and alternative amyloid species were influenced by sample type in a manner similar to Aβ peptides but were generally more stable with respect to delayed centrifugation and short-term storage. GFAP was the only biomarker significantly affected by repeated freeze–thaw cycles, with increased concentrations observed after multiple cycles [50, 51]. In contrast, total tau showed marked instability in whole blood, sensitivity to centrifugation temperature, and vulnerability to prolonged refrigerated storage [52].

Figure 3 illustrates the recommended pre-analytical workflow for blood sample handling to ensure reliable measurement of Alzheimer's disease–related biomarkers. Blood samples are collected by venipuncture using K_2-EDTA plasma, as alternative sample matrices are known to yield systematically different biomarker concentrations. Following blood collection, samples may be maintained at room temperature or cold con-

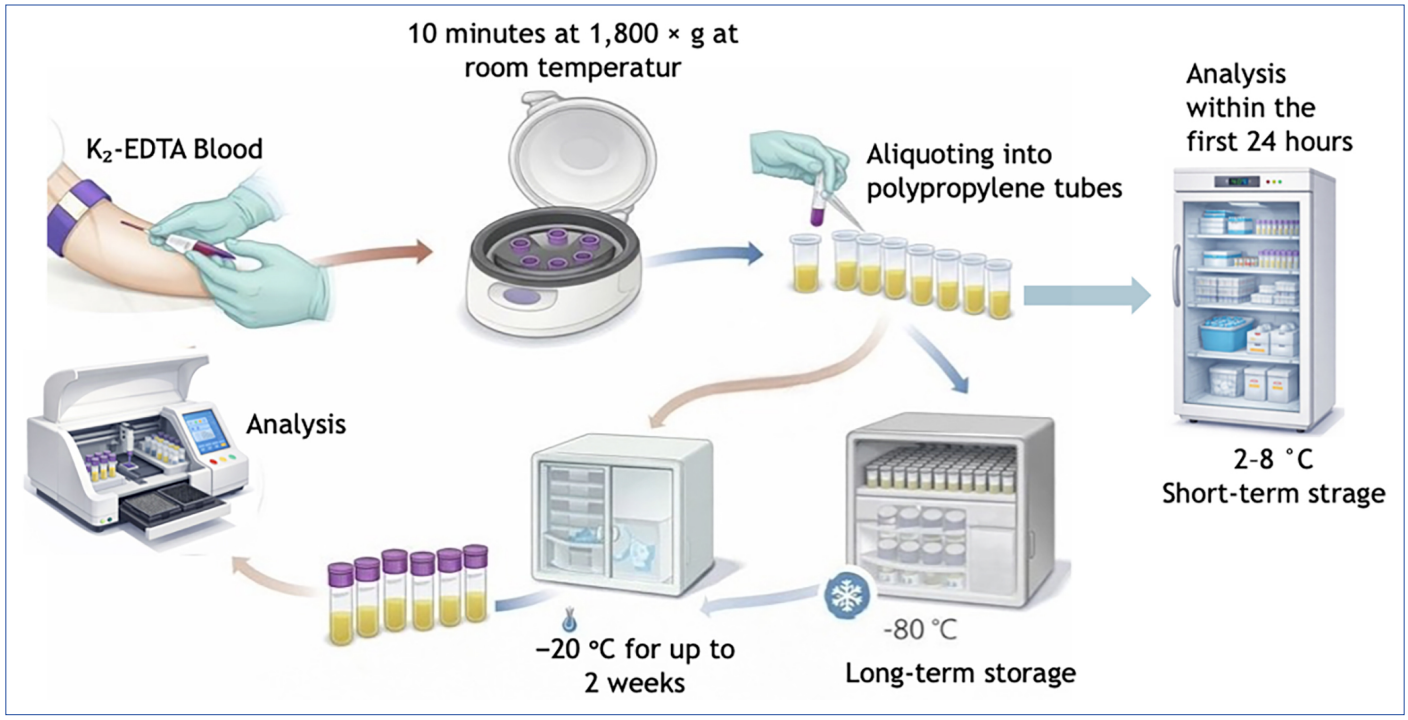

Figure 3. Recommended workflow for blood sample handling for Alzheimer's disease biomarker analysis.

ditions if processed within <3 hours; however, for processing delays of 3–24 hours, samples must be stored at 2–8 °C to prevent biomarker degradation. Plasma separation is performed by centrifugation for 10 minutes at 1,800 × g at room temperature, followed by aliquoting into polypropylene tubes with volumes ranging from 250 to 1000 µL. Post-centrifugation handling allows for short-term storage at 2–8 °C for up to 24 hours or intermediate storage at -20 °C for up to 2 weeks prior to long-term preservation. Long-term storage is conducted at -80 °C, which represents the recommended condition for maintaining biomarker stability. Samples may undergo up to two freeze–thaw cycles without significant impact on measured biomarker concentrations. This workflow emphasizes strict control of sample type, temperature, and processing time, which are critical determinants of analytical reliability in blood-based AD biomarker studies [48].

These findings underscore that analytical sensitivity alone is insufficient without strict control of pre-analytical conditions in blood-based AD biomarker testing.

CSF-Based Alzheimer's Biomarkers

Despite their widespread clinical and research use, significant inter-laboratory and batch-to-batch variability has been reported for CSF biomarker measurements. Three major sources of variability must be considered when interpreting CSF biomarker results or defining diagnostic cut-off values: Pre-analytical factors related to CSF collection, handling, and storage; analytical factors related to assay performance, technician skill, and lot-to-lot differences in reagents; and biological or patient-related factors, such as age and comorbidities [28, 48, 53, 54].

After the implementation of certified reference materials for Aβ1–42, pre-analytical factors are widely regarded as the final critical source of variability limiting harmonization. Differences in tube type, fill volume, sample transfers, storage conditions, and handling procedures can substantially influence measured biomarker concentrations. Among the core biomarkers, Aβ1–42 is particularly susceptible to pre-analytical effects, including adsorption to tube surfaces and changes related to sample volume. The persistence of heterogeneous pre-analytical protocols across centers continues to hinder the establishment of universal cut-off values, complicates clinical interpretation, and poses challenges for patient selection in clinical trials [23, 54–57].

To address this gap, a multidisciplinary workgroup convened by the Alzheimer's Association developed a simplified, standardized pre-analytical protocol for routine clinical CSF biomarker testing, with particular emphasis on Aβ1–42. This unified protocol systematically addresses key pre-analytical variables, including collection method, blood contamination, tube type and filling volume, sample transfers, mixing, transportation, and short-term stability. Broad adoption of such standardized pre-analytical procedures is essential to minimize variability, enable reliable use of biomarker cut-offs, and strengthen clinician confidence in CSF biomarkers as diagnostic tools for Alzheimer's disease [18, 23, 28].

Limitations of Biological Biomarkers

Blood and CSF biomarkers play a critical role in the diagnosis and research of Alzheimer's disease (AD). However, measurement variability across studies, laboratories, and analytical

Table 6. Schematic comparison of Alzheimer's disease cerebrospinal fluid and blood biomarkers

Dimension	CSF biomarkers	Blood (Plasma) biomarkers
Primary Purpose	Definitive biological diagnosis of AD	Screening, risk stratification, triage
Biological Proximity to Brain	High (direct contact with brain extracellular space)	Low–moderate (blood–brain barrier dilution)
Core Biomarkers	Aβ42 ↓, Aβ42/40 ↓ T-tau ↑, P-tau ↑	Aβ42/40 ↓, APP669-711/Aβ42 ↑ Tau ↑, NFL ↑
Pathophysiology Reflected	Amyloid deposition, tau pathology, neurodegeneration	Brain amyloidosis (indirect), neurodegeneration
Specificity for AD	High (especially P-tau, Aβ42/40)	Moderate–low (NFL and tau not AD-specific)
Temporal Sensitivity	Detects pathology very early (preclinical AD)	Early changes possible but later than CSF
Analytical Platforms	ELISA fully automated analyzers, Mass Spectrometry–based Reference Measurement Procedures,	Ultrasensitive immunoassays (Simoa),Immunoprecipitation–Mass Spectrometry
Standardization Status	Advanced (CRMs, reference methods available)	Developing (method-dependent variability)
Inter-laboratory Variability	Reduced with automation and CRMs	Higher; platform- and method-dependent
Pre-analytical Sensitivity	Moderate (tube type, freeze–thaw effects)	High (proteolysis, peripheral interference)
Sample Accessibility	Invasive (lumbar puncture)	Minimally invasive
Clinical Setting	Memory clinics, specialist centers	Primary care, population screening
Regulatory Readiness	High – integrated into NIA-AA biological AD definition	Emerging – not yet standalone diagnostic tools
Key Limitations	Invasiveness, patient acceptance	Lower specificity, strong analytical demands

AD; Alzheimer's disease; CSF: Cerebrospinal fluid; Aβ42: Amyloid beta 42; Aβ40: Amyloid beta 40; Aβ42/40: Ratio of amyloid beta 42 to amyloid beta 40; APP: Amyloid precursor protein; APP669–711/Aβ42: Ratio of APP fragment (amino acids 669–711) to Aβ42; T-tau: Total tau; P-tau: Phosphorylated tau; NFL: Neurofilament light chain; ELISA: Enzyme-linked immunosorbent assay; Simoa: Single molecule array; IP-MS: Immunoprecipitation–mass spectrometry; CRM: Certified reference material; NIA-AA: National institute on aging and alzheimer's association; A/T/N: Amyloid/tau/neurodegeneration; NIA-AA: National institute on aging – alzheimer's association.

platforms remains a major limitation for their widespread clinical implementation. Variability may arise at multiple stages, including assay and kit production, sample collection and storage, laboratory procedures, operator- and instrument-related factors, and data processing [28] (Table 6).

To address this challenge, the Alzheimer's Association launched an international external quality control (QC) and proficiency testing program in 2009. Within this program, 85 laboratories across more than 20 countries analyze standardized CSF samples, with centralized data evaluation enabling interlaboratory comparisons, longitudinal monitoring, and identification of outliers. Early rounds demonstrated coefficients of variation of approximately 25% for CSF Aβ42 and 15–20% for tau biomarkers, exceeding the desired analytical target of 10–15%. Variance component analyses further indicated that batch-to-batch effects represent the dominant source of variability for Aβ42, whereas between-laboratory differences contribute more substantially to variability in tau measurements [18, 23, 28, 45, 54, 57, 58].

Effective standardization therefore requires close collaboration between academia and industry. Major assay manufacturers are developing analytically validated, automation-ready immunoassays aligned with common reference materials, supported by multisite validation studies, training and certification programs, run-validation controls, and ready-to-use calibrators to minimize analytical variability [28, 46, 55, 57].

In parallel, international reference materials and reference measurement procedures are being established. Under the coordination of the International Federation of Clinical Chemistry and Laboratory Medicine (IFCC) and the European Commission's Joint Research Centre (JRC; formerly IRMM), certified reference materials for CSF Aβ42, total tau, and phosphorylated tau are being developed together with accuracy-based reference methods, particularly those based on mass spectrometry. Despite this progress, calibration matrix selection and sample preparation remain key technical challenges in achieving full harmonization [28, 57–59].

Large international QC and proficiency testing initiatives further support assay harmonization by continuously monitoring laboratory performance. As a result of these combined standardization efforts, modern automated immunoassays now demonstrate improved precision, reduced lot-to-lot variability, and lower inter-laboratory variation compared with earlier generations of assays [28, 54, 55].

Another important limitation is the intrinsic sensitivity of biomarker modalities. PET, CSF, and blood-based biomarkers are inherently less sensitive than neuropathologic examination for detecting very early or mild AD neuropathologic change. For example, regional tau PET ligand uptake does not directly equate to Braak staging at autopsy. While this may appear as a limitation, it can also be considered a strength, as abnormal core biomarkers generally reflect clinically meaningful AD pathology rather than incidental or sparse neuropathologic findings [6, 7, 57, 60–62].

From a laboratory medicine perspective, the future clinical implementation of Alzheimer's disease biomarkers will depend less on the discovery of new markers and more on rigorous analytical validation, harmonization, and context-appropriate interpretation of existing assays.

Conclusion

Disease-specific biomarkers are not yet available for all neurodegenerative and age-related brain disorders. As a result, it is not currently possible to determine with certainty which additional pathologies coexist with AD *in vivo* or to quantify the relative contribution of each pathology to the overall clinical phenotype. In conclusion, although current biomarkers provide a powerful framework for identifying AD biology, the frequent presence of comorbid pathologies limits diagnostic certainty, highlighting the continuing need for multimodal evaluation and individualized clinical interpretation. From a laboratory medicine perspective, the clinical value of Alzheimer's disease biomarkers will increasingly depend not on discovery, but on disciplined implementation.

Disclosures

Conflict of Interest Statement: The authors declare that there is no conflict of interest.

Funding: The authors declared that this study has received no financial support.

Use of AI for Writing Assistance: AI was used solely to assist with figure preparation and visual enhancement. No AI tools were used for the generation of scientific content, data analysis, or interpretation.

Peer-review: Externally peer-reviewed.

References

1. Khan S, Barve KH, Kumar MS. Recent advancements in pathogenesis, diagnostics and treatment of Alzheimer's disease. Curr Neuropharmacol 2020;18(11):1106–25. [CrossRef]
2. Twarowski B, Herbet M. Inflammatory processes in Alzheimer's disease-pathomechanism, diagnosis and treatment: A review. Int J Mol Sci 2023;24(7):6518. [CrossRef]
3. Hansson O. Biomarkers for neurodegenerative diseases. Nat Med 2021;27(6):954–63. [CrossRef]
4. Rajendran K, Krishnan UM. Biomarkers in Alzheimer's disease. Clin Chim Acta 2024;562:119857. [CrossRef]
5. Jack CR Jr, Albert MS, Knopman DS, McKhann GM, Sperling RA, Carrillo MC, et al. Introduction to the recommendations from the National Institute on Aging-Alzheimer's Association workgroups on diagnostic guidelines for Alzheimer's disease. Alzheimers Dement 2011;7(3):257–62. [CrossRef]
6. Jack CR Jr, Bennett DA, Blennow K, Carrillo MC, Dunn B, Haeberlein SB, et al. NIA-AA research framework: Toward a biological definition of Alzheimer's disease. Alzheimers Dement 2018;14(4):535–62. [CrossRef]
7. Jack CR Jr, Andrews JS, Beach TG, Buracchio T, Dunn B, Graf A, et al. Revised criteria for diagnosis and staging of Alzheimer's disease: Alzheimer's Association Workgroup. Alzheimers Dement 2024;20(8):5143–69. [CrossRef]
8. Burnham SC, Coloma PM, Li QX, Collins S, Savage G, Laws S, et al. Application of the NIA-AA research framework: Towards a biological definition of Alzheimer's disease using cerebrospinal fluid biomarkers in the AIBL study. J Prev Alzheimers Dis 2019;6(4):248–55. [CrossRef]
9. Salloway S, Sperling R, Fox NC, Blennow K, Klunk W, Raskind M, et al. Two phase 3 trials of bapineuzumab in mild-to-moderate Alzheimer's disease. N Engl J Med 2014;370(4):322–33. [CrossRef]
10. Novak G, Fox N, Clegg S, Nielsen C, Einstein S, Lu Y, et al. Changes in brain volume with bapineuzumab in mild to moderate Alzheimer's disease. J Alzheimers Dis 2016;49(4):1123–34. [CrossRef]
11. Iulita MF, Bejanin A, Vilaplana E, Carmona-Iragui M, Benejam B, Videla L, et al. Association of biological sex with clinical outcomes and biomarkers of Alzheimer's disease in adults with Down syndrome. Brain Commun 2023;5(2):fcad074. [CrossRef]
12. Atri A, Dickerson BC, Clevenger C, Karlawish J, Knopman D, Lin PJ, et al. Alzheimer's Association clinical practice guideline for the diagnostic evaluation, testing, counseling, and disclosure of suspected Alzheimer's disease and related disorders (DETeCD-ADRD): Executive summary of recommendations for primary care. Alzheimers Dement 2025;21(6):e14333. [CrossRef]
13. Shi Q, Hou J, Peng X, Xu Z, Wang Y, Cao D. Magnetic resonance imaging analysis for Alzheimer's disease diagnosis using artificial intelligence: Methods, challenges, and opportunities. Ageing Res Rev 2026;113:102943. [CrossRef]
14. Dubois B, von Arnim CAF, Burnie N, Bozeat S, Cummings J. Biomarkers in Alzheimer's disease: Role in early and differential diagnosis and recognition of atypical variants. Alzheimers Res Ther 2023;15(1):175. [CrossRef]
15. Arslan B, Zetterberg H, Ashton NJ. Blood-based biomarkers in Alzheimer's disease-moving towards a new era of diagnostics. Clin Chem Lab Med 2024;62(6):1063–9. [CrossRef]
16. Karikari TK, Pascoal TA, Ashton NJ, Janelidze S, Benedet AL, Rodriguez JL, et al. Blood phosphorylated tau 181 as a biomarker for Alzheimer's disease: A diagnostic performance and prediction modelling study using data from four prospective cohorts. Lancet Neurol 2020;19(5):422–33. [CrossRef]
17. Hansson O, Edelmayer RM, Boxer AL, Carrillo MC, Mielke MM, Rabinovici GD, et al. The Alzheimer's Association appropriate use recommendations for blood biomarkers in Alzheimer's disease. Alzheimers Dement 2022;18(12):2669–86. [CrossRef]
18. Hansson O, Batrla R, Brix B, Carrillo MC, Corradini V, Edelmayer RM, et al. The Alzheimer's Association international guidelines for handling of cerebrospinal fluid for routine clinical measurements of amyloid β and tau. Alzheimers Dement 2021;17(9):1575–82. [CrossRef]
19. van Oostveen WM, de Lange ECM. Imaging techniques in Alzheimer's disease: A review of applications in early diagnosis and longitudinal monitoring. Int J Mol Sci 2021;22(4):2110. [CrossRef]
20. Jack CR Jr, Bennett DA, Blennow K, Carrillo MC, Feldman HH, Frisoni GB, et al. A/T/N: An unbiased descriptive classification scheme for Alzheimer disease biomarkers. Neurology 2016;87(5):539–47. [CrossRef]
21. Wang ZB, Tan L, Gao PY, Ma YH, Fu Y, Sun Y, et al. Associations of the A/T/N profiles in PET, CSF, and plasma biomarkers with Alzheimer's disease neuropathology at autopsy. Alzheimers Dement 2023;19(10):4421–35. [CrossRef]

22. Jack CR Jr, Knopman DS, Chételat G, Dickson D, Fagan AM, Frisoni GB, et al. Suspected non-Alzheimer disease pathophysiology-concept and controversy. Nat Rev Neurol 2016;12(2):117–24. [CrossRef]
23. Blennow K, Zetterberg H. Biomarkers for Alzheimer's disease: Current status and prospects for the future. J Intern Med 2018;284(6):643–63. [CrossRef]
24. Pichet Binette A, Smith R, Salvadó G, Tideman P, Glans I, van Westen D, et al. Evaluation of the revised criteria for biological and clinical staging of Alzheimer disease. JAMA Neurol 2025;82(7):666–75. [CrossRef]
25. Palmqvist S, Whitson HE, Allen LA, Suarez-Calvet M, Galasko D, Karikari TK, et al. Alzheimer's Association clinical practice guideline on the use of blood-based biomarkers in the diagnostic workup of suspected Alzheimer's disease within specialized care settings. Alzheimers Dement 2025;21(7):e70535. [CrossRef]
26. Qiu Y, Jacobs DM, Messer K, Salmon DP, Wellington CL, Stukas S, et al. Prognostic value of plasma biomarkers for informing clinical trial design in mild-to-moderate Alzheimer's disease. Alzheimers Res Ther 2025;17(1):97. [CrossRef]
27. Manuilova E, Schrurs I, Rutz S, McIlwrick S, Goldhardt O, Sommer P, et al. Elecsys CSF AD immunoassays: Sample stability for a new pre-analytical protocol for fresh CSF. Alzheimers Dement 2025;21(10):e70797. [CrossRef]
28. Carrillo MC, Blennow K, Soares H, Lewczuk P, Mattsson N, Oberoi P, et al. Global standardization measurement of cerebrospinal fluid for Alzheimer's disease: An update from the Alzheimer's Association Global Biomarkers Consortium. Alzheimers Dement 2013;9(2):137–40. [CrossRef]
29. Ossenkoppele R, van der Kant R, Hansson O. Tau biomarkers in Alzheimer's disease: Towards implementation in clinical practice and trials. Lancet Neurol 2022;21(8):726–34. [CrossRef]
30. Olsson B, Lautner R, Andreasson U, Öhrfelt A, Portelius E, Bjerke M, et al. CSF and blood biomarkers for the diagnosis of Alzheimer's disease: A systematic review and meta-analysis. Lancet Neurol 2016;15(7):673–84. [CrossRef]
31. Brickman AM, Manly JJ, Honig LS, Sanchez D, Reyes-Dumeyer D, Lantigua RA, et al. Plasma p-tau181, p-tau217, and other blood-based Alzheimer's disease biomarkers in a multi-ethnic, community study. Alzheimers Dement 2021;17(8):1353–64. [CrossRef]
32. Horie K, Salvadó G, Koppisetti RK, Janelidze S, Barthélemy NR, He Y, et al. Plasma MTBR-tau243 biomarker identifies tau tangle pathology in Alzheimer's disease. Nat Med 2025;31(6):2044–53. [CrossRef]
33. Gaetani L, Blennow K, Calabresi P, Di Filippo M, Parnetti L, Zetterberg H. Neurofilament light chain as a biomarker in neurological disorders. J Neurol Neurosurg Psychiatry 2019;90(8):870–81. [CrossRef]
34. Fuloria NK, Sekar M, Porwal O, Ansari MT, Biswas A, Narain K, et al. Neurofilament light chain in Alzheimer's disease. Clin Chim Acta 2026;578:120580. [CrossRef]
35. Carter SF, Herholz K, Rosa-Neto P, Pellerin L, Nordberg A, Zimmer ER. Astrocyte biomarkers in Alzheimer's disease. Trends Mol Med 2019;25(2):77–95. [CrossRef]
36. Shetty D, Brahmbhatt S, Desai A, Bathla G, Mohan S, Gupta V,vet al. Glial fibrillary acidic protein astrocytopathy: Review of pathogenesis, imaging features, and radiographic mimics. AJNR Am J Neuroradiol 2024;45(10):1394–402. [CrossRef]
37. Abu-Rumeileh S, Erhart DK, Barba L, Konen FF, Stapf C, Senel M, et al. CSF beta-synuclein, SNAP-25, and neurogranin in infectious and autoimmune inflammatory neurologic diseases. Neurol Neuroimmunol Neuroinflamm 2025;12(6):e200491. [CrossRef]
38. Alcolea D, Beeri MS, Rojas JC, Gardner RC, Lleó A. Blood biomarkers in neurodegenerative diseases: Implications for the clinical neurologist. Neurology 2023;101(4):172–80. [CrossRef]
39. Jack CR Jr, Wiste HJ, Weigand SD, Therneau TM, Lowe VJ, Knopman DS, et al. Defining imaging biomarker cut points for brain aging and Alzheimer's disease. Alzheimers Dement 2017;13(3):205–16. [CrossRef]
40. Basellini MJ, Kothuis JM, Comincini A, Pezzoli G, Cappelletti G, Mazzetti S. Pathological pathways and alpha-synuclein in Parkinson's disease: A view from the periphery. Front Biosci 2023;28(2):33. [CrossRef]
41. Wolk DA, Nelson PT, Apostolova L, Arfanakis K, Boyle PA, Carlsson CM, et al. Clinical criteria for limbic-predominant age-related TDP-43 encephalopathy. Alzheimers Dement 2025;21(1):e14202. [CrossRef]
42. Hansson O, Blennow K, Zetterberg H, Dage J. Blood biomarkers for Alzheimer's disease in clinical practice and trials. Nat Aging 2023;3(5):506–19. [CrossRef]
43. Heneka MT, Morgan D, Jessen F. Passive anti-amyloid β immunotherapy in Alzheimer's disease-opportunities and challenges. Lancet 2024;404(10468):2198–2208. [CrossRef]
44. Suzuki N, Hatta T, Ito M, Kusakabe KI. Anti-amyloid-β antibodies and anti-tau therapies for Alzheimer's disease: Recent advances and perspectives. Chem Pharm Bull 2024;72(7):602–9. [CrossRef]
45. Frisoni GB, Hansson O, Nichols E, Garibotto V, Schindler SE, van der Flier WM, et al. New landscape of the diagnosis of Alzheimer's disease. Lancet 2025;406(10510):1389–1407. [CrossRef]
46. Verberk IMW, Misdorp EO, Koelewijn J, Ball AJ, Blennow K, Dage JL, et al. Characterization of pre-analytical sample handling effects on a panel of Alzheimer's disease-related blood-based biomarkers: Results from the Standardization of Alzheimer's Blood Biomarkers (SABB) working group. Alzheimers Dement 2022;18(8):1484–97. [CrossRef]
47. Panikkar D, Vivek S, Crimmins E, Faul J, Langa KM, Thyagarajan B. Pre-analytical variables influencing stability of blood--based biomarkers of neuropathology. J Alzheimers Dis 2023;95(2):735–48. [CrossRef]
48. Verberk IMW, Gouda M, Antwi-Berko D, van Leeuwenstijn M, Bongers B, Houtkamp IM, et al. Evidence-based standardized sample handling protocol for accurate blood-based Alzheimer's disease biomarker measurement: Results and consensus of the Global Biomarker Standardization Consortium. Alzheimers Dement 2025;21(10):e70752. [CrossRef]
49. Chen Y, Zeng X, Diaz JL, Sehrawat A, Lafferty TK, Boslett JJ, et al. Effect of blood collection tube containing protease inhibitors on the pre-analytical stability of Alzheimer's disease plasma biomarkers. J Neurochem 2024;168(9):2736–50. [CrossRef]

50. van Lierop ZYGJ, Verberk IMW, van Uffelen KWJ, Koel-Simmelink MJA, In 't Veld L, Killestein J, et al. Pre-analytical stability of serum biomarkers for neurological disease: Neurofilament-light, glial fibrillary acidic protein and contactin-1. Clin Chem Lab Med 2022;60(6):842–50. [CrossRef]
51. Choucair I, Lee TL, Van Eldik LJ, Dage JL, Gold BT, Abner EL, et al. Storage-dependent variability in Alzheimer disease-related plasma biomarker results using the Fujirebio Lumipulse G1200 platform. J Neuropathol Exp Neurol 2025;84(12):1143–51. [CrossRef]
52. Bali D, Hansson O, Janelidze S. Effects of certain pre-analytical factors on the performance of plasma phospho-tau217. Alzheimers Res Ther 2024;16(1):31. [CrossRef]
53. Vanderstichele H, Demeyer L, Janelidze S, Coart E, Stoops E, Mauroo K, et al. Recommendations for cerebrospinal fluid collection for the analysis by ELISA of neurogranin trunc P75, α-synuclein, and total tau in combination with Aβ(1–42)/Aβ(1–40). Alzheimers Res Ther 2017;9(1):40. [CrossRef]
54. Mattsson N, Andreasson U, Persson S, Arai H, Batish SD, Bernardini S, et al. The Alzheimer's Association external quality control program for cerebrospinal fluid biomarkers. Alzheimers Dement 2011;7(4):386–95.e6. [CrossRef]
55. Schauer SP, Mylott WR Jr, Yuan M, Jenkins RG, Rodney Mathews W, Honigberg LA, et al. Preanalytical approaches to improve recovery of amyloid-β peptides from CSF as measured by immunological or mass spectrometry-based assays. Alzheimers Res Ther 2018;10(1):118. [CrossRef]
56. Pannee J, Portelius E, Minthon L, Gobom J, Andreasson U, Zetterberg H, et al. Reference measurement procedure for CSF amyloid beta (Aβ)1–42 and the CSF Aβ1–42/Aβ1–40 ratio-a cross-validation study against amyloid PET. J Neurochem 2016;139(4):651–8. [CrossRef]
57. Pannee J, Shaw LM, Korecka M, Waligorska T, Teunissen CE, Stoops E, et al. The global Alzheimer's Association round robin study on plasma amyloid β methods. Alzheimers Dement (Amst) 2021;13(1):e12242. [CrossRef]
58. Ashton NJ, Keshavan A, Brum WS, Andreasson U, Arslan B, Droescher M, et al. The Alzheimer's Association Global Biomarker Standardization Consortium plasma phospho-tau Round Robin study. Alzheimers Dement 2025;21(2):e14508. [CrossRef]
59. Arnerić SP, Batrla-Utermann R, Beckett L, Bittner T, Blennow K, Carter L, et al. Cerebrospinal fluid biomarkers for Alzheimer's disease: A view of the regulatory science qualification landscape from the Coalition Against Major Diseases CSF Biomarker Team. J Alzheimers Dis 2017;55(1):19–35. [CrossRef]
60. Braak H, Del Tredici K. The pathological process underlying Alzheimer's disease in individuals under thirty. Acta Neuropathol 2011;121(2):171–81. [CrossRef]
61. Villemagne VL, Doré V, Burnham SC, Masters CL, Rowe CC. Imaging tau and amyloid-β proteinopathies in Alzheimer disease and other conditions. Nat Rev Neurol 2018;14(4):225–36. [CrossRef]
62. Blennow K, Hampel H, Weiner M, Zetterberg H. Cerebrospinal fluid and plasma biomarkers in Alzheimer disease. Nat Rev Neurol 2010;6(3):131–44. [CrossRef]

INTERNATIONAL JOURNAL OF
MEDICAL BIOCHEMISTRY

DOI: 10.14744/ijmb.2026.79847
Int J Med Biochem 2026;9(1):69–70

Letter to the Editor

Trans fat-induced metabolic and endothelial injury: A convergent pathway accelerating atherogenesis

Mustafa Sahin[1], Nazli Koc[1], Okan Dikker[2]

[1]Department of Medical Biochemistry, Hitit University Faculty of Medicine, Corum, Türkiye
[2]Department of Medical Biochemistry, University of Health Sciences, Istanbul Prof. Dr. Cemil Taşcıoğlu City Hospital, Istanbul, Türkiye

How to cite this article: Sahin M, Koc N, Dikker O. Trans fat-induced metabolic and endothelial injury: A convergent pathway accelerating atherogenesis. Int J Med Biochem 2026;9(1):69–70.

Dear Editor,

Despite substantial progress in global food policy, recent analyses demonstrate that industrial trans fatty acids (TFAs) remain detectable in a wide range of commercially prepared foods, including baked goods, confectionery products, frying oils, and fast-food items [1]. Even though overall population exposure has declined in many regions, residual intake persists and may still be sufficient to exert biologically relevant effects. Accumulating evidence indicates that TFAs may act through dual, interconnected pathways—metabolic dysregulation and vascular injury—that collectively may contribute to atherogenesis beyond lipid profile changes alone.

From a metabolic perspective, TFAs have been reported to influence hepatic lipid handling. They have been associated with increased de novo lipogenesis, impaired β-oxidation, and worsening hepatic insulin resistance, potentially contributing to the development and progression of non-alcoholic fatty liver disease (NAFLD) [2, 3]. NAFLD in turn may promotes increased very-low-density lipoprotein (VLDL) secretion, elevating circulating low-density lipoprotein (LDL) concentrations [4]. Importantly, hepatic steatosis and systemic inflammation may enhance oxidative stress, potentially rendering LDL particles more susceptible to oxidative modification—a critical step driving macrophage lipid uptake and foam cell formation [4, 5].

It has also been noted that TFAs may be associated with an increase in visceral fat accumulation independently of total calorie load [6]. Visceral adipose tissue behaves as an active endocrine organ, releasing pro-inflammatory cytokines, adipokines, and free fatty acids. These mediators may aggravate systemic inflammation, intensify insulin resistance, and impose additional stress on the vascular endothelium, thereby fostering a metabolic environment permissive to atherosclerotic progression [6, 7].

Concurrently, TFAs have been associated with markers of vascular dysfuntion. They may impair endothelial nitric oxide (NO) bioavailability, increase reactive oxygen species, and activate NF-κB–dependent inflammatory cascades. These changes can promote monocyte recruitment and increase endothelial permeability by upregulating adhesion molecules such as VCAM-1, ICAM-1, and E-selectin; these are important early stages of atherogenesis [7, 8]. As LDL particles—already elevated and rendered more oxidation-prone by metabolic dysregulation—enter this inflammatory subendothelial compartment, they undergo rapid conversion into oxidized LDL (oxLDL).

OxLDL may promote macrophage recruitment and uptake via scavenger receptors, facilitating the formation of foam cells, a hallmark of early atherosclerotic lesions [8, 9]. ABCA1 and ABCG1 are key transporters mediating macrophage cholesterol efflux and reverse cholesterol transport, processes critically involved in limiting foam cell formation and atherogenesis [9]. While direct human evidence linking TFAs to modulation of these transporters remains limited, disturbances in lipid metabolism and inflammatory signaling associated with TFA exposure may have implications for macrophage cholesterol handling. These mechanisms may facilitate the transition from fatty streaks to more advanced, rupture-prone plaques.

Recent mechanistic studies suggest that individuals with NAFLD, metabolic syndrome, diabetes, or pre-existing endothelial dysfunction may exhibit heightened vascular susceptibility to ox-LDL-driven foam cell formation and plaque progression [10]. As

Address for correspondence: Mustafa Sahin, MD. Department of Medical Biochemistry, Hitit University Faculty of Medicine, Corum, Türkiye
Phone: +90 364 219 30 00 **E-mail:** sahinmustafa@hitit.edu.tr **ORCID:** 0000-0001-6073-563X

Submitted: January 15, 2026 **Revised:** February 05, 2026 **Accepted:** February 09, 2026 **Available Online:** February 18, 2026

the prevalence of these conditions rises globally, the synergistic toxicity of TFAs across metabolic and vascular pathways becomes increasingly concerning. The integration of molecular, metabolic, and vascular evidence underscores that TFAs should be regarded not only as dyslipidemic nutrients but as potent accelerators of atherogenesis through multiple reinforcing mechanisms.

Given this convergent model—whereby TFAs elevate and oxidize LDL, promote hepatic steatosis, increase visceral obesity, impair endothelial function, and accelerate foam cell formation—it is imperative to adopt a more prevention-oriented framework. Even minimal residual exposure may be sufficient to activate these atherogenic processes. Thus, regulatory strategies should extend beyond simple manufacturing restrictions to include rigorous surveillance of imported and commercially prepared foods. Improved labeling practices, mandatory trans fat disclosure, and random market sampling may further safeguard the food environment.

Clinically, greater emphasis is needed on dietary counselling. Patients—especially those with NAFLD, obesity, diabetes, or established cardiovascular disease—should be explicitly advised to avoid all sources of trans fats. Positioning TFAs as preventable cardiovascular risk factors may improve adherence and help reduce long-term morbidity.

Disclosures

Conflict of Interest Statement: The authors have no conflicts of interest to declare.

Funding: The authors declared that this study received no financial support.

Use of AI for Writing Assistance: No AI technologies utilized.

Authorship Contributions: Concept – M.S., N.K., O.D.; Design – M.S.; Supervision – N.K.; Resources – M.S., N.K., O.D.; Materials – M.S., O.D.; Data collection and/or processing – M.S., N.K.; Analysis and/or interpretation – M.S., O.D.; Writing – M.S., O.D.; Critical review – M.S., N.K., O.D.

Peer-review: Externally peer-reviewed.

References

1. Niforou A, Magriplis E, Klinaki E, Niforou K, Naska A. On account of trans fatty acids and cardiovascular disease risk - There is still need to upgrade the knowledge and educate consumers. Nutr Metab Cardiovasc Dis 2022;32(8):1811–8. [CrossRef]
2. Arab JP, Arrese M, Trauner M. Recent Insights into the pathogenesis of nonalcoholic fatty liver disease. Annu Rev Pathol 2018;13:321–50. [CrossRef]
3. Wang DD, Hu FB. Dietary fat and risk of cardiovascular disease: Recent controversies and advances. Annu Rev Nutr 2017;37:423–46. [CrossRef]
4. van Zwol W, van de Sluis B, Ginsberg HN, Kuivenhoven JA. VLDL biogenesis and secretion: It takes a village. Circ Res 2024;134(2):226–44. [CrossRef]
5. Hong CG, Florida E, Li H, Parel PM, Mehta NN, Sorokin AV. Oxidized low-density lipoprotein associates with cardiovascular disease by a vicious cycle of atherosclerosis and inflammation: A systematic review and meta-analysis. Front Cardiovasc Med 2023;9:1023651. [CrossRef]
6. Kolb H. Obese visceral fat tissue inflammation: From protective to detrimental? BMC Med 2022;20(1):494. [CrossRef]
7. Cesaro A, De Michele G, Fimiani F, Acerbo V, Scherillo G, Signore G, et al. Visceral adipose tissue and residual cardiovascular risk: A pathological link and new therapeutic options. Front Cardiovasc Med 2023;10:1187735. [CrossRef]
8. Jiang H, Zhou Y, Nabavi SM, Sahebkar A, Little PJ, Xu S, et al. Mechanisms of oxidized ldl-mediated endothelial dysfunction and ıts consequences for the development of atherosclerosis. Front Cardiovasc Med 2022;9:925923. [CrossRef]
9. Chistiakov DA, Melnichenko AA, Myasoedova VA, Grechko AV, Orekhov AN. Mechanisms of foam cell formation in atherosclerosis. J Mol Med 2017;95(11):1153–65. [CrossRef]
10. Guo J, Du L. An update on ox-LDL-inducing vascular smooth muscle cell-derived foam cells in atherosclerosis. Front Cell Dev Biol 2024;12:1481505. [CrossRef]